

Supporting Information

Chiral self-sorting behaviour of [2.2]paracyclophane-based bis(pyridine) ligands

J. Anhäuser,^a R. Puttreddy,^b Y. Lorenz,^a A. Schneider,^a M. Engeser,^a K. Rissanen,^b A. Lützen^a

^a Kekulé-Institut für Organische Chemie und Biochemie
Rheinische Friedrich-Wilhelms-Universität Bonn
Gerhard-Domagk-Str. 1, 53121 Bonn, Germany

^b University of Jyväskylä
Department of Chemistry, Nanoscience Center
P.O. Box 35, 40014 Jyväskylä, Finland

Table of contents

General experimental information.....	2
Synthesis route.....	3
Synthesis and characterization of ligand precursors.....	3
4,15-Bis-(4-trimethylsilylphenyl)[2.2]paracyclophane 2	3
4,15-Bis-(4-iodophenyl)[2.2]paracyclophane 3	10
Synthesis and characterization of ligands.....	14
4,15-Bis-(4-(pyridin-4-yl)phenyl)[2.2]paracyclophane 4	14
4,15-Bis-(4-(pyridin-3-yl)phenyl)[2.2]paracyclophane 5	22
Self-assembly and characterization of palladium(II) complexes.....	30
[Pd ₂ (dppp) ₂ 4] ₂ (OTf) ₄ in dichloromethane:acetonitrile 1:1.....	30
[Pd ₂ (dppp) ₂ 4] ₂ (OTf) ₄ in acetonitrile.....	40
[Pd ₂ 5] ₄ (BF ₄) ₄ in acetonitrile.....	51
[Pd ₂ 5] ₄ (BF ₄) ₄ in dimethyl sulfoxide.....	59
NMR experiments concerning the kinetics of structural rearrangements upon mixing of preassembled enantiomerically pure complexes [Pd ₂ {(<i>R</i> _p)- 5] ₄ (BF ₄) ₄ and [Pd ₂ {(<i>S</i> _p)- 5] ₄ (BF ₄) ₄	66
X-ray crystallography.....	68
References.....	69

General experimental information

All reactions with air and moisture sensitive compounds were performed under argon atmosphere using standard Schlenk techniques, oven-dried glassware and dry solvents.

The following chemicals were obtained commercially from *Alfa Aesar*, *Sigma-Aldrich*, *Carbolution*, *Fluorochem* or *abcr* and used as received: 4-(trimethylsilyl)phenylboronic acid, caesium fluoride, tetrakis(triphenylphosphine)palladium(0), iodine monochloride, 4-pyridinylboronic acid, tricyclohexylphosphine, potassium phosphate, 3-pyridinylboronic acid, tetrakis(acetonitrile)palladium(II) tetrafluoroborate.

The following chemicals were synthesized according to known literature synthesis procedures: 4,15-diiodo[2.2]paracyclophane (*rac*)-**1**,¹ tris(dibenzylideneacetone)dipalladium(0)-chloroform,² [1,3-bis(diphenylphosphino)propane]palladium(II) triflate.^{3,4}

All solvents were obtained from commercial sources. Dry solvents were obtained from the solvent purification system *MS-SPS 800* from *MBraun*. Other reaction solvents and solvents for specific rotation value, UV-Vis or CD measurements were solvents of *p.a.* grade. For flash column chromatography freshly distilled solvents of technical grade and for high performance liquid chromatography solvents of HPLC grade were used.

Thin-layer chromatography was performed on silica gel-coated aluminium plates with fluorescent indicator F254 from *Merck*. Detection was done by UV-light (254 and 366 nm).

Products were purified by flash column chromatography on silica gel 60 (particle size 0.040-0.063 mm) from *Merck* or on reversed phase silica gel (C18-RP, 17% C, 0.048-0.065 mm) from *Acros Organics*.

¹H, ¹³C, ¹⁹F, ³¹P, H,H-COSY, HSQC, HMBC and ¹H-2D-DOSY NMR experiments were performed on a *Bruker Avance I 400* spectrometer, a *Bruker Avance I 500* spectrometer, a *Bruker Avance III HD 500* spectrometer with a *Prodigy* cryo probe or a *Bruker Avance III HD 700* spectrometer with a *cryo* probe. ¹H NMR chemical shifts are reported relative to residual non-deuterated solvent as internal standard. ¹³C NMR chemical shifts are reported relative to deuterated solvent as internal standard. ¹⁹F and ³¹P chemical shifts are reported relative to a mixture of trifluoroacetic acid-d₁ (¹⁹F: δ = -76.6 ppm) and phosphoric acid-d₃ (³¹P: δ = 0.0 ppm) in D₂O as external standard using a *Wilma*[®] coaxial insert from *Sigma Aldrich*. All shifts are reported on the δ scale in ppm and NMR multiplicities are abbreviated as s (singlet), d (doublet), t (triplet), dd (doublet of doublets), ddd (doublet of doublet of doublets) or m (multiplet). Coupling constants *J* are reported in Hertz. All spectra were processed using the *MestReNova 8.0.1* program from *Mestrelab*. ¹H-2D-DOSY NMR spectra were evaluated using the software *Topspin 3.5* from *Bruker* and the *Stokes-Einstein equation*, normally used for spherical particles, with a correction factor for ellipsoids (**equation 1**).⁵

$$D = \frac{k_B T}{6 \pi \eta f R_h}$$

Equation 1: *Stokes-Einstein equation*. *D* = diffusion constant, *k_B* = Boltzmann constant, *T* = temperature, *η* = viscosity of solvent, *f* = correction factor for ellipsoids, *R_h* = hydrodynamic radius.

(High-resolution) electrospray ionization mass spectra in positive mode (ESI(+)-MS) were measured on an *Orbitrap XL* mass spectrometer from *Thermo Fischer Scientific* or a *micrOTOF-Q* time-of-flight mass spectrometer from *Bruker Daltonics*. Electron ionization mass spectra (EI-MS) were measured on a *MAT 95 XL* or a *MAT 90* sector field mass spectrometer from *Thermo Finnigan*.

Elementary analyses were performed on a *Vario EL* elemental analyzer from *Heraeus*.

Melting points were determined with a *DigiMelt MPA 161* instrument from *Stanford Research Systems*.

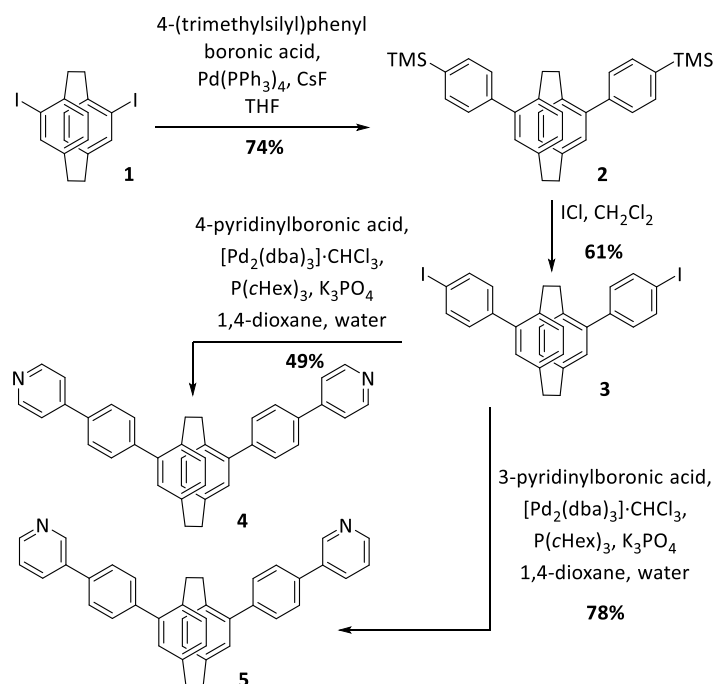
UV-Vis spectra were measured on a *Specord 200* instrument from *Analytik Jena* and analysed using the software *WinASPECT 1.7.2.0*. Quartz glass cuvettes from *Hellma Analytics* with a layer thickness of 10 mm (solutions of ligand precursors/ligands) and 0.01 mm (complex solutions) were used.

Circular dichroism spectra were measured on a *J-810* spectrometer from *Jasco*. Quartz glass cuvettes from *Hellma Analytics* with a layer thickness of 1 mm (solutions of ligand precursors/ligands) and 0.01 mm (complex solutions) were used.

Specific rotation values were measured on an *Anton Paar Model MCP 150* polarimeter with a standard wavelength of 589 nm using a cuvette with a layer thickness of 100 mm.

High performance liquid chromatography on analytical scale was performed on a *PLATINblue* HPLC system from *Knauer*, equipped with two pumps, an online degasser and a photodiode array detector *PDA-1* with a deuterium and tungsten-halogen lamp (190-1000 nm). For analytical HPLC resolution a *CHIRALPAK® IA* column (4.6 mm \varnothing , 250 mm) by *Daicel* or a *CHIRALPAK® IB* column (4.6 mm \varnothing , 250 mm) by *Daicel* was used. High performance liquid chromatography on semi-preparative scale was performed on an *Azura* HPLC system from *Knauer*, equipped with a binary HPG pump *P 6.1L*, an online degasser, a multi wavelength detector *MWL 2.1L* with deuterium lamp (190-700 nm) and a fraction collector. For semi-preparative HPLC resolution a *CHIRALPAK® IA* column (20mm \varnothing , 250 mm) by *Daicel* or a *CHIRALPAK® IB* column (20 mm \varnothing , 250 mm) by *Daicel* was used.

Synthesis route



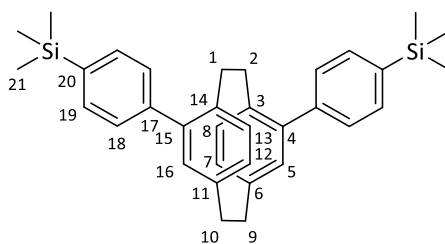
Scheme S1: Synthesis route to ligand **4** and **5**.

Synthesis and characterization of ligand precursors

4,15-Bis-(4-trimethylsilylphenyl)[2.2]paracyclophane **2**

Under an atmosphere of argon, (*rac*)-**1**¹ (900 mg, 1.96 mmol, 1.00 eq.), 4-(trimethylsilyl)phenylboronic acid (875 mg, 4.51 mmol, 2.30 eq.), caesium fluoride (1.79 mg, 11.8 mmol, 6.00 eq.), tetrakis(triphenylphosphine)palladium(0) (226 mg, 0.196 mmol, 10.0 mol%) were dissolved in dry tetrahydrofuran (75 mL). The reaction mixture was degassed at room temperature and then, heated to reflux for 48 h. After cooling to room temperature the solution was quenched by the addition of saturated aqueous ethylenediaminetetraacetic acid disodium salt solution and dichloromethane. The mixture was extracted with dichloromethane. The combined organic layers were washed with brine, dried with anhydrous magnesium sulphate and the solvent was removed under reduced pressure. The crude product was subjected to flash

column chromatography on silica gel (cyclohexane/dichloromethane 10:1) to give (*rac*)-**2** (733 mg, 1.45 mmol, 74%) as a white solid.



Chemical formula: $C_{34}H_{40}Si_2$

Exact mass: 504.2669 u

Molecular weight: 504.86 g/mol

1H NMR (500.1 MHz, $CDCl_3$, 298 K): δ [ppm] = 7.63-7.60 (m, 4H, H-19), 7.49-7.46 (m, 4H, H-18), 6.72 (d, 2H, H-5, H-16, $^4J_{5,7} = ^4J_{16,12} = 1.9$ Hz), 6.68 (d, 2H, H-8, H-13, $^3J_{8,7} = ^3J_{13,12} = 7.8$ Hz), 6.56 (dd, 2H, H-7, H-12, $^3J_{7,8} = ^3J_{12,13} = 7.8$ Hz, $^4J_{7,5} = ^4J_{12,16} = 1.9$ Hz), 3.26-3.07 (m, 6H, H-1, H-2, H-9, H-10), 2.64-2.55 (m, 2H, H-1, H-2), 0.33 (s, 18H, H-21).

^{13}C NMR (125.8 MHz, $CDCl_3$, 298 K): δ [ppm] = 142.7 (C-4, C-15), 141.7 (C-17), 139.6 (C-6, C-11), 138.8 (C-20), 137.6 (C-3, C-14), 133.7 (C-19), 132.5 (C-8, C-13), 132.0 (C-5, C-16), 131.5 (C-7, C-12), 129.1 (C-18), 35.3 (C-9, C-10), 33.5 (C-1, C-2), -0.84 (C-21).

MS (EI) *m/z* (intens. %): 504.3 (73) [**2**] $^+$, 489.3 (11) [**2**-CH $_3$] $^+$, 416.2 (33) [**2**-C $_4$ H $_{12}$ Si] $^+$, 356.3 (7) [**2**-C $_9$ H $_{12}$ Si] $^+$, 237.2 (58) [**2**-C $_{18}$ H $_{23}$ Si] $^+$, 73.1 (100) [C $_3$ H $_9$ Si] $^+$; HR-MS (EI) *m/z*: calculated for $C_{34}H_{40}Si_2$ [**2**] $^+$: 504.2669, found: 504.2672.

Elementary analysis: calculated for $C_{34}H_{40}Si_2$: C: 80.89, H: 7.99, found: C: 80.70, H: 7.98.

Melting point: 111 °C

R_f (cyclohexane/dichloromethane 5:1): 0.48

UV-Vis (CH_3CN , $c = 1.98 \mu M$): λ [nm] = 233, 285.

HPLC analytical (CHIRALPAK[®] IB, methanol/ethanol (90:10 v/v), 1 mL/min): (*R*_p)-**2** $t_R = 4.55$ min, (*S*_p)-**2** $t_R = 4.98$ min.

HPLC semi-preparative recycling mode (CHIRALPAK[®] IB, methanol/ethanol (90:10 v/v), 18 mL/min): (*R*_p)-**2** 99% ee, (*S*_p)-**2** 97% ee.

Specific rotation: (-)-(*R*_p)-**2**: $[\alpha]_D^{23} = -442^\circ$ ($c = 2.00$ mg/mL = 3.96 mM, CH_2Cl_2), (+)-(*S*_p)-**2**: $[\alpha]_D^{23} = +420^\circ$ ($c = 2.00$ mg/mL = 3.96 mM, CH_2Cl_2).

CD (CH_3CN , $c = 198 \mu M$): λ [nm] ($\Delta\epsilon$ [L/(mol cm)]) = (*R*_p)-**2**: 214 (-76), 228 (+36), 292 (-88), 237 (+11), 251 (-91); (*S*_p)-**2**: 214 (+84), 228 (-36), 237 (+13), 251 (-100), 292 (+98).

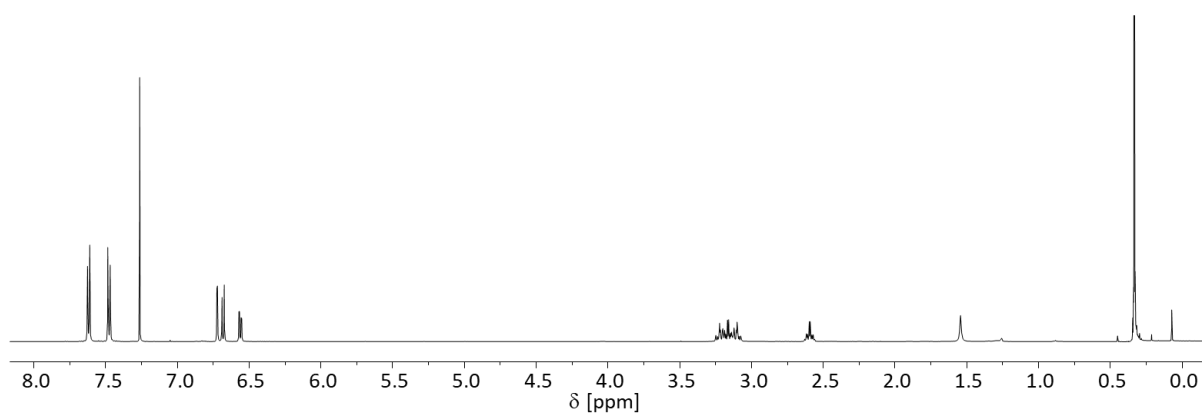


Figure S1: ^1H NMR spectrum (500.1 MHz, CDCl_3 , 298 K) of **2**.

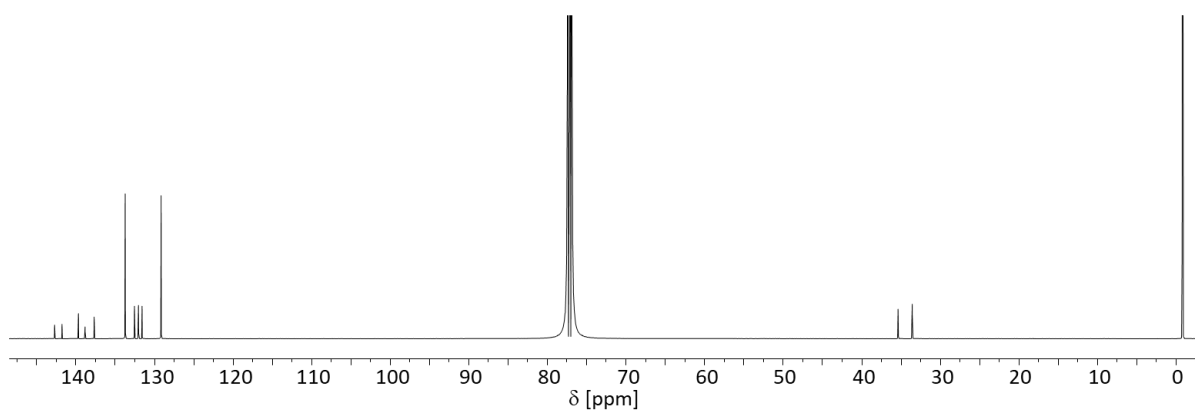


Figure S2: ^{13}C NMR spectrum (125.8 MHz, CDCl_3 , 298 K) of **2**.

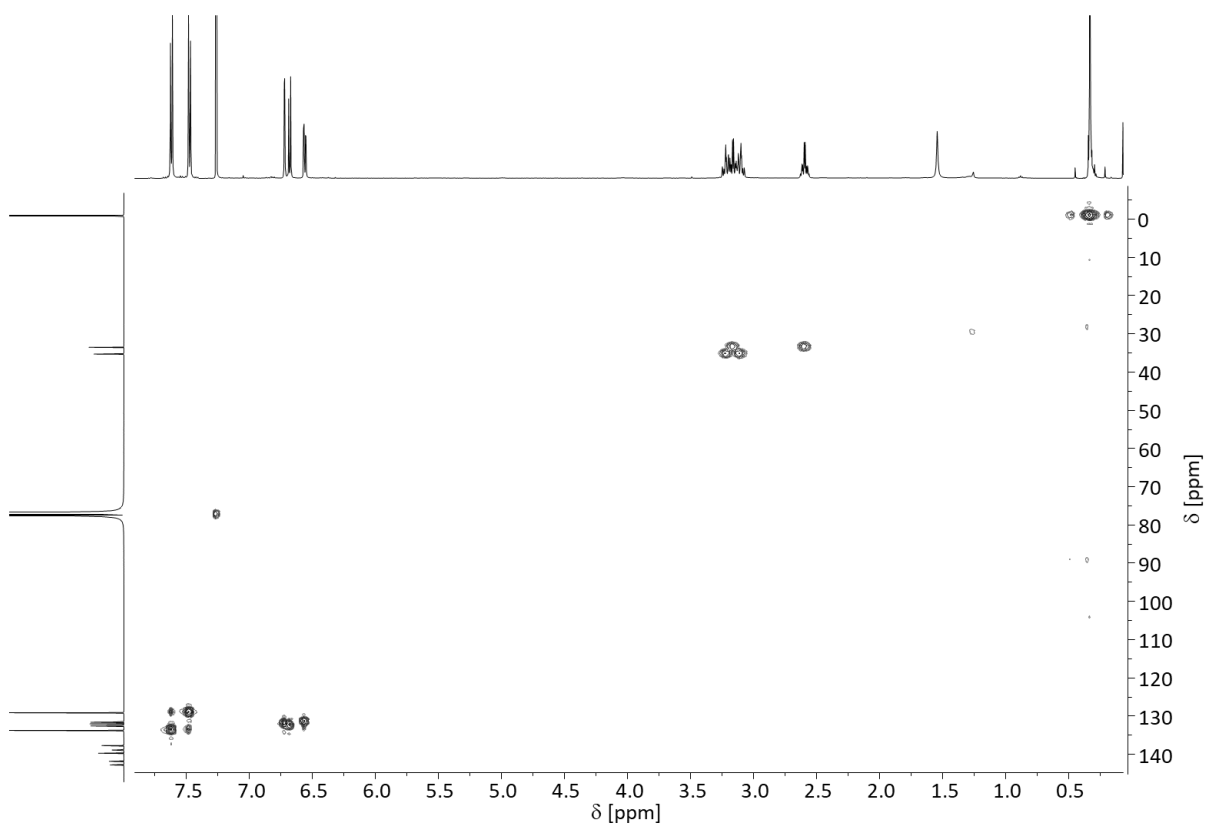


Figure S3: ^1H , ^{13}C -HSQC NMR spectrum (500.1 MHz, 125.8 MHz, CDCl_3 , 298 K) of **2**.

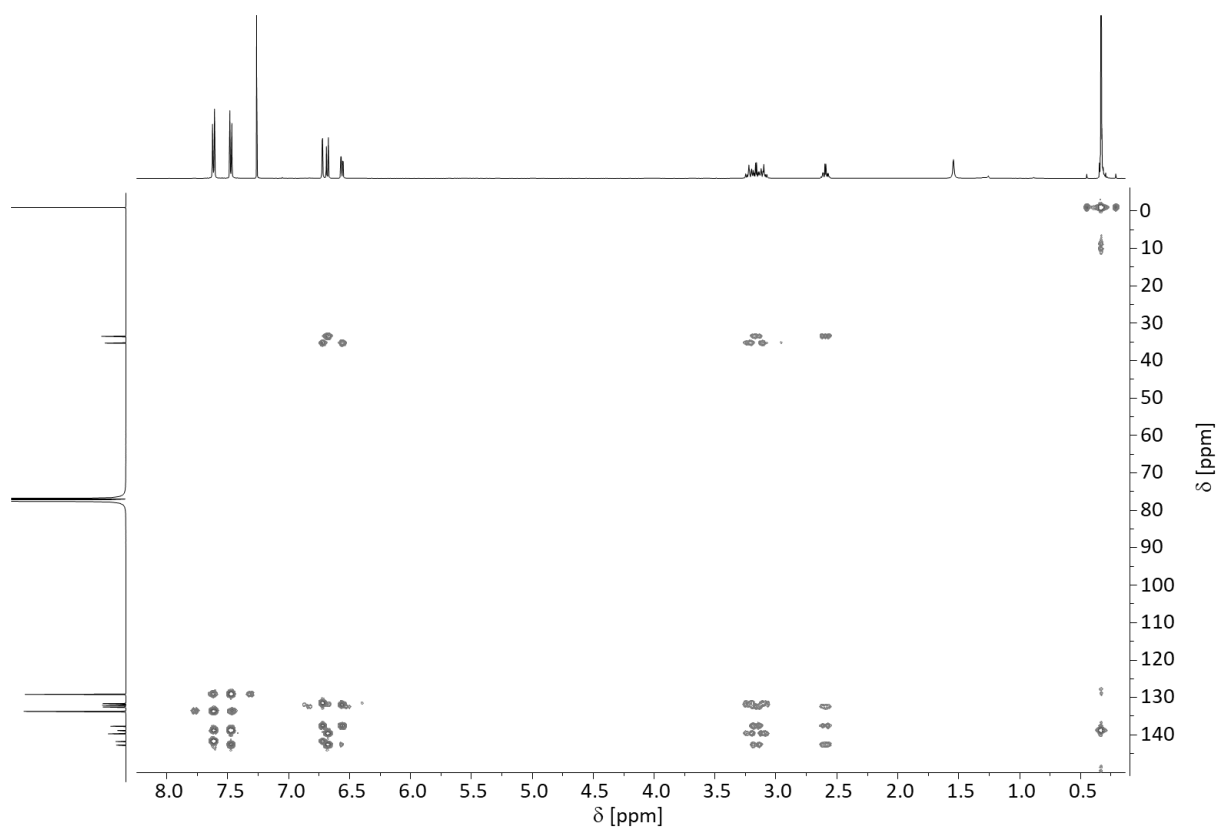


Figure S4: ^1H , ^{13}C -HMBC NMR spectrum (500.1 MHz, 125.8 MHz, CDCl_3 , 298 K) of **2**.

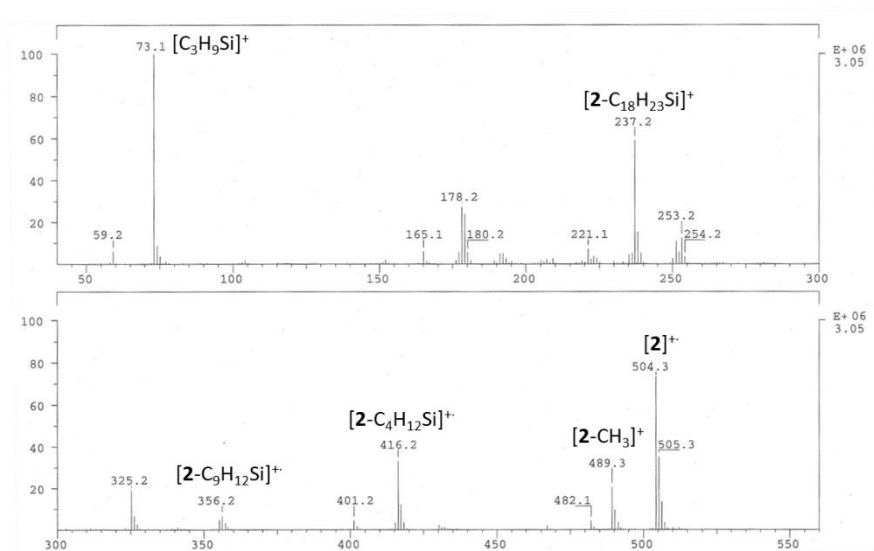


Figure S5: EI mass spectrum of **2**.

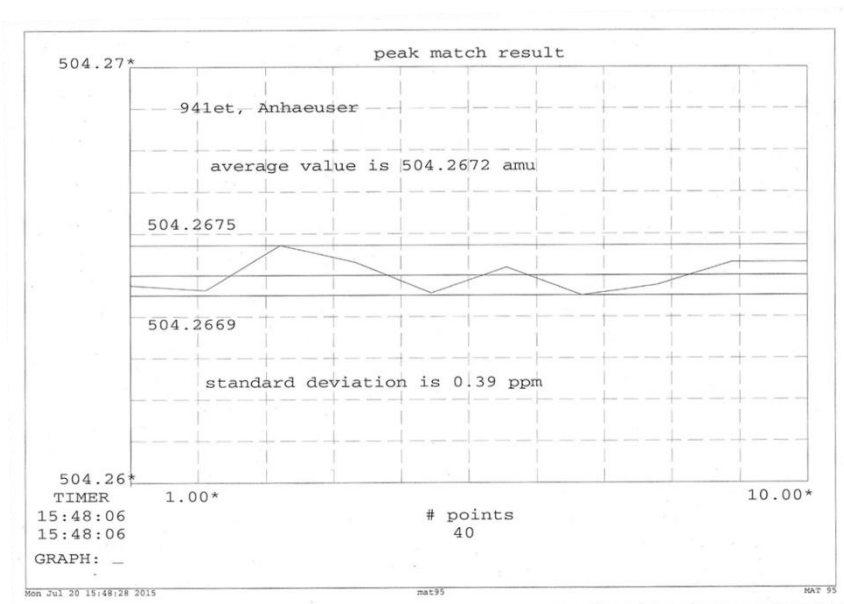


Figure S6: High resolution accurate mass determinations for **2**.

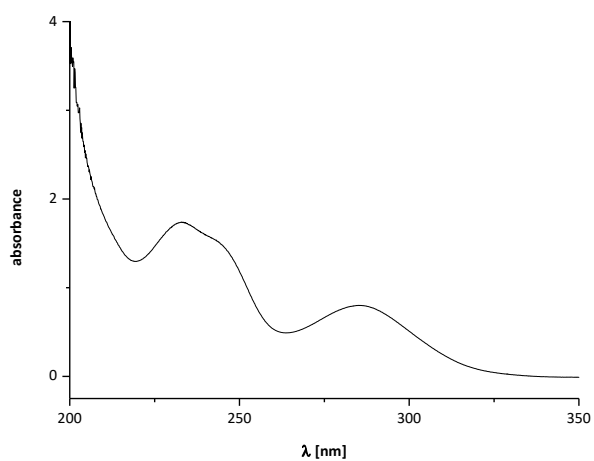


Figure S7: Non-normalized UV-Vis spectrum of **2** ($c = 1.98 \mu\text{M}$, CH_3CN).

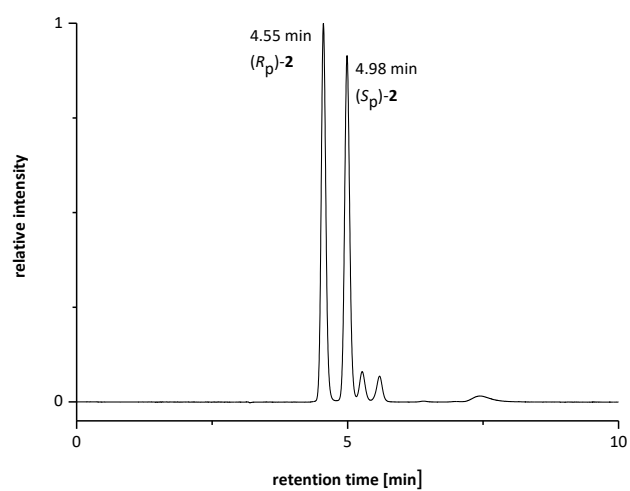


Figure S8: Chromatogram of chiral resolution of **2** via analytical HPLC (chiral stationary phase: *CHIRALPAK*[®] IB column, eluent: methanol/ethanol (90:10 v/v), flow rate: 1 mL/min). When upscaling to semi-preparative mode, the flow rate was increased to 18 mL/min.

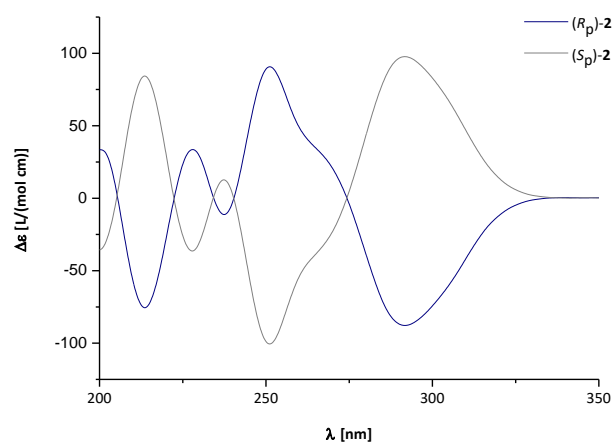
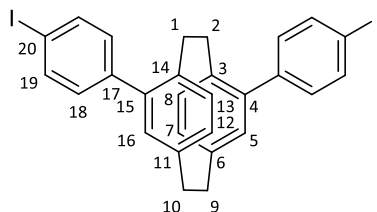


Figure S9: CD spectra of **2** ($c = 198 \mu\text{M}$, CH_3CN).

4,15-Bis-(4-iodophenyl)[2.2]paracyclophane **3**

Under an atmosphere of argon, (*rac*)-/(*R_p*)-/(*S_p*)-**2** (350 mg, 0.693 mmol, 1.00 eq.) was dissolved in dry dichloromethane (5 mL) and cooled to 0 °C. At 0 °C iodine monochloride solution (1.40 mL, 1 M in dichloromethane, 1.40 mmol, 2.00 eq.) was added slowly over 45 min and the red reaction mixture was stirred at 0 °C for further 45 min. Then, it was warmed up to room temperature and stirred for another hour. Subsequently, saturated aqueous sodium sulphite solution was added and the mixture was stirred until discolouration. The phases were separated and the aqueous phase was extracted with dichloromethane. The combined organic layers were washed with brine, dried with anhydrous magnesium sulphate and the solvent was removed under reduced pressure. The crude product was subjected to flash column chromatography on silica gel (cyclohexane/dichloromethane 20:1) to give (*rac*)-/(*R_p*)-/(*S_p*)-**3** (260 mg, 0.425 mmol, 61%) as a white solid.



Chemical formula: C₂₈H₂₂I₂

Exact mass: 611.9811

Molecular weight: 612.29 g/mol

¹H NMR (500.1 MHz, CDCl₃, 298 K): δ [ppm] = 7.82-7.78 (m, 4H, H-19), 7.24-7.21 (m, 4H, H-18), 6.65 (d, 2H, H-5, H-16, ⁴J_{5,7} = ⁴J_{16,12} = 1.9 Hz), 6.64 (d, 2H, H-8, H-13, ³J_{8,7} = ³J_{13,12} = 7.8 Hz), 6.55 (dd, 2H, H-7, H-12, ³J_{7,8} = ³J_{12,13} = 7.8 Hz, ⁴J_{7,5} = ⁴J_{12,16} = 1.9 Hz), 3.25-3.18 (m, 2H, H-9, H-10), 3.16-3.05 (m, 4H, H-1, H-2, H-9, H-10), 2.56-2.48 (m, 2H, H-1, H-2).

¹³C NMR (125.8 MHz, CDCl₃, 298 K): δ [ppm] = 141.5 (C-4, C-15), 140.7 (C-17), 140.0 (C-6, C-11), 137.9 (C-19), 137.3 (C-3, C-14), 132.4 (C-8, C-13), 131.8 (C-5, C-16), 131.6 (C-7, C-12), 131.6 (C-18), 93.0 (C-20), 35.2 (C-9, C-10), 33.5 (C-1, C-2).

MS (EI) *m/z* (intens. %): 611.8 (47) [**3**]⁺, 485.0 (58) [**3**-I]⁺, 304.9 (45) [**3**-C₁₄H₁₂I]⁺, 179.0 (100) [**3**-C₁₄H₁₁I₂]⁺; HR-MS (EI) *m/z*: calculated for C₂₈H₂₂I₂ [**3**]⁺: 611.9811, found: 611.9816.

Elementary analysis: calculated for C₂₈H₂₂I₂ · $\frac{1}{3}$ C₆H₆: C: 56.45, H: 3.79, found: C: 56.37, H: 4.18.

Melting point: 229 °C

R_f (cyclohexane/dichloromethane 5:1): 0.47

UV-Vis (CH₃CN, c = 16.3 μM): λ [nm] = 245, 288.

Specific rotation: (-)-(*R_p*)-**3**: [α]_D²³ = -354° (c = 2.00 mg/mL = 4.90 mM, CH₂Cl₂), (+)-(*S_p*)-**3**: [α]_D²³ = +370° (c = 2.00 mg/mL = 4.90 mM, CH₂Cl₂).

CD (CH₃CN, c = 163 μM): λ [nm] (Δε [L/(mol cm)]) = (*R_p*)-**3**: 217 (-78), 231 (+36), 242 (-40), 255 (+80), 297 (-97); (*S_p*)-**3**: 217 (+61), 231 (-28), 242 (+32), 255 (-61), 296 (+77).

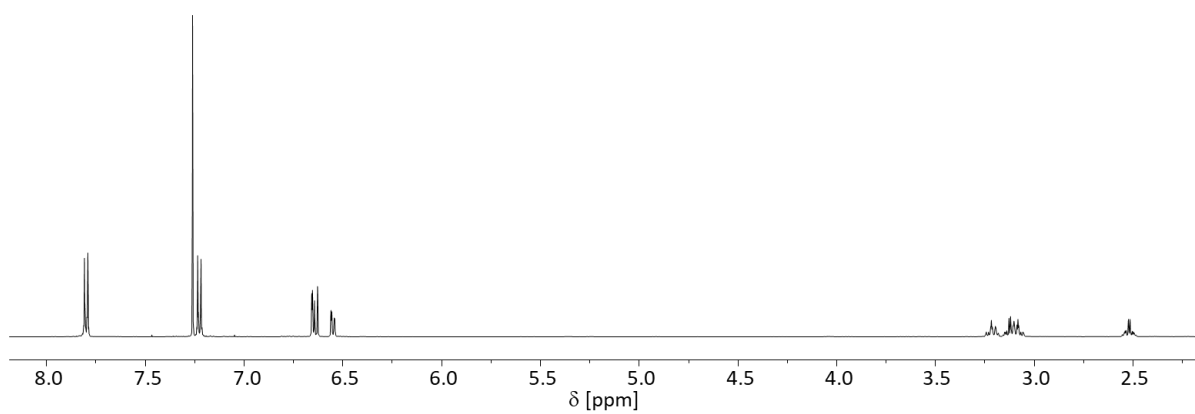


Figure S10: ^1H NMR spectrum (500.1 MHz, CDCl_3 , 298 K) of **3**.

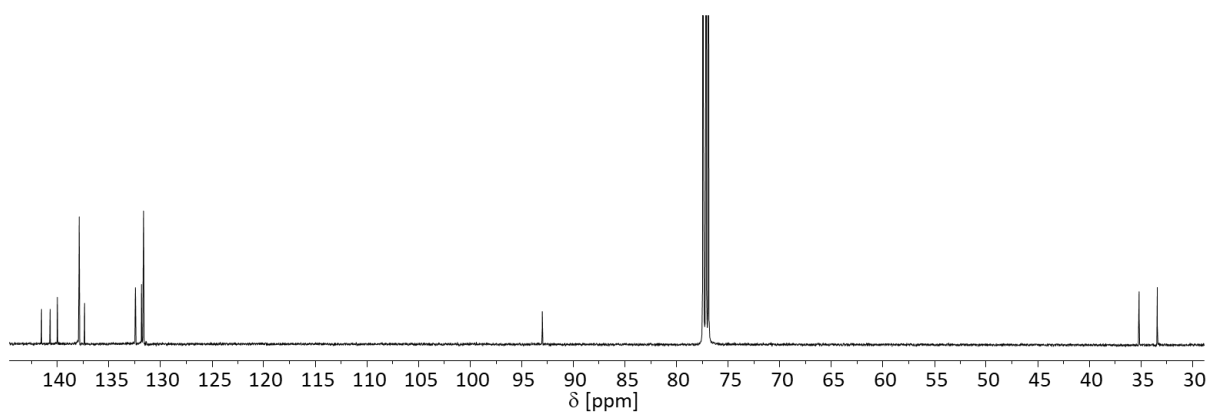


Figure S11: ^{13}C NMR spectrum (125.8 MHz, CDCl_3 , 298 K) of **3**.

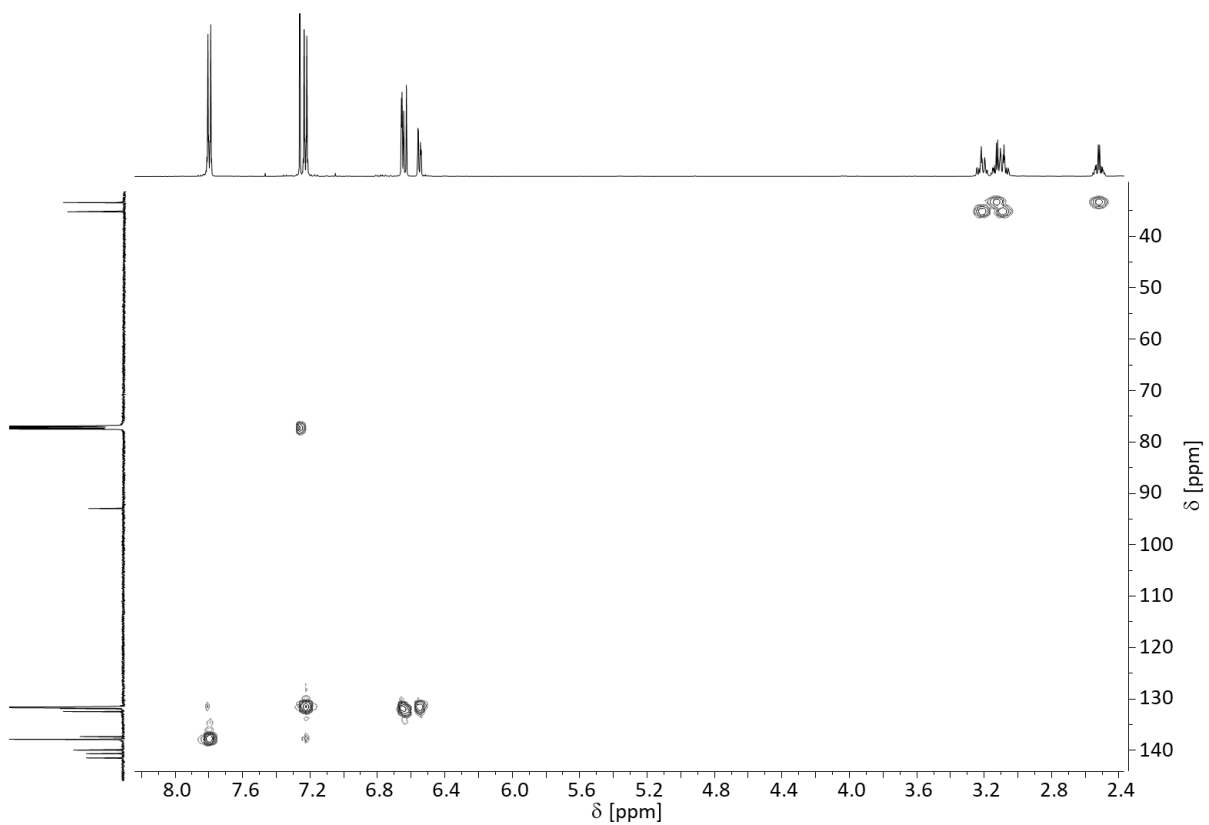


Figure S12: ^1H , ^{13}C -HSQC NMR spectrum (500.1 MHz, 125.8 MHz, CDCl_3 , 298 K) of **3**.

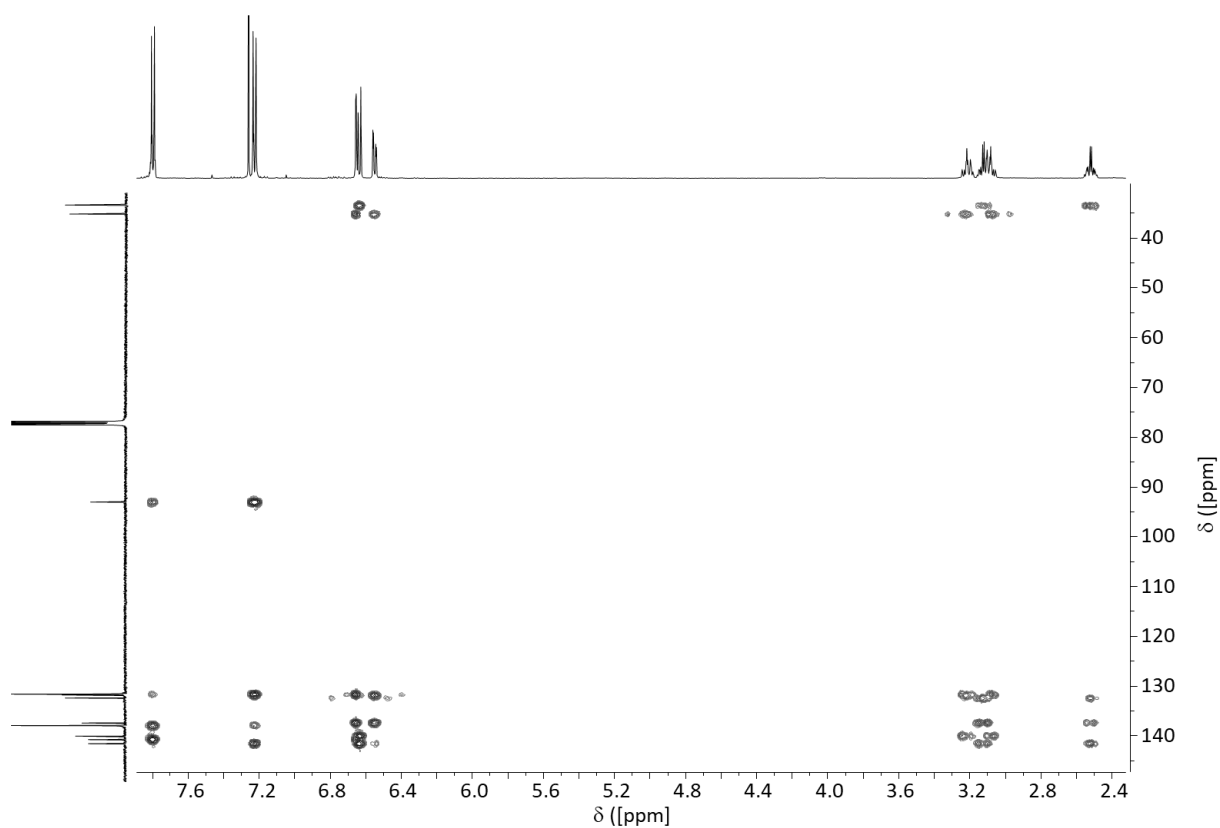


Figure S13: ^1H , ^{13}C -HMBC NMR spectrum (500.1 MHz, 125.8 MHz, CDCl_3 , 298 K) of **3**.

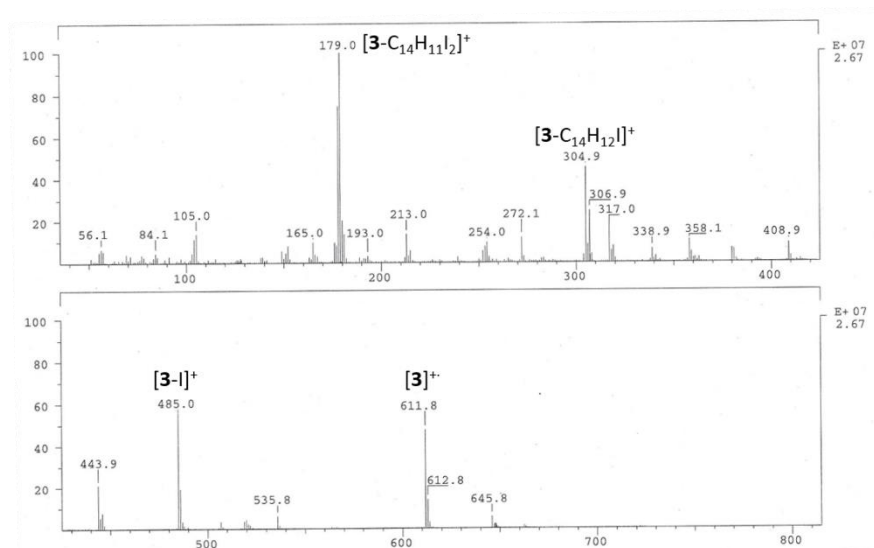


Figure S14: EI mass spectrum of **3**.

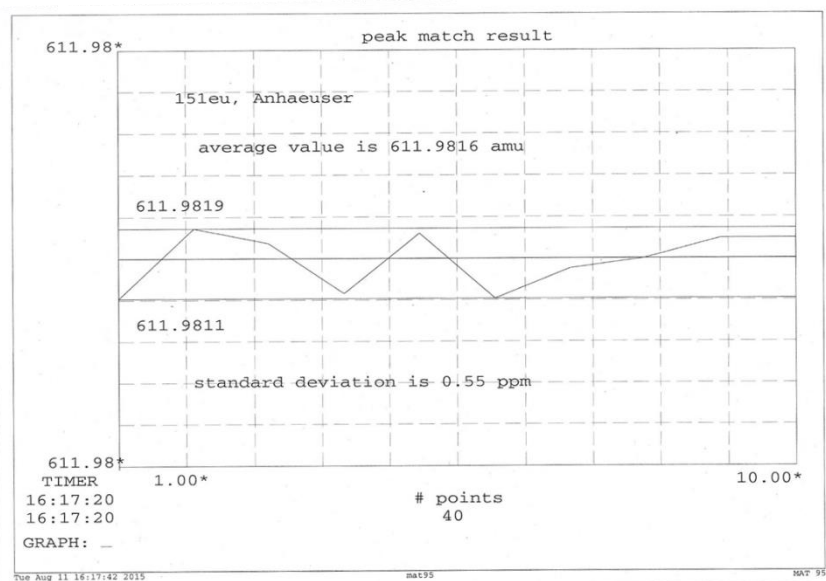


Figure S15: High resolution accurate mass determinations for **3**.

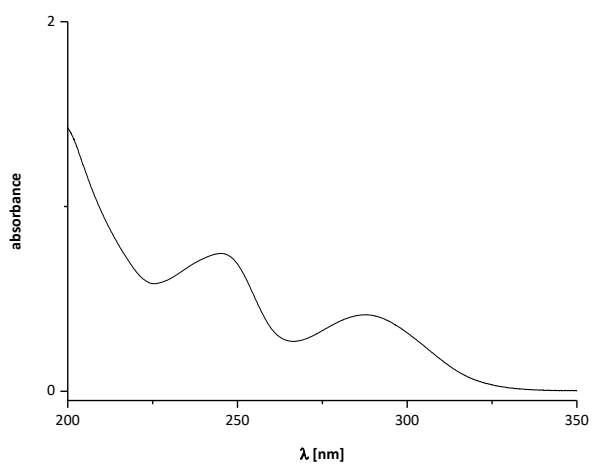


Figure S16: Non-normalized UV-Vis spectrum of **3** ($c = 16.3 \mu\text{M}$, CH_3CN).

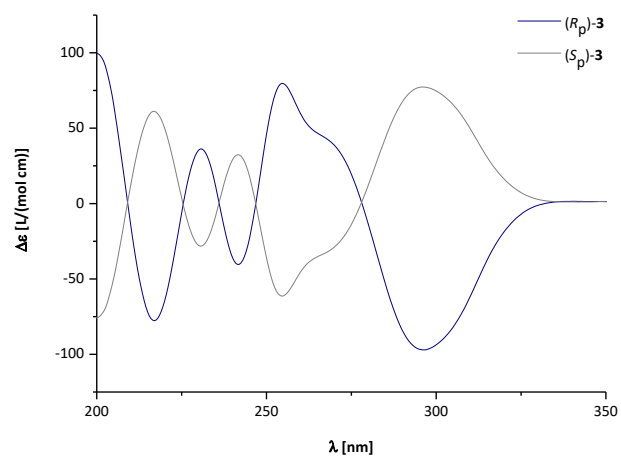
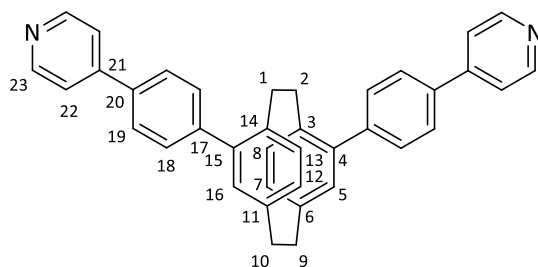


Figure S17: CD spectra of **3** ($c = 163 \mu\text{M}$, CH_3CN).

Synthesis and characterization of ligands

4,15-Bis-(4-(pyridin-4-yl)phenyl)[2.2]paracyclophane **4**

Under an atmosphere of argon, (*rac*)-**3** (200 mg, 0.327 mmol, 1.00 eq.), 4-pyridinylboronic acid (92.4 mg, 0.752 mmol, 2.30 eq.), tris(dibenzylideneacetone)dipalladium(0)-chloroform (33.8 mg, 0.0327 mmol, 10.0 mol%), tricyclohexylphosphine (22.9 mg, 0.0818 mmol, 25.0 mol%) und potassium phosphate (208 mg, 1.96 mmol, 6.00 eq.) were dissolved in 1,4-dioxane (7.2 mL) and water (2.1 mL). The reaction mixture was degassed at room temperature and then, heated to reflux for 48 h. After cooling to room temperature the solution was quenched by the addition of saturated aqueous ethylenediaminetetraacetic acid disodium salt solution and dichloromethane. The mixture was extracted with dichloromethane. The combined organic layers were washed with brine, dried with anhydrous magnesium sulphate and the solvent was removed under reduced pressure. The crude product was subjected to flash column chromatography on silica gel (cyclohexane/ethyl acetate 1:1 + 0.5% triethylamine) and reversed-phase silica gel (chloroform/methanol 1:1) to give (*rac*)-**4** (82.9 mg, 0.161 mmol, 49%) as a white solid.



Chemical formula: C₃₈H₃₀N₂

Exact mass: 514.2409 u

Molecular weight: 514.67 g/mol

¹H NMR (500.1 MHz, CD₂Cl₂, 298 K): δ [ppm] = 8.70-8.66 (m, 4H, H-23), 7.82-7.80 (m, 4H, H-19), 7.66-7.64 (m, 4H, H-18) 7.63-7.61 (m, 4H, H-22), 6.79 (d, 2H, H-5, H-16, ⁴J_{5,7} = ⁴J_{16,12} = 1.9 Hz), 6.75 (d, 2H, H-8, H-13, ³J_{8,7} = ³J_{13,12} = 7.8 Hz), 6.66 (dd, 2H, H-7, H-12, ³J_{7,8} = ³J_{12,13} = 7.8 Hz, ⁴J_{7,5} = ⁴J_{12,16} = 1.9 Hz), 3.31-3.20 (m, 4H, H-1, H-2, H-9, H-10), 3.18-3.10 (m, 2H, H-9, H-10), 2.61-2.53 (m, 2H, H-1, H-2).

¹³C NMR (125.8 MHz, CD₂Cl₂, 298 K): δ [ppm] = 150.9 (C-23), 148.3 (C-21), 142.6 (C-17), 142.2 (C-4, C-15), 140.6 (C-6, C-11), 138.1 (C-3, C-14), 137.1 (C-20), 133.0 (C-8, C-13), 132.4 (C-5, C-16), 132.1 (C-7, C-12), 130.9 (C-18), 127.7 (C-19), 122.0 (C-22), 35.6 (C-9, C-10), 34.0 (C-1, C-2).

¹H NMR (700.4 MHz, CD₂Cl₂:CD₃CN 1:1, 298 K): δ [ppm] = 8.62-8.59 (m, 4H, H-23), 7.79-7.77 (m, 4H, H-19), 7.62-7.58 (m, 8H, H-18, H-22), 6.74 (d, 2H, H-5, H-16, ⁴J_{5,7} = ⁴J_{16,12} = 1.8 Hz), 6.68 (d, 2H, H-8, H-13, ³J_{8,7} = ³J_{13,12} = 7.8 Hz), 6.63 (dd, 2H, H-7, H-12, ³J_{7,8} = ³J_{12,13} = 7.8 Hz, ⁴J_{7,5} = ⁴J_{12,16} = 1.8 Hz), 3.23-3.15 (m, 4H, H-1, H-2, H-9, H-10), 3.11-3.05 (m, 2H, H-9, H-10), 2.51-2.45 (m, 2H, H-1, H-2).

¹³C NMR (176.1 MHz, CD₂Cl₂:CD₃CN 1:1, 298 K): δ [ppm] = 150.6 (C-23), 147.7 (C-21), 142.2 (C-17), 141.8 (C-4, C-15), 140.3 (C-6, C-11), 137.6 (C-3, C-14), 136.6 (C-20), 132.6 (C-8, C-13), 132.0 (C-5, C-16), 131.8 (C-7, C-12), 130.6 (C-18), 127.4 (C-19), 121.5 (C-22), 35.0 (C-9, C-10), 33.6 (C-1, C-2).

¹H NMR (700.4 MHz, CD₃CN, 298 K): δ [ppm] = 8.68-8.66 (m, 4H, H-23), 7.90-7.87 (m, 4H, H-19), 7.73-7.71 (m, 4H, H-22), 7.70-7.68 (m, 4H, H-18), 6.84 (d, 2H, H-5, H-16, ⁴J_{5,7} = ⁴J_{16,12} = 1.7 Hz), 6.75 (dd, 2H, H-7, H-12, ³J_{7,8} = ³J_{12,13} = 7.8 Hz, ⁴J_{7,5} = ⁴J_{12,16} = 1.7 Hz), 6.73 (d, 2H, H-8, H-13, ³J_{8,7} = ³J_{13,12} = 7.8 Hz), 3.29-3.20 (m, 4H, H-1, H-2, H-9, H-10), 3.16-3.11 (m, 2H, H-9, H-10), 2.53-2.47 (m, 2H, H-1, H-2).

¹³C NMR (176.1 MHz, CD₃CN, 298 K): δ [ppm] = 151.3 (C-23), 148.3 (C-21), 143.0 (C-17), 142.5 (C-4, C-15), 141.3 (C-6, C-11), 138.2 (C-3, C-14), 137.2 (C-20), 133.4 (C-8, C-13), 132.8 (C-5, C-16), 132.7 (C-7, C-12), 131.4 (C-18), 128.2 (C-19), 122.3 (C-22), 35.5 (C-9, C-10), 34.3 (C-1, C-2).

MS (ESI+) *m/z*: 515.2475 [**4**+H]⁺, 258.1273 [**4**+2H]²⁺; HR-MS (ESI+) *m/z*: calculated for C₃₈H₃₁N₂ [**4**+H]⁺: 515.2482, found: 515.2475.

Elementary analysis: calculated for $C_{38}H_{30}N_2 \cdot \frac{1}{6} CH_2Cl_2$: C: 86.69, H: 5.78, N: 5.30, found: C: 86.83, H: 6.00, N: 5.21.

Melting point: 240 °C (decomposition)

R_f (cyclohexane/ethyl acetate 1:1 + 0.5% triethylamine): 0.12

UV-Vis (CH_3CN , $c = 19.4 \mu M$): λ [nm] = 261, 302.

HPLC analytical (*CHIRALPAK*[®] IA, dichloromethane/ethanol (95:5 v/v), 1 mL/min): (S_p)-**4** $t_R = 3.69$ min, (R_p)-**4** $t_R = 5.65$ min.

HPLC semi-preparative (*CHIRALPAK*[®] IA, dichloromethane/ethanol (95:5 v/v), 15 mL/min): (S_p)-**4** > 99% ee, (R_p)-**4** 98% ee.

Specific rotation: (-)-(S_p)-**4**: $[\alpha]_D^{20} = -656^\circ$ ($c = 2.00$ mg/mL = 3.89 mM, CH_2Cl_2), (+)-(R_p)-**4**: $[\alpha]_D^{20} = +619^\circ$ ($c = 2.00$ mg/mL = 3.89 mM, CH_2Cl_2).

CD (CH_3CN , $c = 194 \mu M$): λ [nm] ($\Delta\epsilon$ [L/(mol cm)]) = (R_p)-**4**: 212 (-9), 236 (+31), 247 (+11), 266 (+38), 313 (-87); (S_p)-**4**: 211 (+5), 236 (-27), 247 (-9), 266 (-34), 313 (+83).

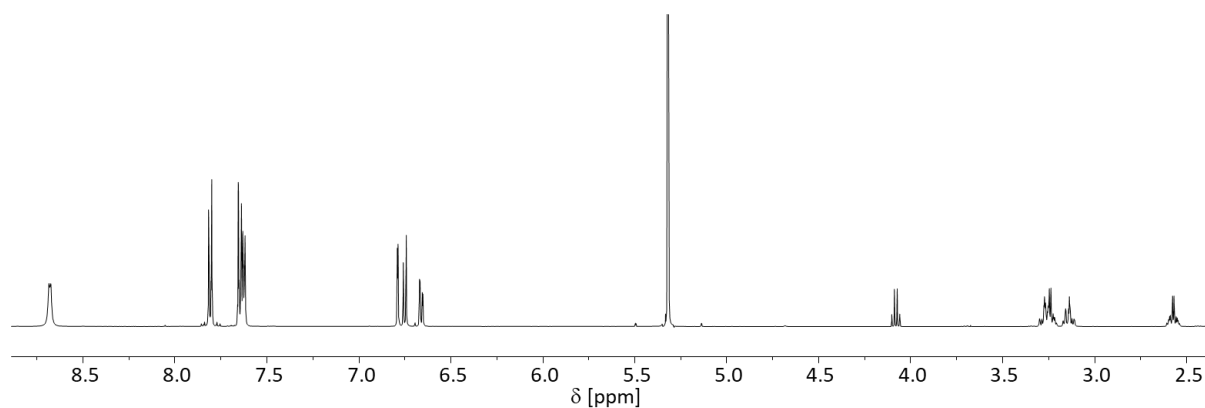


Figure S18: 1H NMR spectrum (500.1 MHz, CD_2Cl_2 , 298 K) of **4**.

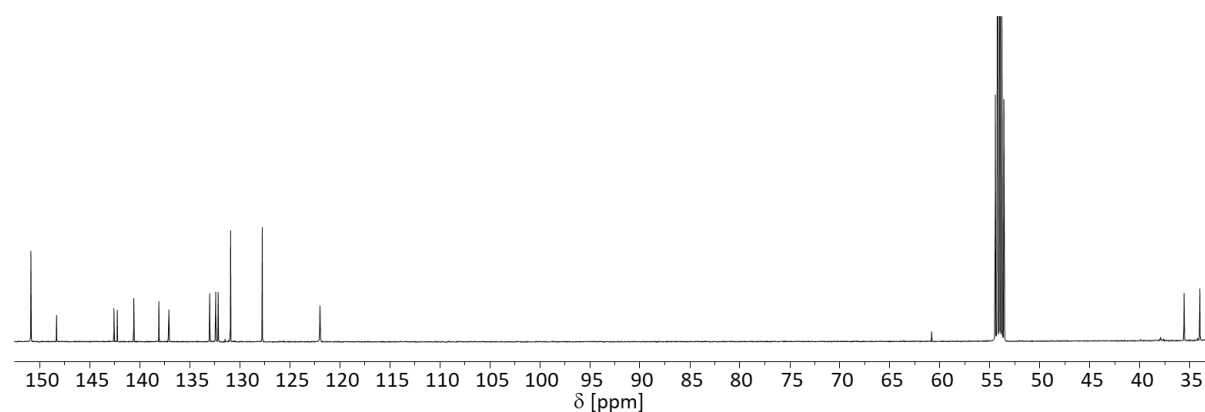


Figure S19: ^{13}C NMR spectrum (125.8 MHz, CD_2Cl_2 , 298 K) of **4**.

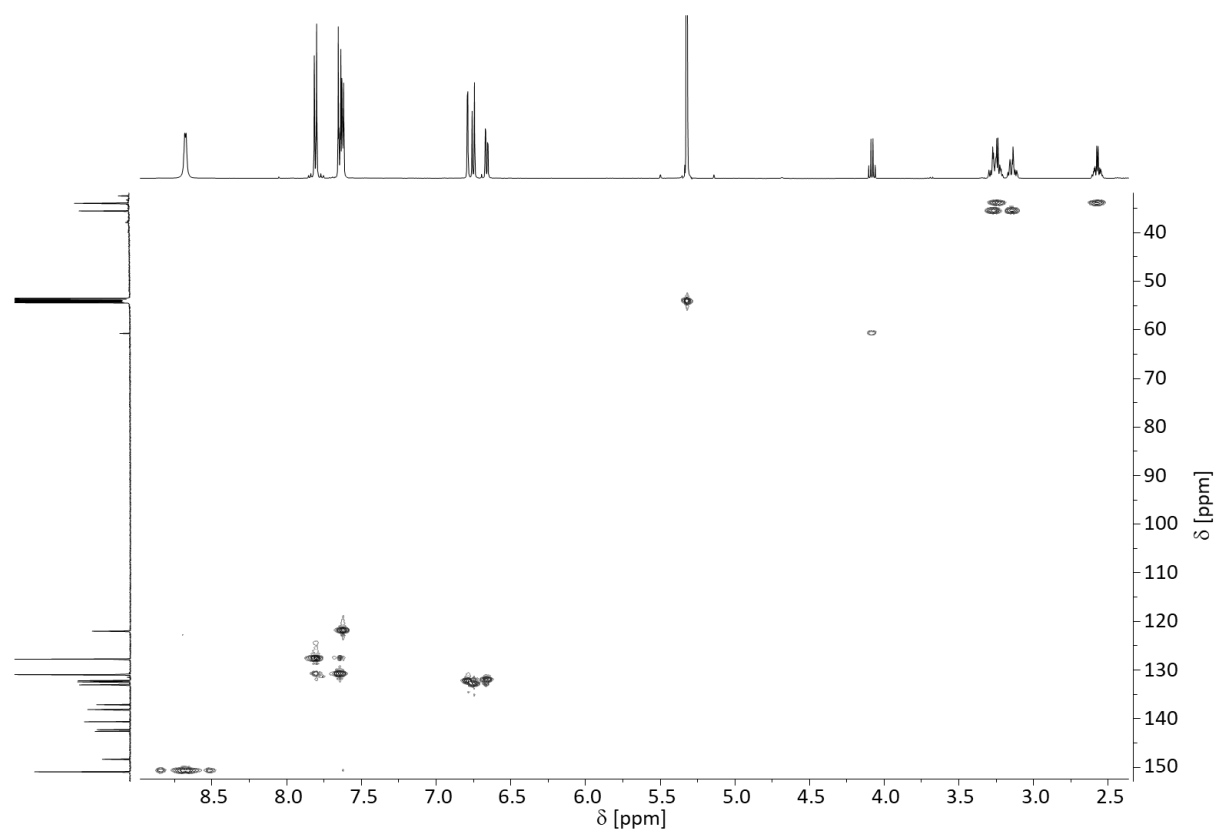


Figure S20: ^1H , ^{13}C -HSQC NMR spectrum (500.1 MHz, 125.8 MHz, CD_2Cl_2 , 298 K) of **4**.

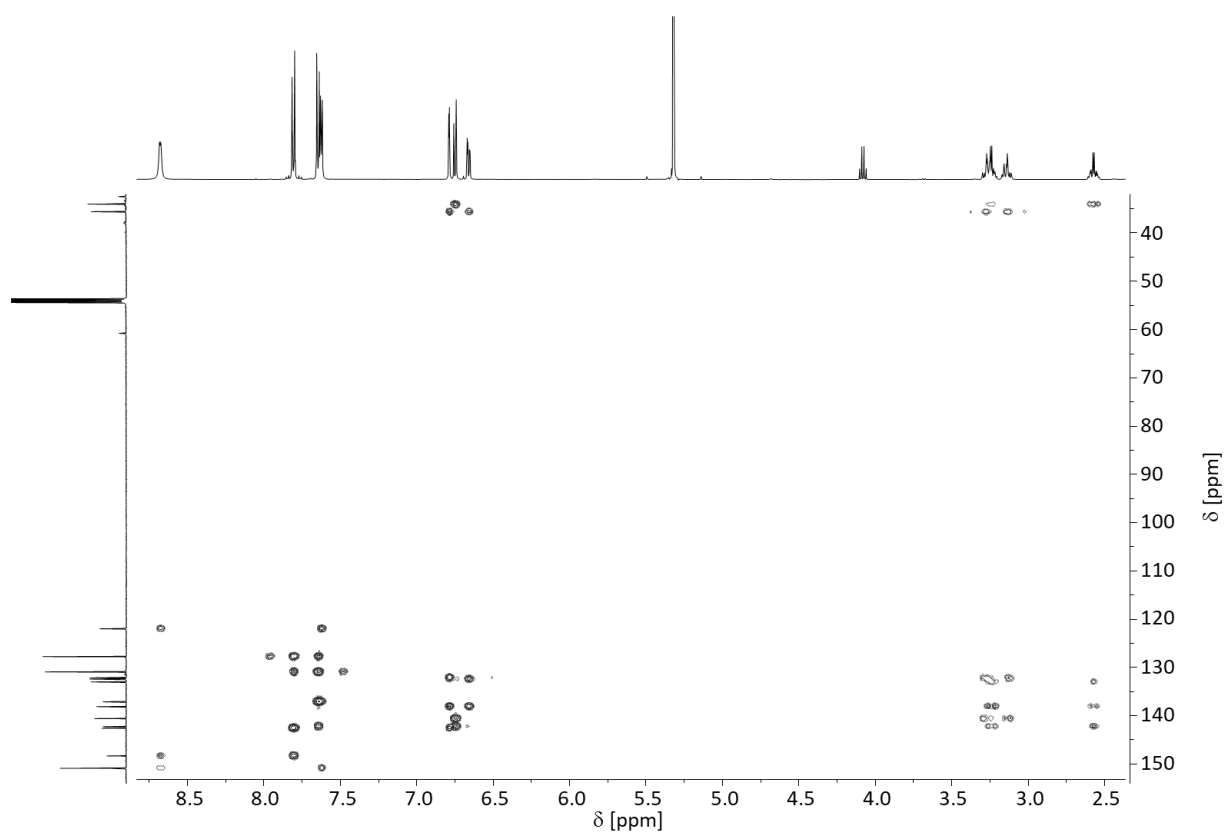


Figure S21: ^1H , ^{13}C -HMBC NMR spectrum (500.1 MHz, 125.8 MHz, CD_2Cl_2 , 298 K) of **4**.

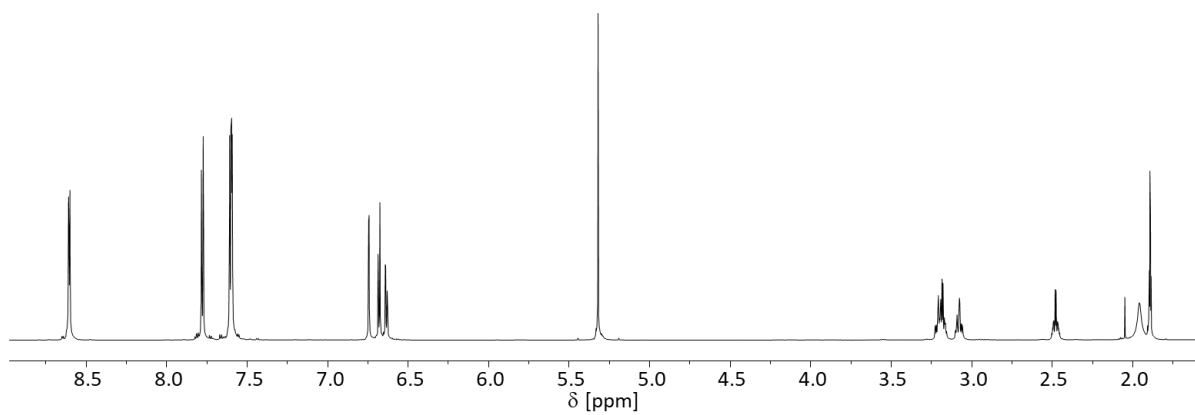


Figure S22: ^1H NMR spectrum (700.4 MHz, $\text{CD}_2\text{Cl}_2:\text{CH}_3\text{CN}$ 1:1, 298 K) of **4**.

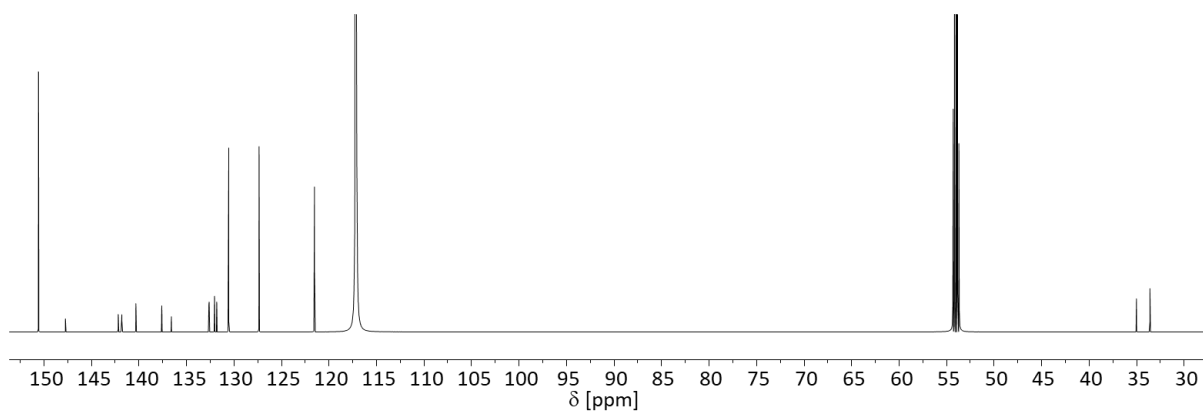


Figure S23: ^{13}C NMR spectrum (176.1 MHz, $\text{CD}_2\text{Cl}_2:\text{CD}_3\text{CN}$ 1:1, 298 K) of **4**.

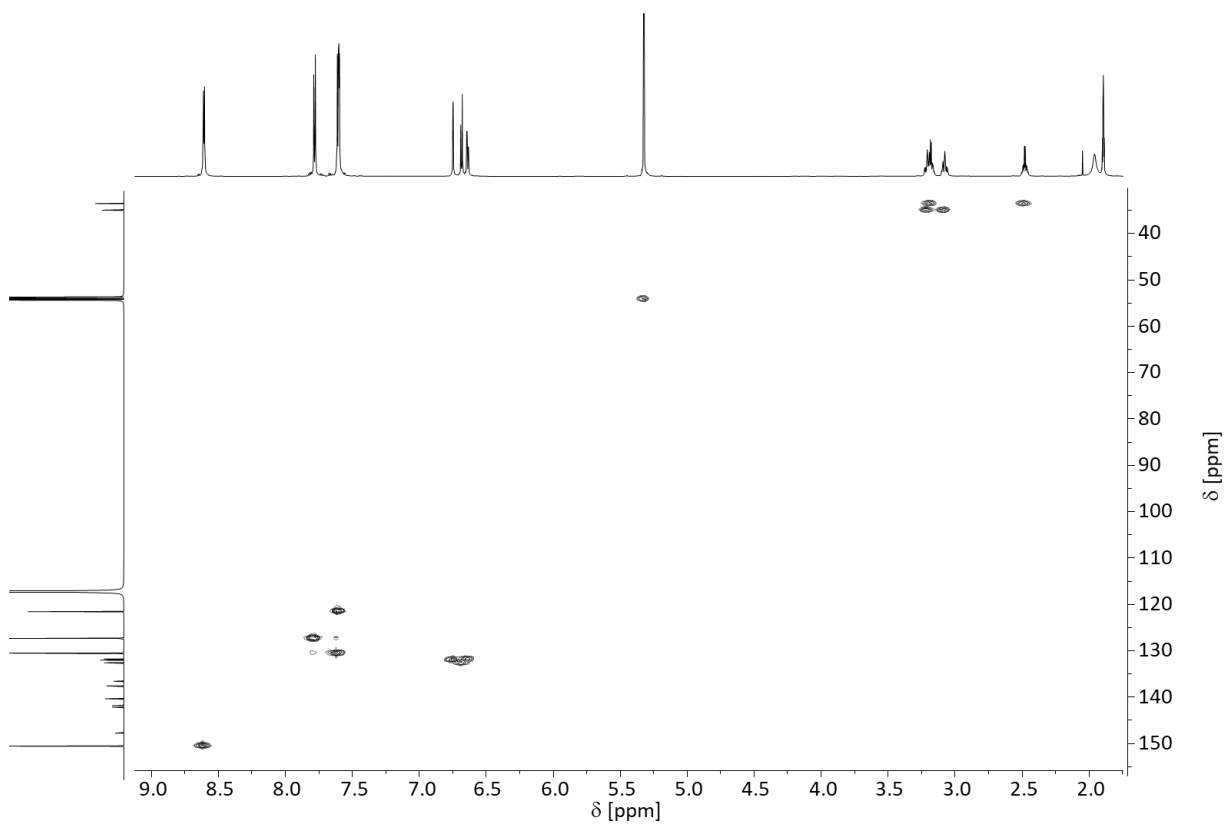


Figure S24: ^1H , ^{13}C -HSQC NMR spectrum (700.4 MHz, 176.1, $\text{CD}_2\text{Cl}_2:\text{CH}_3\text{CN}$ 1:1, 298 K) of **4**.

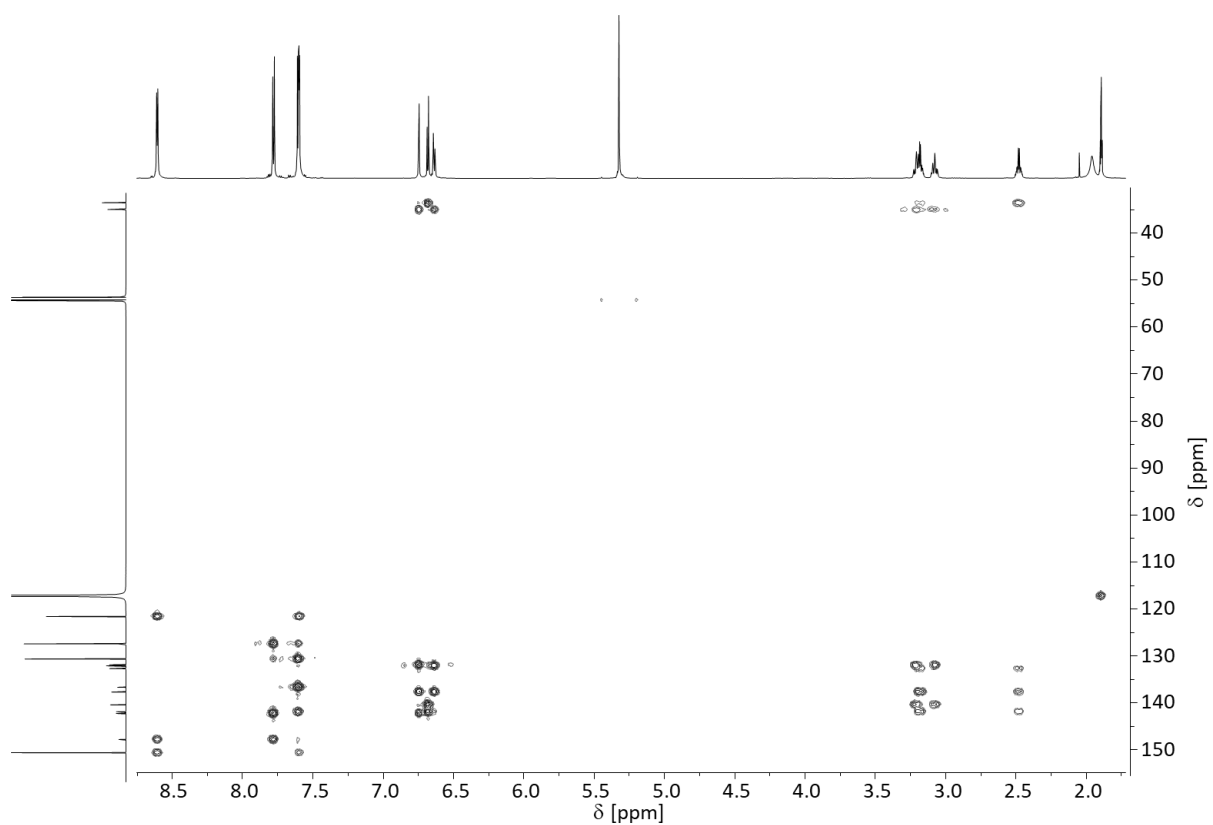


Figure S25: ^1H , ^{13}C -HMBC NMR spectrum (700.4, 176.1 MHz, $\text{CD}_2\text{Cl}_2:\text{CH}_3\text{CN}$ 1:1, 298 K) of **4**.

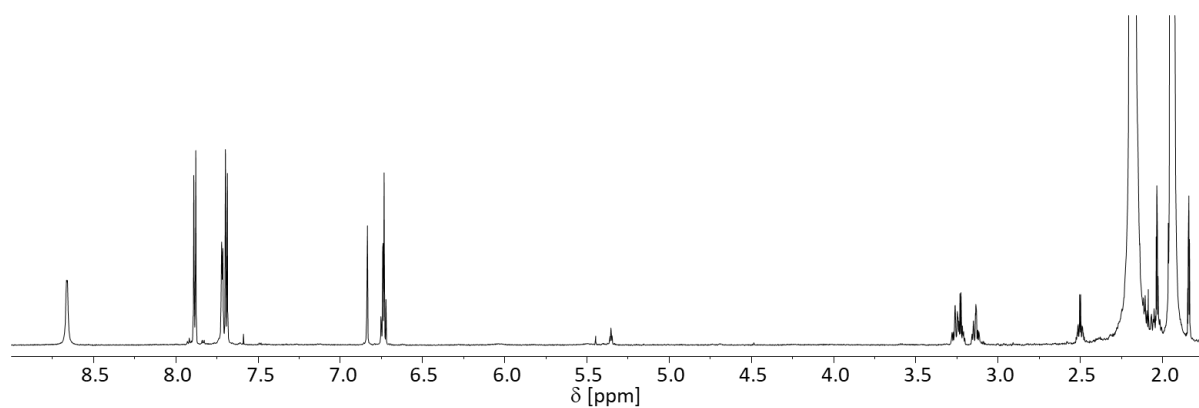


Figure S26: ^1H NMR spectrum (700.4 MHz, CH_3CN , 298 K) of **4**.

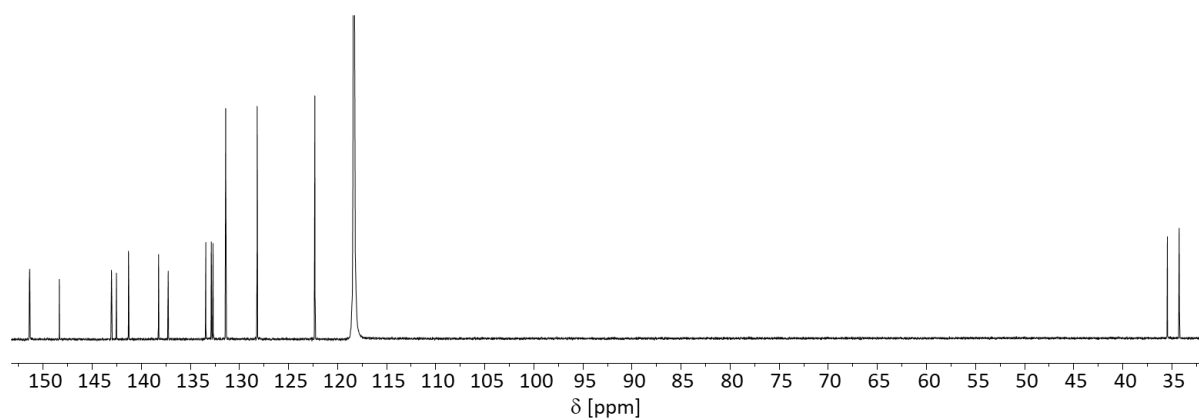


Figure S27: ^{13}C NMR spectrum (176.1 MHz, CD_3CN , 298 K) of **4**.

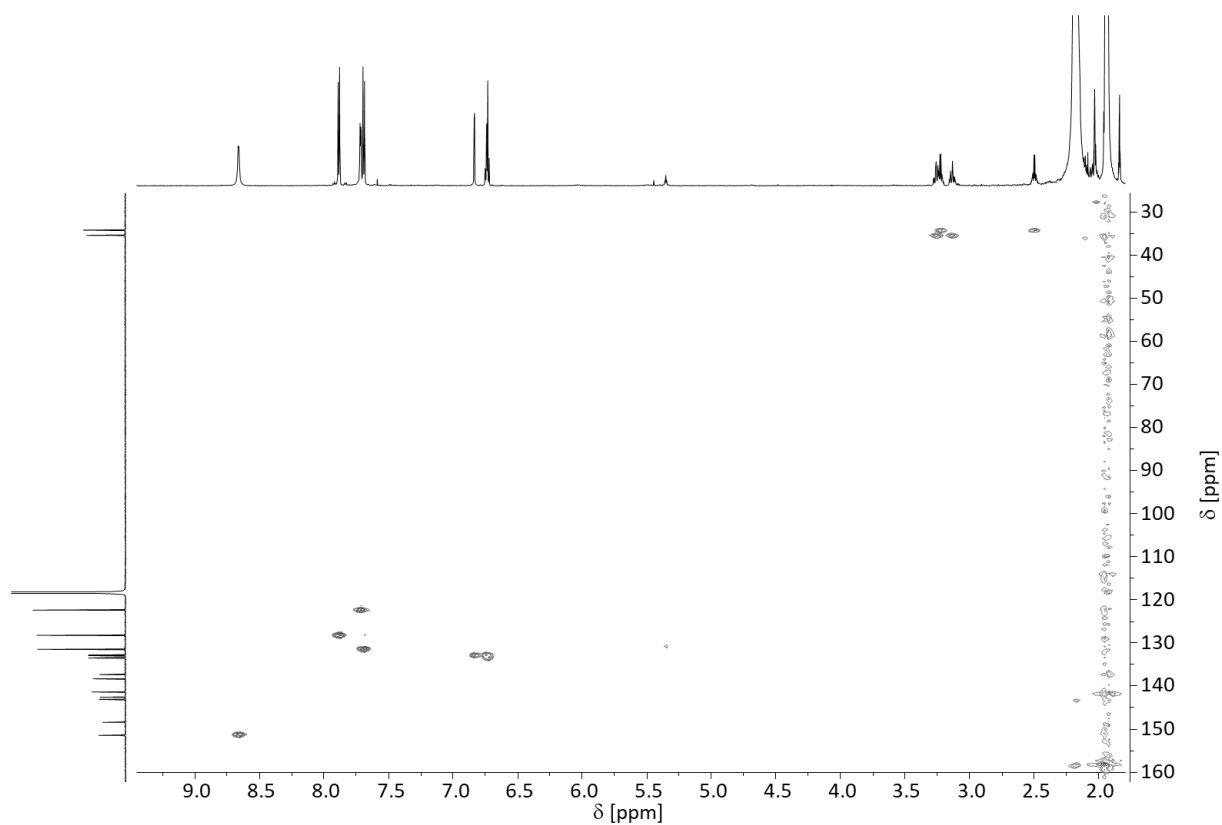


Figure S28: ^1H , ^{13}C -HSQC NMR spectrum (700.4 MHz, 176.1 MHz, CH_3CN , 298 K) of **4**.

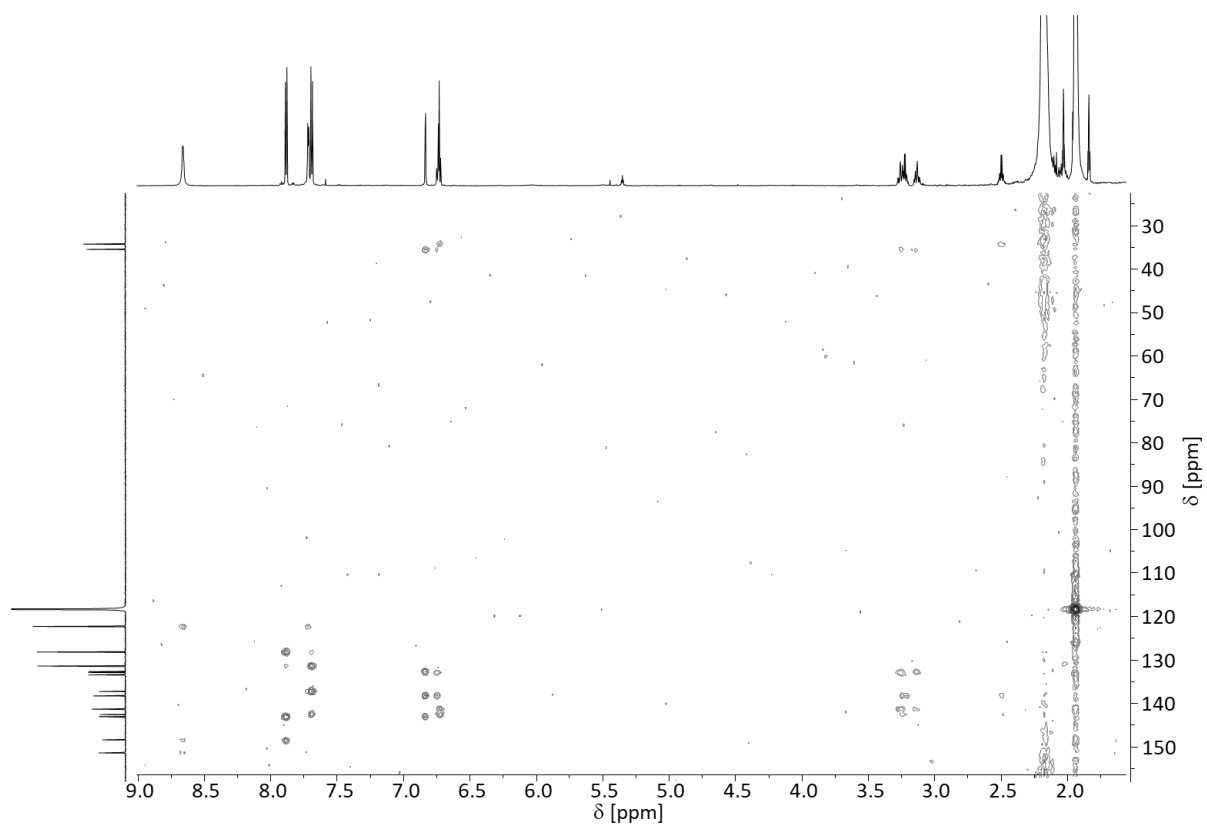


Figure S29: ^1H , ^{13}C -HMBC NMR spectrum (700.4 MHz, 176.1 MHz, CH_3CN , 298 K) of **4**.

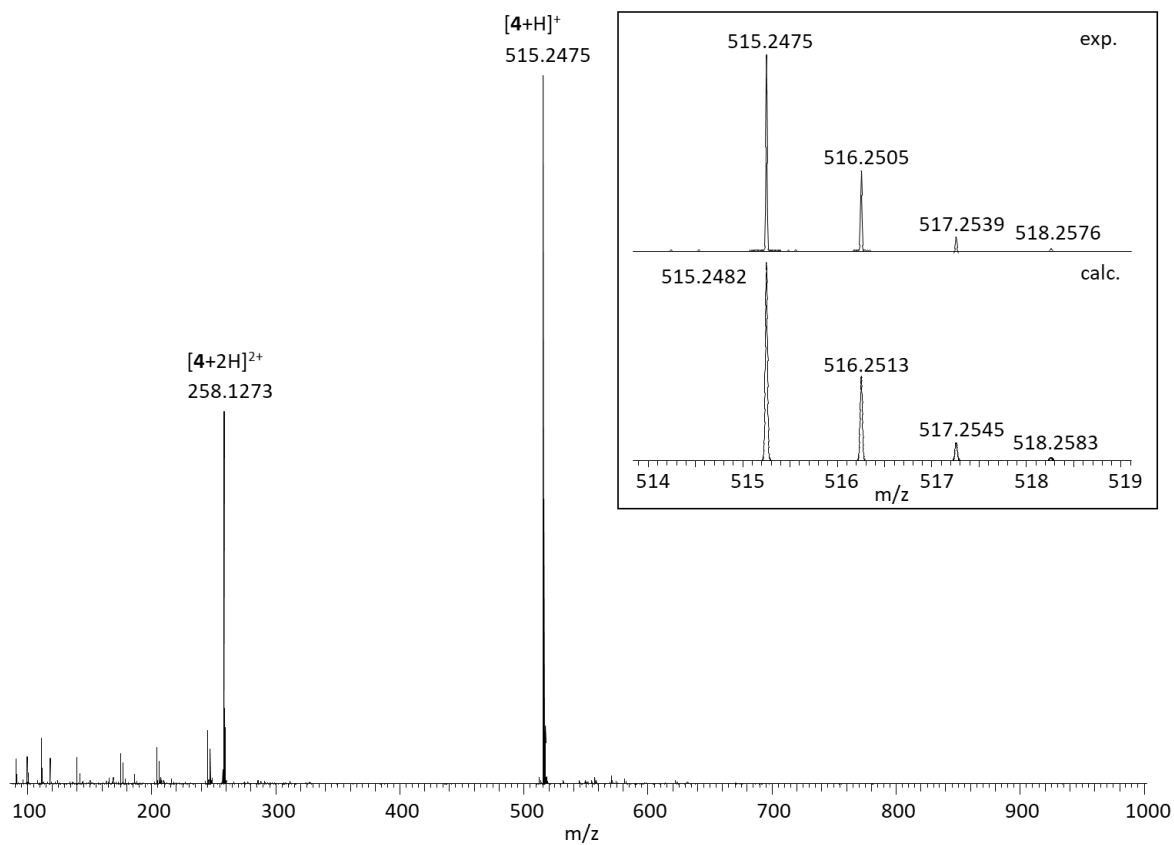


Figure S30: ESI positive mass spectrum of **4**.

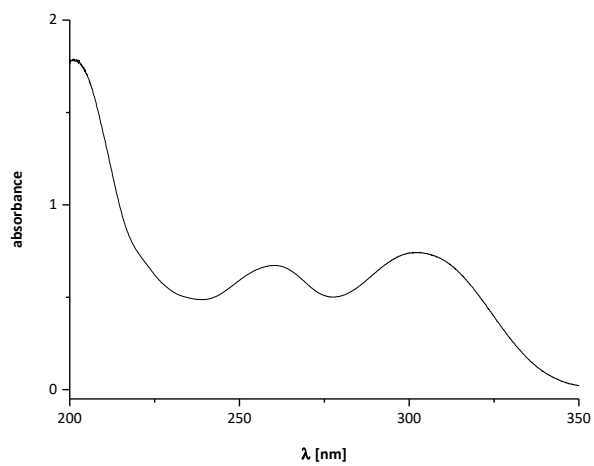


Figure S31: Non-normalized UV-Vis spectrum of **4** ($c = 19.4 \mu\text{M}$, CH_3CN).

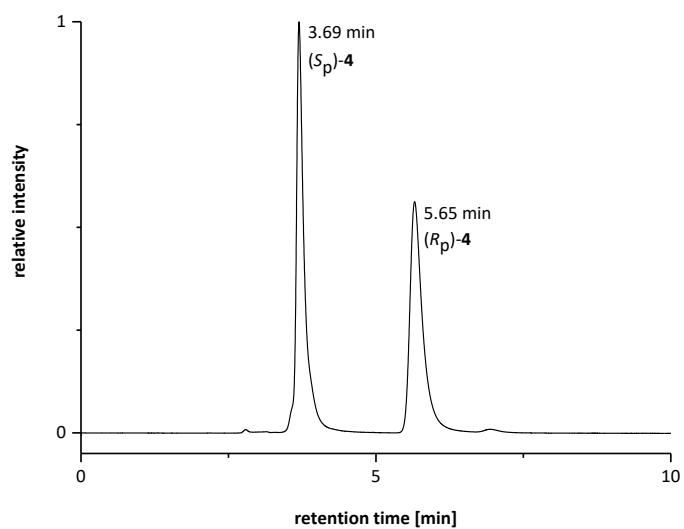


Figure S32: Chromatogram of chiral resolution of **4** via analytical HPLC (chiral stationary phase: *CHIRALPAK*[®] IA column, eluent: dichloromethane/ethanol (95:5 v/v), flow rate: 1 mL/min). When upscaling to semi-preparative mode, the flow rate was increased to 15 mL/min.

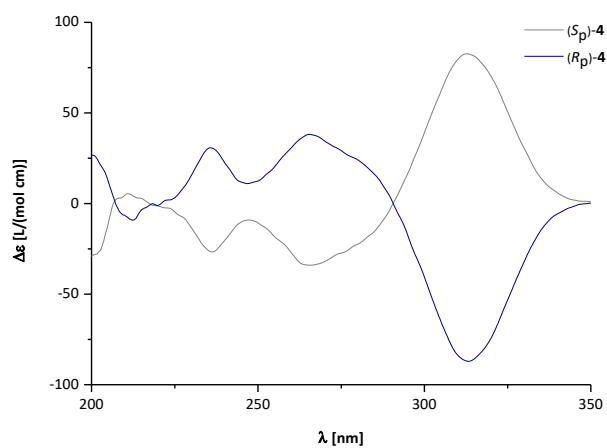
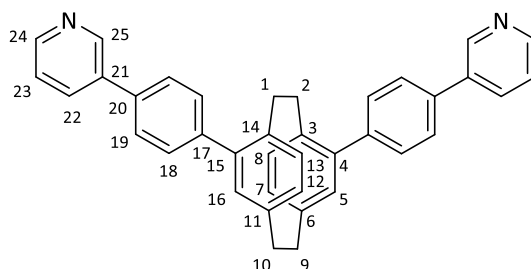


Figure S33: CD spectra of **4** ($c = 194 \mu\text{M}$, CH_3CN).

4,15-Bis-(4-(pyridin-3-yl)phenyl)[2.2]paracyclophane 5

Under an atmosphere of argon, (*rac*)-/(*R_p*)-/(*S_p*)-**3** (150 mg, 0.245 mmol, 1.00 eq.), 3-pyridinylboronic acid (69.3 mg, 0.564 mmol, 2.30 eq.), tris(dibenzylideneacetone)dipalladium(0)-chloroform (25.4 mg, 0.0245 mmol, 10.0 mol%), tricyclohexylphosphine (17.2 mg, 0.0613 mmol, 25.0 mol%) und potassium phosphate (156 mg, 1.47 mmol, 6.00 eq.) were dissolved in 1,4-dioxane (7.2 mL) and water (2.1 mL). The reaction mixture was degassed at room temperature and then, heated to reflux for 48 h. After cooling to room temperature the solution was quenched by the addition of saturated aqueous ethylenediaminetetraacetic acid disodium salt solution and dichloromethane. The mixture was extracted with dichloromethane. The combined organic layers were washed with brine, dried with anhydrous magnesium sulphate and the solvent was removed under reduced pressure. The crude product was subjected to flash column chromatography on silica gel (cyclohexane/ethyl acetate 1:1 + 0.5% triethylamine) to give (*rac*)-/(*R_p*)-/(*S_p*)-**5** (98.9 mg, 0.192 mmol, 78%) as a white solid.



Chemical formula: C₃₈H₃₀N₂

Exact mass: 514.2409 u

Molecular weight: 514.67 g/mol

¹H NMR (500.1 MHz, CD₂Cl₂, 298 K): δ [ppm] = 8.94 (dd, 2H, H-25, ⁴J_{25,22} = 2.4 Hz, ⁵J_{25,23} = 0.9 Hz), 8.59 (dd, 2H, H-24, ³J_{24,23} = 4.8 Hz, ⁴J_{24,22} = 1.6 Hz), 7.99 (ddd, 2H, H-22, ³J_{22,23} = 7.9 Hz, ⁴J_{22,25} = 2.4 Hz, ⁴J_{22,24} = 1.6 Hz), 7.76-7.73 (m, 4H, H-19), 7.65-7.62 (m, 4H, H-18), 7.41 (ddd, 2H, H-23, ³J_{23,22} = 7.9 Hz, ³J_{23,24} = 4.8 Hz, ⁵J_{23,25} = 0.9 Hz), 6.79 (d, 2H, H-5, H-16, ⁴J_{5,7} = ⁴J_{16,12} = 1.9 Hz), 6.76 (d, 2H, H-8, H-13, ³J_{8,7} = ³J_{13,12} = 7.8 Hz), 6.65 (dd, 2H, H-7, H-12, ³J_{7,8} = ³J_{12,13} = 7.8 Hz, ⁴J_{7,5} = ⁴J_{12,16} = 1.9 Hz), 3.30-3.21 (m, 4H, H-1, H-2, H-9, H-10), 3.17-3.10 (m, 2H, H-9, H-10), 2.63-2.54 (m, 2H, H-1, H-2).

¹³C NMR (125.8 MHz, CD₂Cl₂, 298 K): δ [ppm] = 149.1 (C-24), 148.8 (C-25), 142.3 (C-4, C-15), 141.5 (C-17), 140.5 (C-6, C-11), 138.1 (C-3, C-14), 136.9 (C-20), 136.7 (C-21), 134.6 (C-22), 133.0 (C-8, C-13), 132.4 (C-5, C-16), 132.0 (C-7, C-12), 130.9 (C-18), 127.8 (C-19), 124.1 (C-23), 35.6 (C-9, C-10), 34.0 (C-1, C-2).

¹H NMR (500.1 MHz, CD₃CN, 298 K): δ [ppm] = 8.95 (dd, 2H, H-25, ⁴J_{25,22} = 2.5 Hz, ⁵J_{25,23} = 0.9 Hz), 8.59 (dd, 2H, H-24, ³J_{24,23} = 4.8 Hz, ⁴J_{24,22} = 1.6 Hz), 8.08 (ddd, 2H, H-22, ³J_{22,23} = 7.9 Hz, ⁴J_{22,25} = 2.4 Hz, ⁴J_{22,24} = 1.6 Hz), 7.83-7.80 (m, 4H, H-19), 7.70-7.66 (m, 4H, H-18), 7.46 (ddd, 2H, H-23, ³J_{23,22} = 7.9 Hz, ³J_{23,24} = 4.8 Hz, ⁵J_{23,25} = 0.9 Hz), 6.84-6.83 (m, 2H, H-5, H-16), 6.76-6.71 (m, 4H, H-8, H-13, H-7, H-12), 3.29-3.20 (m, 4H, H-1, H-2, H-9, H-10), 3.17-3.10 (m, 2H, H-9, H-10), 2.55-2.47 (m, 2H, H-1, H-2).

¹³C NMR (125.8 MHz, CD₃CN, 298 K): δ [ppm] = 149.6 (C-24), 149.0 (C-25), 142.6 (C-4, C-15), 142.0 (C-17), 141.2 (C-6, C-11), 138.2 (C-3, C-14), 137.2 (C-20), 136.8 (C-21), 135.1 (C-22), 133.4 (C-8, C-13), 132.8 (C-5, C-16), 132.6 (C-7, C-12), 131.3 (C-18), 128.3 (C-19), 124.8 (C-23), 35.5 (C-9, C-10), 34.3 (C-1, C-2).

¹H NMR (500.1 MHz, DMSO-d₆, 298 K): δ [ppm] = 9.00 (dd, 2H, H-25, ⁴J_{25,22} = 2.4 Hz, ⁵J_{25,23} = 0.9 Hz), 8.60 (dd, 2H, H-24, ³J_{24,23} = 4.8 Hz, ⁴J_{24,22} = 1.6 Hz), 8.18 (ddd, 2H, H-22, ³J_{22,23} = 7.9 Hz, ⁴J_{22,25} = 2.4 Hz, ⁴J_{22,24} = 1.6 Hz), 7.90-7.87 (m, 4H, H-19), 7.67-7.64 (m, 4H, H-18), 7.53 (ddd, 2H, H-23, ³J_{23,22} = 7.9 Hz, ³J_{23,24} = 4.8 Hz, ⁵J_{23,25} = 0.9 Hz), 6.82 (d, 2H, H-5, H-16, ⁴J_{5,7} = ⁴J_{16,12} = 1.8 Hz), 6.75 (dd, 2H, H-7, H-12, ³J_{7,8} = ³J_{12,13} = 7.8 Hz, ⁴J_{7,5} = ⁴J_{12,16} = 1.8 Hz), 6.63 (d, 2H, H-8, H-13, ³J_{8,7} = ³J_{13,12} = 7.8 Hz), 3.24-3.08 (m, 4H, H-1, H-2, H-9, H-10), 2.50-2.10 (m, 2H, H-1, H-2).

^{13}C NMR (125.8 MHz, DMSO- d_6 , 298 K): δ [ppm] = 148.5 (C-24), 147.6 (C-25), 141.3 (C-4, C-15), 140.5 (C-17), 139.7 (C-6, C-11), 136.6 (C-3, C-14), 135.5 (C-20), 135.2 (C-21), 134.0 (C-22), 132.1 (C-8, C-13), 131.7 (C-5, C-16, C-7, C-12), 130.1 (C-18), 127.1 (C-19), 123.9 (C-23), 34.4 (C-9, C-10), 33.1 (C-1, C-2).

MS (ESI+) m/z : 515.2480 [$5+H$] $^+$, 258.1277 [$5+2H$] $^{2+}$; HR-MS (ESI+) m/z : calculated for $\text{C}_{38}\text{H}_{31}\text{N}_2$ [$5+H$] $^+$: 515.2482, found: 515.2480.

Elementary analysis: calculated for $\text{C}_{38}\text{H}_{30}\text{N}_2 \cdot 2 \text{C}_6\text{H}_6 \cdot 2.5 \text{H}_2\text{O}$: C: 86.69, H: 5.78, N: 5.30, found: C: 86.83, H: 6.00, N: 5.21.

Melting point: 255 °C (decomposition)

R_f (cyclohexane/ethyl acetate 1:1 + 0.5% triethylamine): 0.18

UV-Vis (CH_3CN , $c = 19.4 \mu\text{M}$): λ [nm] = 256, 298.

Specific rotation: (-)-(R_p)-**5**: $[\alpha]_D^{23} = -570^\circ$ ($c = 2.00 \text{ mg/mL} = 5.83 \text{ mm}$, CH_2Cl_2), (+)-(S_p)-**5**: $[\alpha]_D^{23} = +556^\circ$ ($c = 2.00 \text{ mg/mL} = 5.83 \text{ mm}$, CH_2Cl_2).

CD (CH_3CN , $c = 194 \mu\text{M}$): λ [nm] ($\Delta\epsilon$ [L/(mol cm)]) = (R_p)-**5**: 217 (-41), 234 (+64), 248 (+11), 263 (+49), 310 (-118); (S_p)-**5**: 217 (+43), 231 (-68), 247 (-11), 263 (-51), 311 (+125).

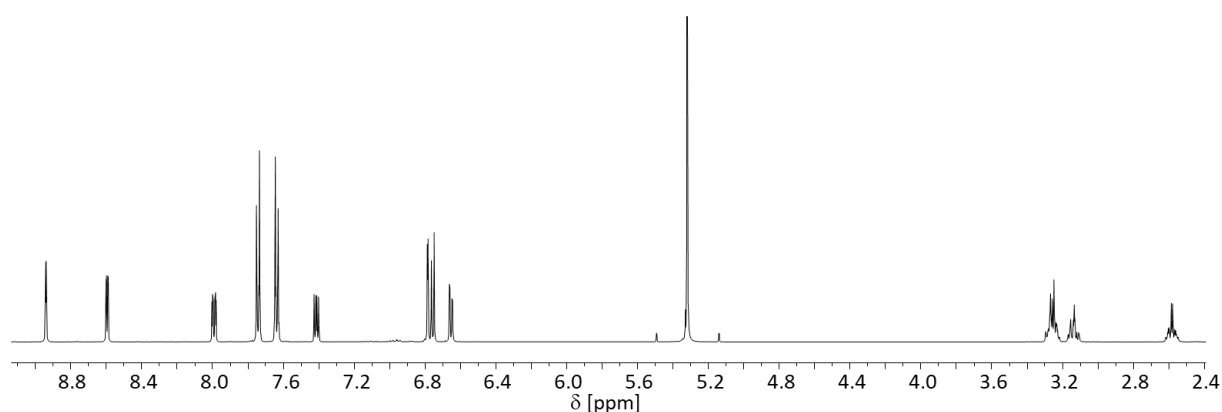


Figure S34: ^1H NMR spectrum (500.1 MHz, CD_2Cl_2 , 298 K) of **5**.

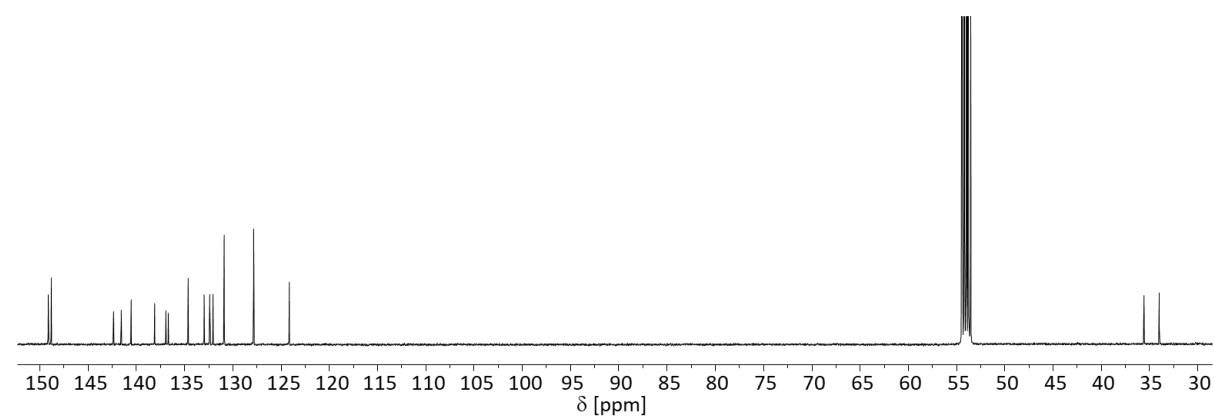


Figure S35: ^{13}C NMR spectrum (125.8 MHz, CD_2Cl_2 , 298 K) of **5**.

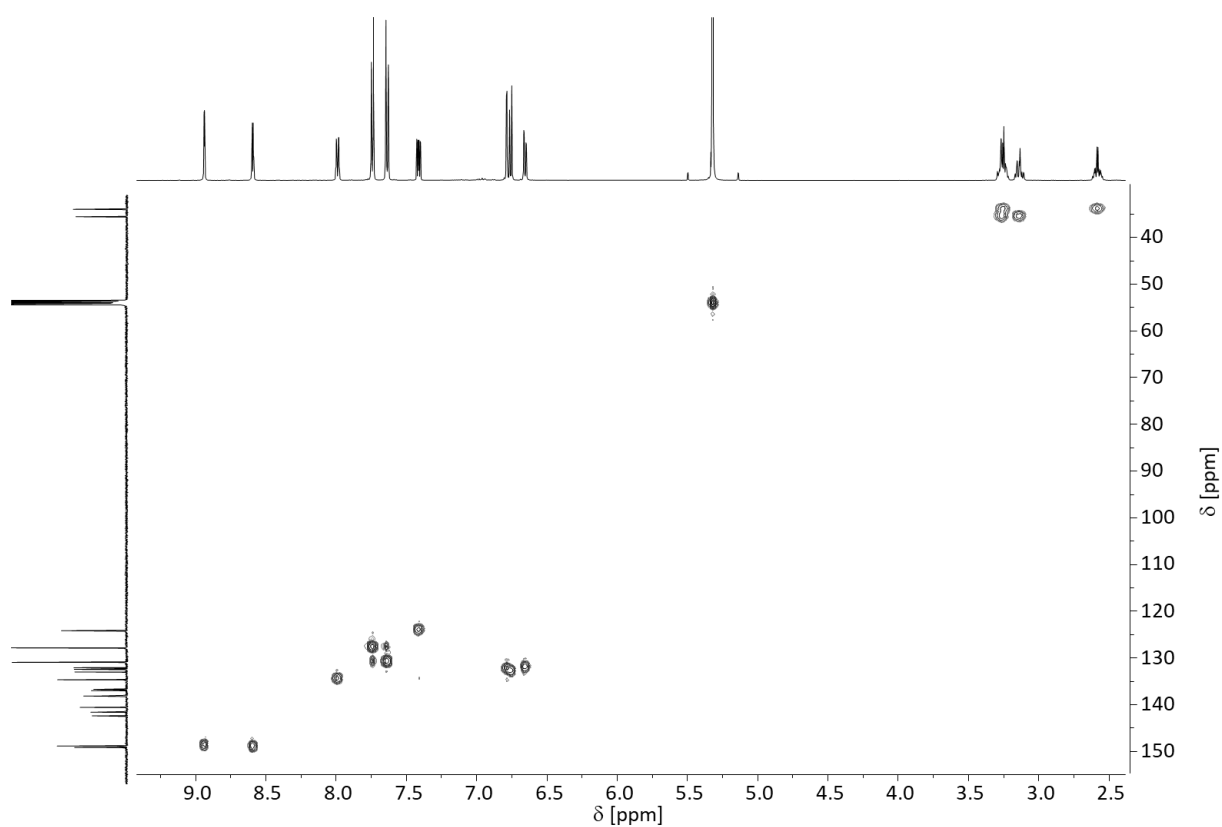


Figure S36: ^1H , ^{13}C -HSQC NMR spectrum (500.1 MHz, 125.8 MHz, CD_2Cl_2 , 298 K) of **5**.

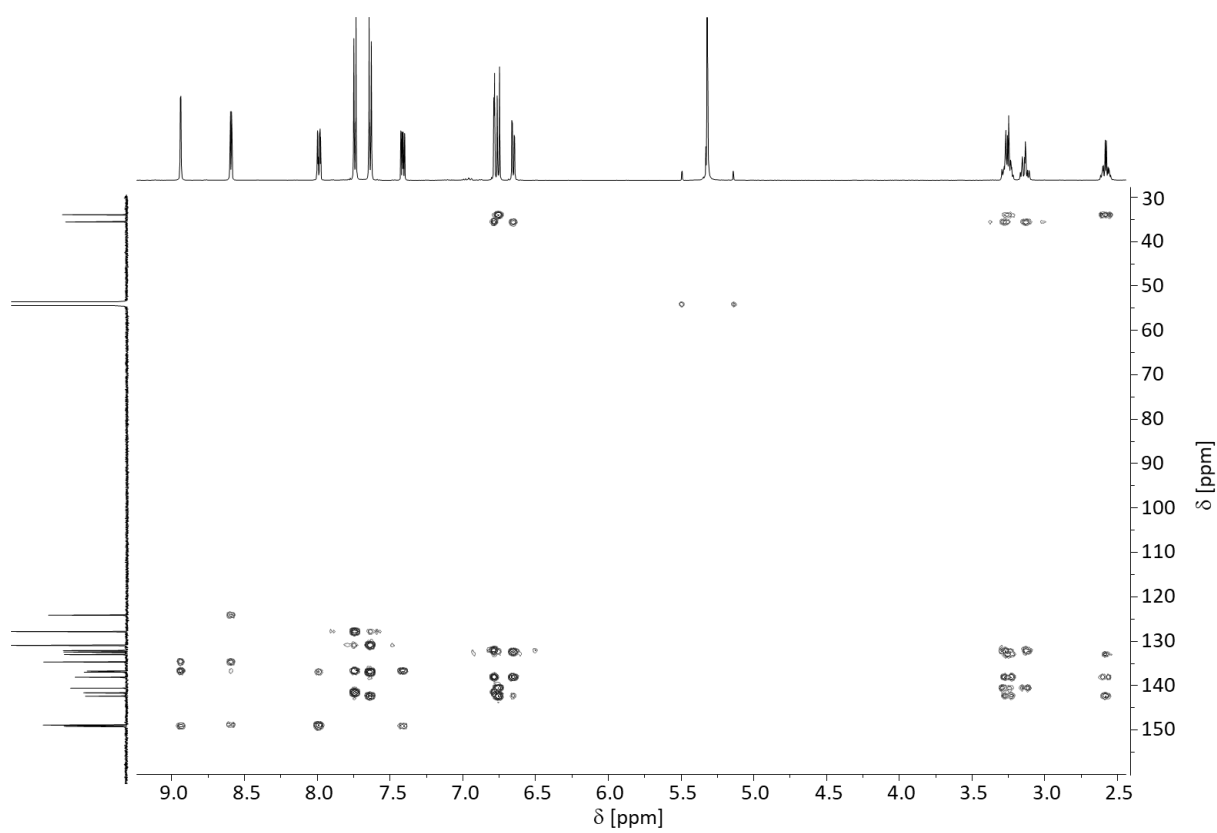


Figure S37: ^1H , ^{13}C -HMBC-NMR spectrum (500.1 MHz, 125.8 MHz, CD_2Cl_2 , 298 K) of **5**.

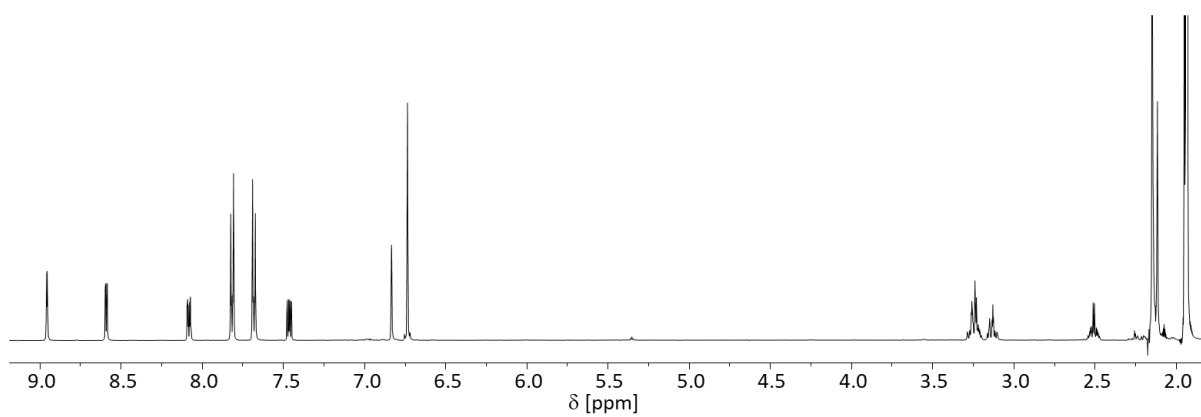


Figure S38: ^1H NMR spectrum (500.1 MHz, CD_3CN , 298 K) of **5**:

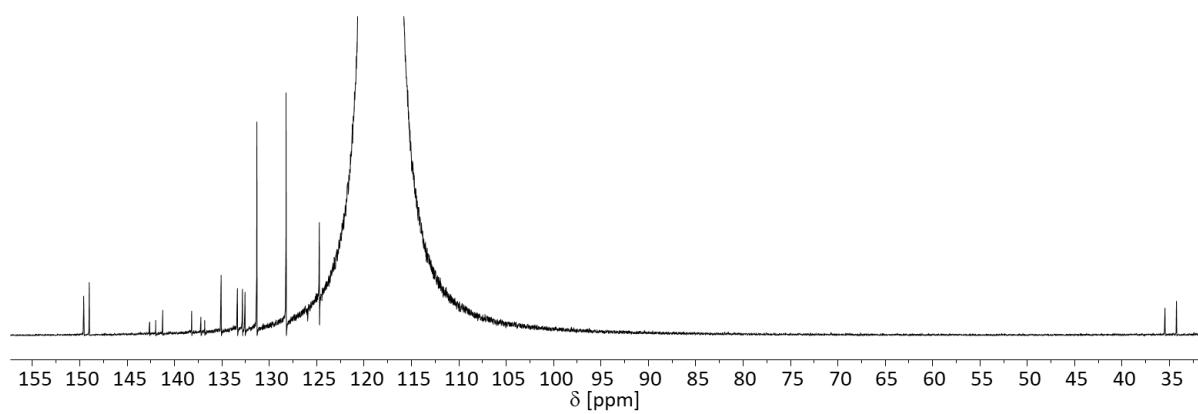


Figure S39: ^{13}C NMR spectrum (125.8 MHz, CD_3CN , 298 K) of **5**.

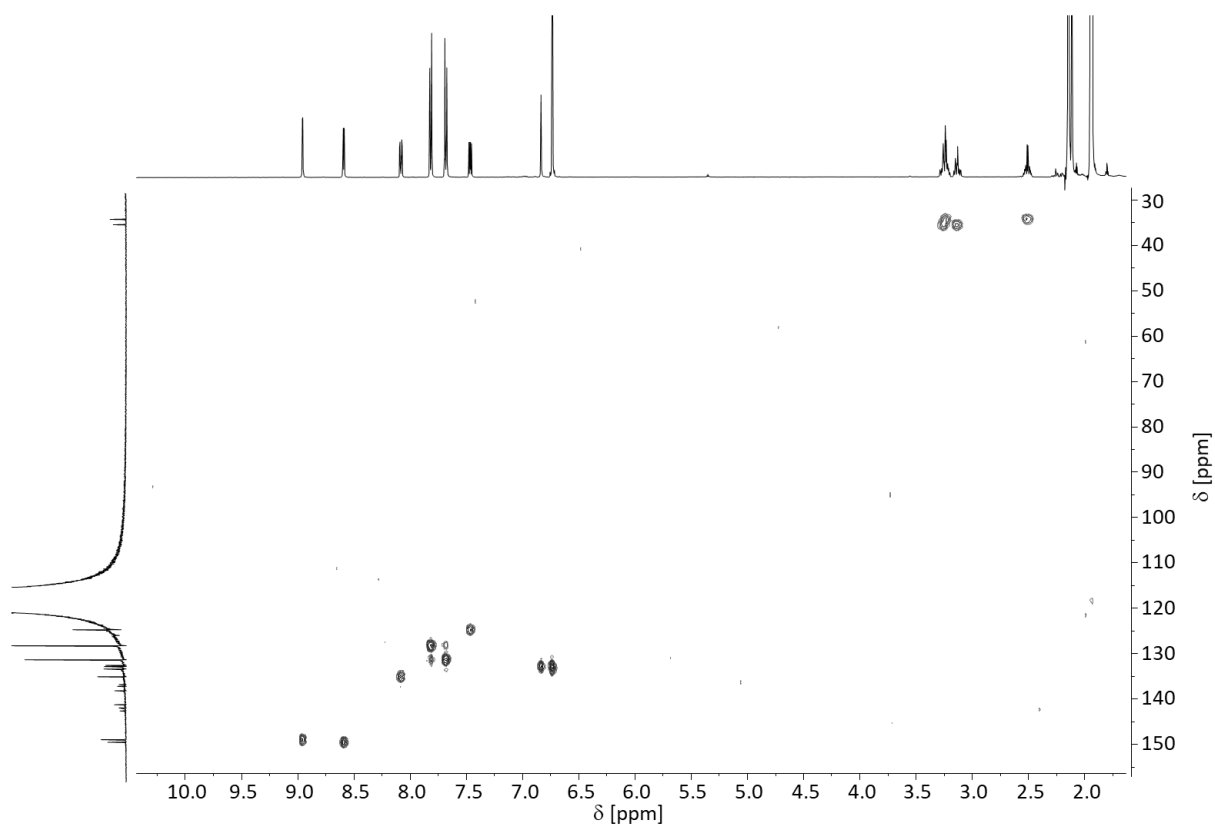


Figure S40: ^1H , ^{13}C -HSQC NMR spectrum (500.1 MHz, 125.8 MHz, CD_3CN , 298 K) of **5**.

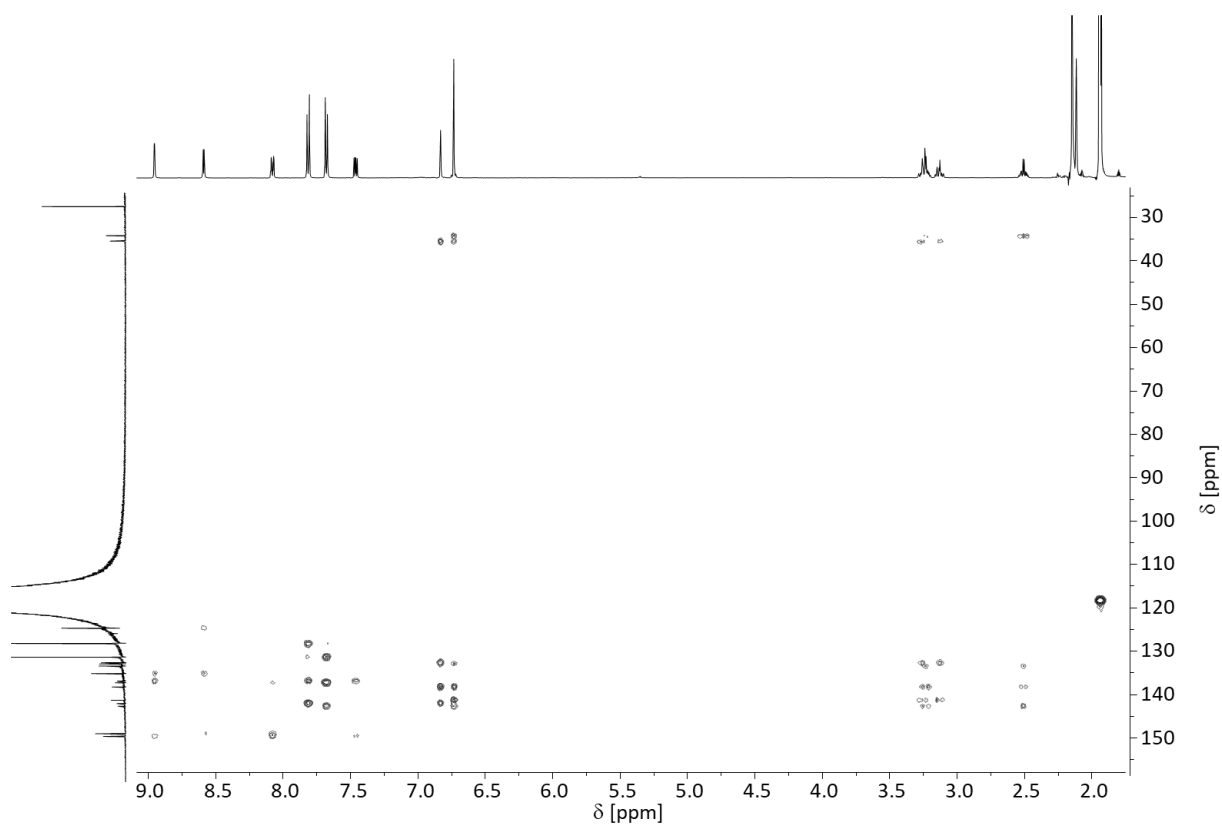


Figure S41: ^1H , ^{13}C -HMBC NMR spectrum (500.1 MHz, 125.8 MHz, CD_3CN , 298 K) of **5**.

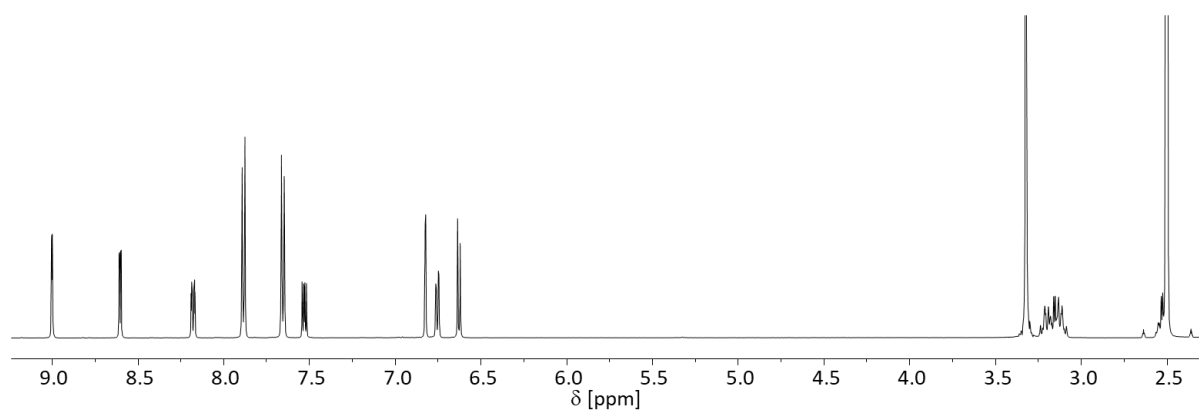


Figure S42: ^1H NMR spectrum (500.1 MHz, DMSO-d_6 , 298 K) of **5**:

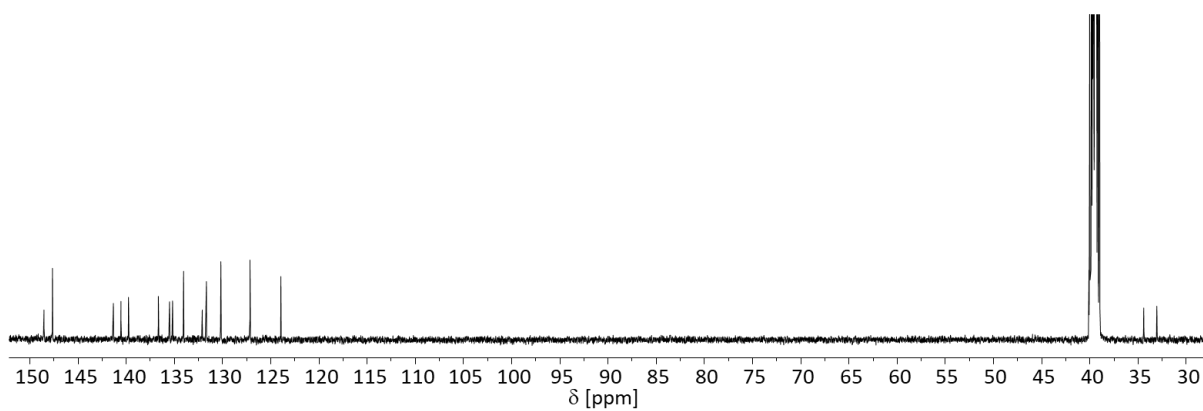


Figure S43: ^{13}C NMR spectrum (125.8 MHz, DMSO-d_6 , 298 K) of **5**.

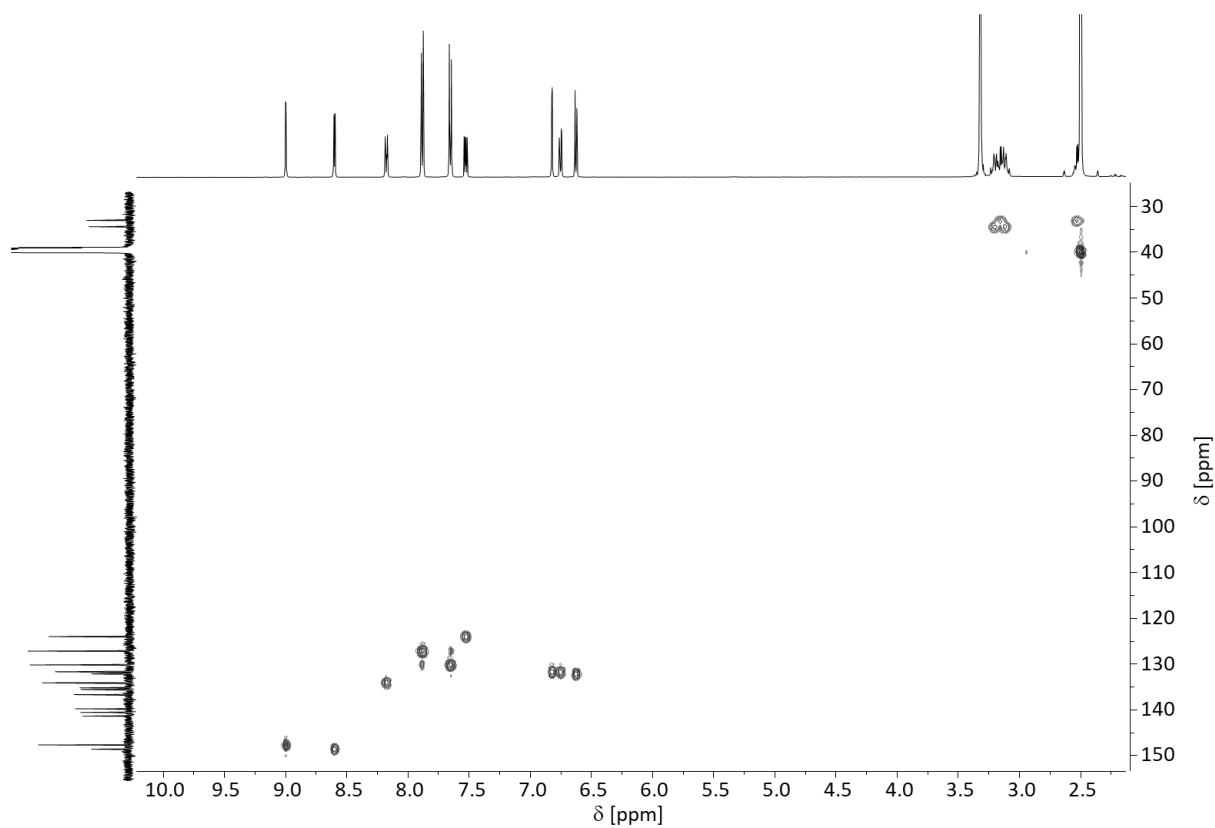


Figure S44: ^1H , ^{13}C -HSQC NMR spectrum (500.1 MHz, 125.8 MHz, DMSO- d_6 , 298 K) of **5**.

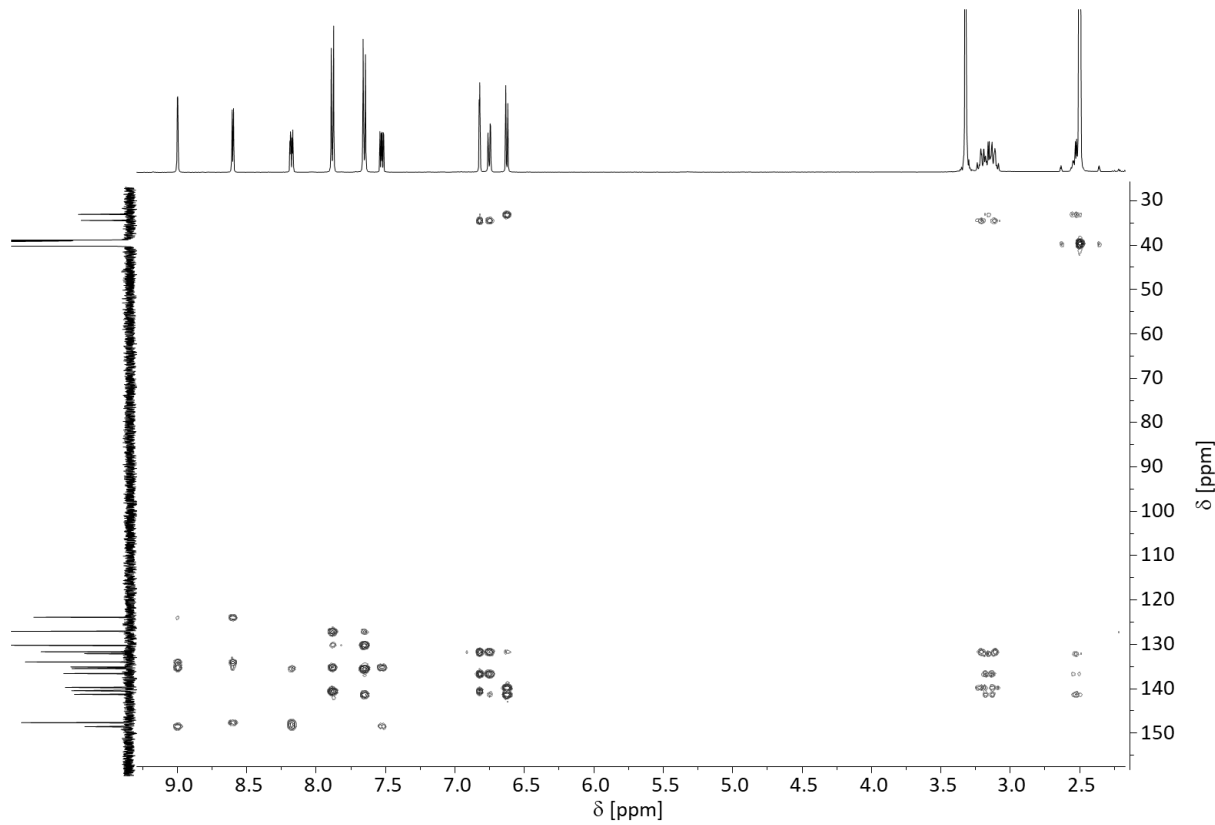


Figure S45: ^1H , ^{13}C -HMBC NMR spectrum (500.1 MHz, 125.8 MHz, DMSO- d_6 , 298 K) of **5**.

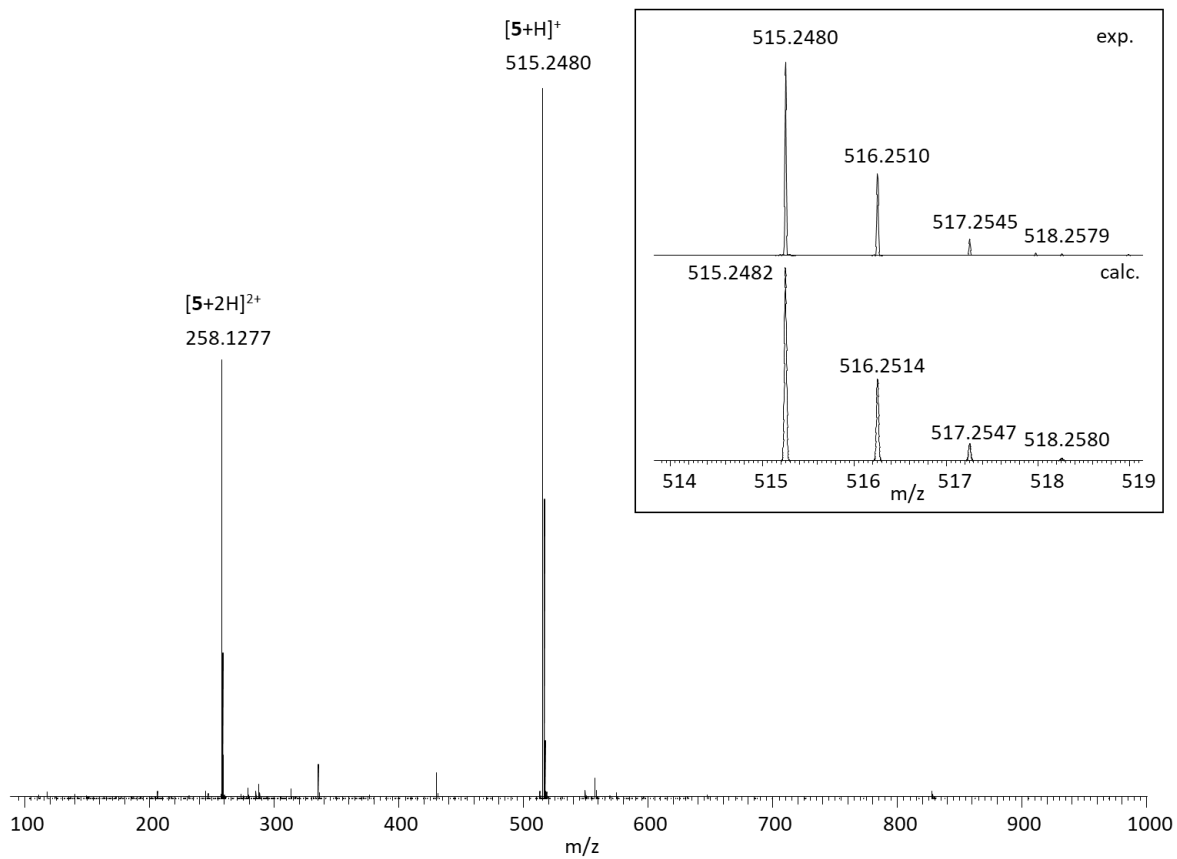


Figure S46: ESI positive mass spectrum of **5**.

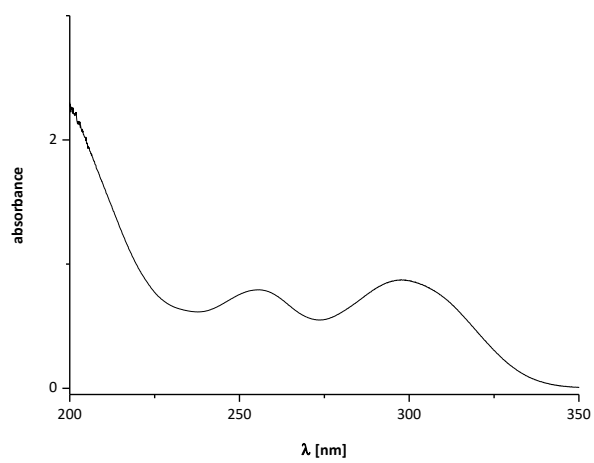


Figure S47: Non-normalized UV-Vis spectrum of **5** ($c = 19.4 \mu\text{M}$, CH_3CN).

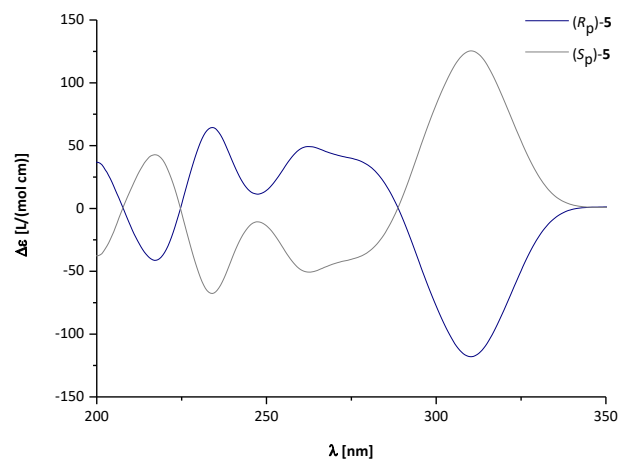
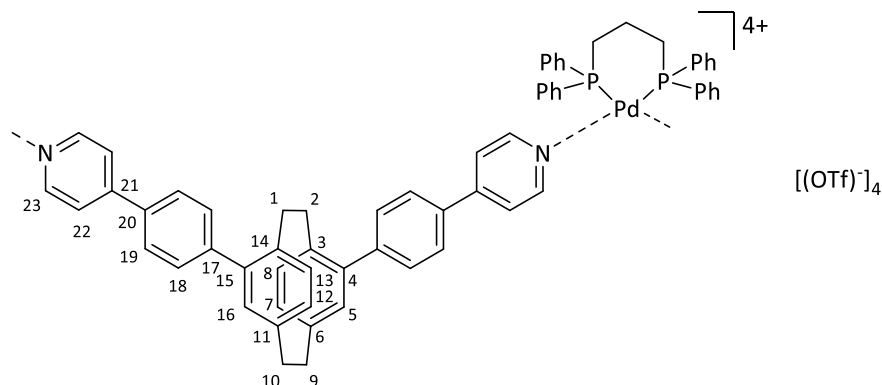


Figure S48: CD spectra of **5** ($c = 194 \mu\text{M}$, CH_3CN).

Self-assembly and characterization of palladium(II) complexes

[Pd₂(dppp)₂]₂(OTf)₄ in dichloromethane:acetonitrile 1:1

(*rac*)-, (*R_p*)- or (*S_p*)-**4** (2.88 mg, 5.60 μmol, 1.00 eq.) was dissolved in deuterated dichloromethane (0.3 mL) and a solution of [Pd(dppp)](OTf)₂ (4.61 mg, 5.64 μmol, 1.01 eq.) in deuterated acetonitrile (0.3 mL) was added. The mixture was filtrated.



[Pd₂(dppp)₂{(*S_p*)-**4**]₂(OTf)₄

¹H NMR (700.4 MHz, CD₃CN:CD₂Cl₂ 1:1, 298 K): δ [ppm] = 8.69-8.64 (m, 8H, H-23), 7.72-7.50 (m, 40H, H-18, H-19, dppp-Ph_{ortho}, dppp-Ph_{para}), 7.44-7.34 (m, 24H, H-22, dppp-Ph_{meta}), 6.72-6.65 (m, 12H, H-5, H-7, H-8, H-12, H-13, H-16), 3.32-2.90 (m, 24H, H-1, H-2, H-9, H-10, dppp-CH₂-PPh₂), 2.33-2.21 (m, 4H, dppp-CH₂).

¹³C NMR (176.1 MHz, CD₃CN:CD₂Cl₂ 1:1, 298 K): δ [ppm] = 150.5 (C-23), 143.8*, 141.4*, 141.0*, 137.8*, 133.8*, 133.1*, 133.0*, 132.5*, 132.0*, 131.0*, 130.2*, 128.0*, 122.7*, 120.9*, 35.2*, 33.9*.

*Signals could not be unambiguously assigned.

³¹P-NMR (202.1 MHz, CD₃CN:CD₂Cl₂ 1:1, 298 K): δ [ppm] = 8.37 (s, dppp-P).

¹H-DOSY-NMR (700.4 MHz, CD₃CN:CD₂Cl₂ 1:1, 298 K): D = 5.88 · 10⁻¹⁰ m²s⁻¹, R_H = 11.7 Å.

MS (ESI+) *m/z*: 516.6 [Pd₂(dppp)₂{(*S_p*)-**4**]₂⁴⁺ and [Pd(dppp){(*S_p*)-**4**}]²⁺, 536.6 [Pd(dppp){(*S_p*)-**4**}(CH₃CN)]²⁺, 553.0 {[Pd(dppp)]Cl}⁺, 666.9 {[Pd(dppp)]OTf}⁺, 738.4 {[Pd₂(dppp)₂{(*S_p*)-**4**]₂OTf}³⁺, 773.2 [Pd(dppp){(*S_p*)-**4**}]²⁺, 1183.2 {[Pd₂(dppp)₂{(*S_p*)-**4**]₂(OTf)₂}²⁺ and {[Pd(dppp){(*S_p*)-**4**}]OTf⁺.

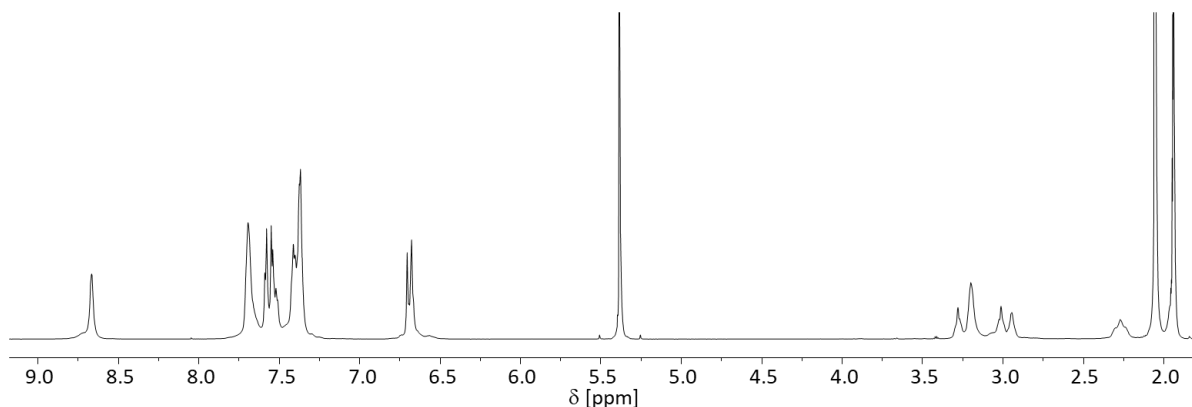


Figure S49: ¹H NMR spectrum (700.4 MHz, CD₃CN:CD₂Cl₂ 1:1, 298 K) of [Pd₂(dppp)₂{(*S_p*)-**4**]₂(OTf)₄.

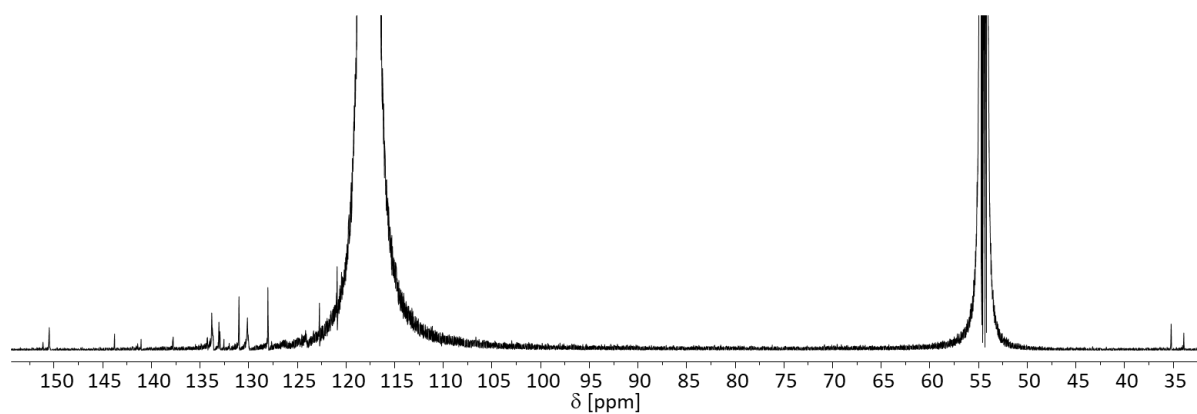


Figure S50: ^{13}C NMR spectrum (176.1 MHz, $\text{CD}_3\text{CN}:\text{CD}_2\text{Cl}_2$ 1:1, 298 K) of $[\text{Pd}_2(\text{dppp})_2\{(\text{S}_p)\text{-4}\}_2](\text{OTf})_4$.

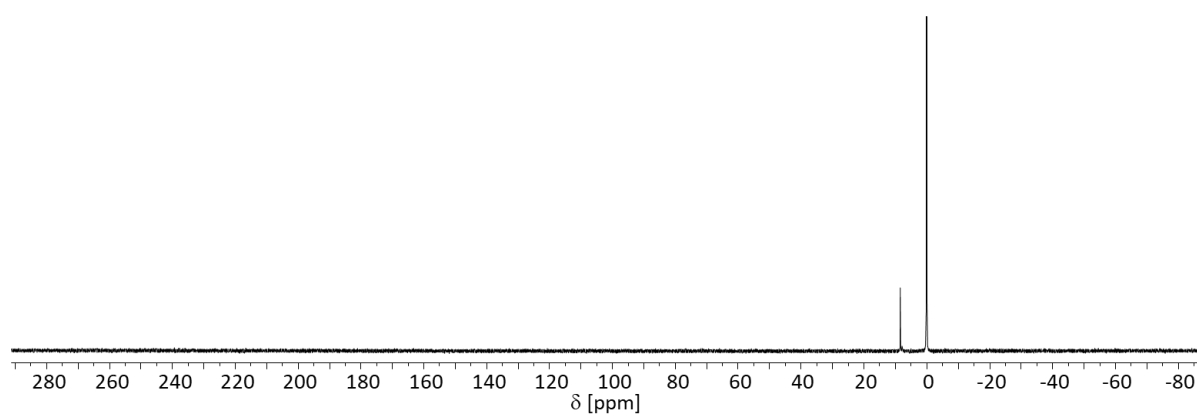


Figure S51: ^{31}P NMR spectrum (202.1 MHz, $\text{CD}_3\text{CN}:\text{CD}_2\text{Cl}_2$ 1:1, 298 K) of $[\text{Pd}_2(\text{dppp})_2\{(\text{S}_p)\text{-4}\}_2](\text{OTf})_4$.

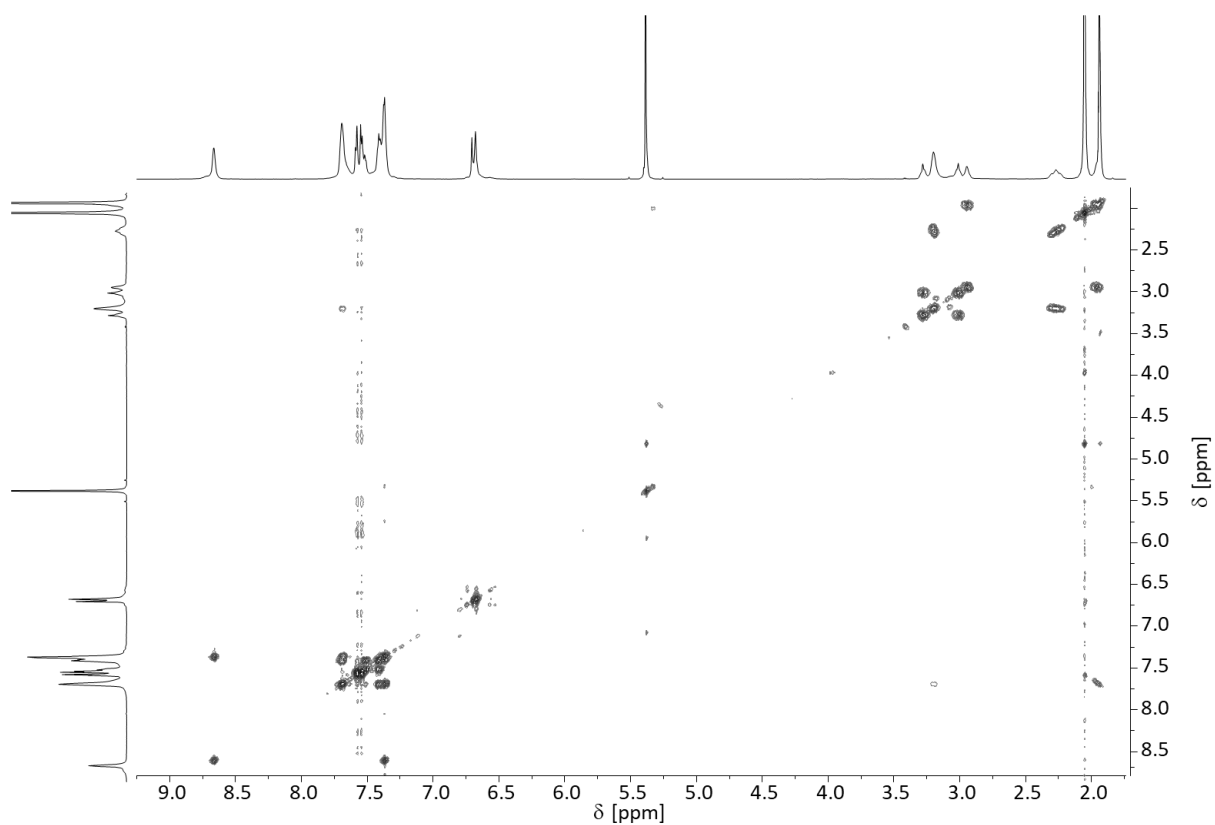


Figure S52: ^1H , ^1H -COSY NMR spectrum (700.4 MHz, $\text{CD}_3\text{CN}:\text{CD}_2\text{Cl}_2$ 1:1, 298 K) of $[\text{Pd}_2(\text{dppp})_2\{(\text{S}_p)\text{-4}\}_2](\text{OTf})_4$.

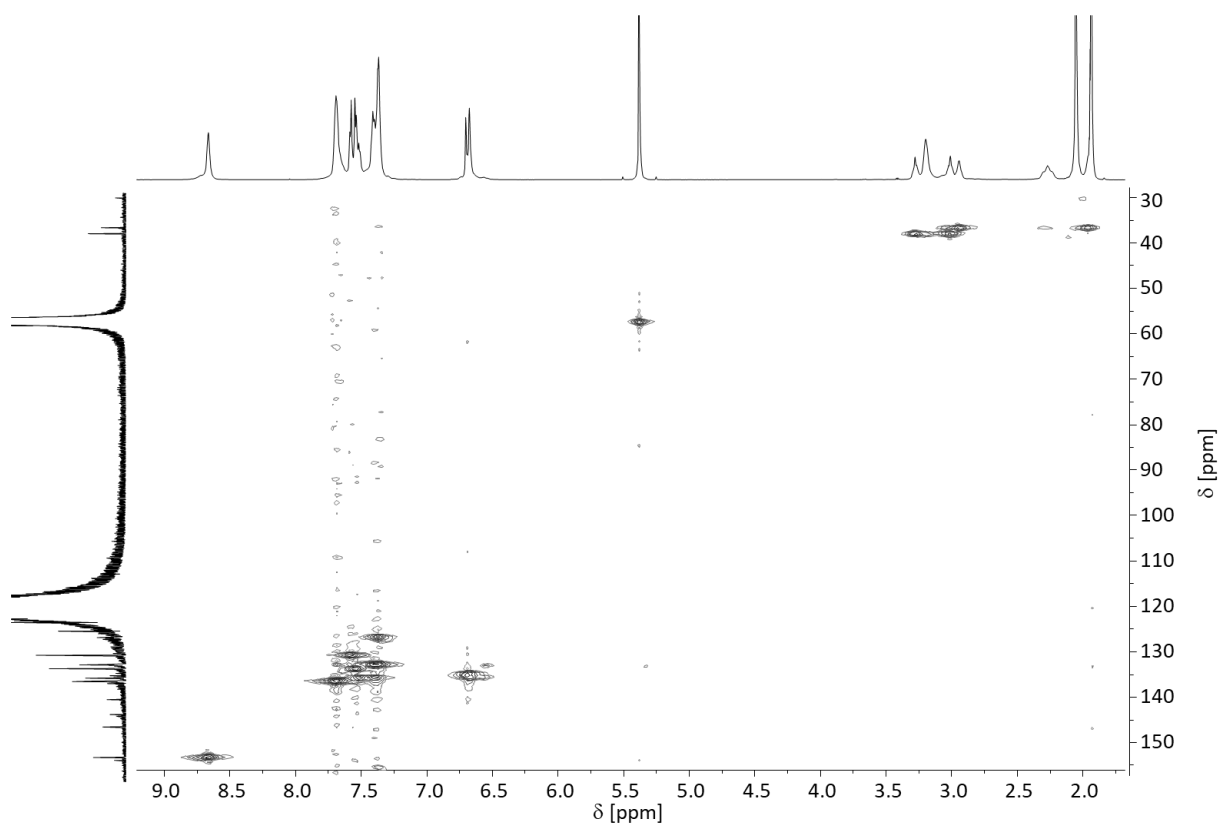


Figure S53: ^1H , ^{13}C -HSQC NMR spectrum (700.4 MHz, 176.1 MHz, $\text{CD}_3\text{CN}:\text{CD}_2\text{Cl}_2$ 1:1, 298 K) of $[\text{Pd}_2(\text{dppp})_2\{(\text{S}_p)\text{-4}\}_2](\text{OTf})_4$.

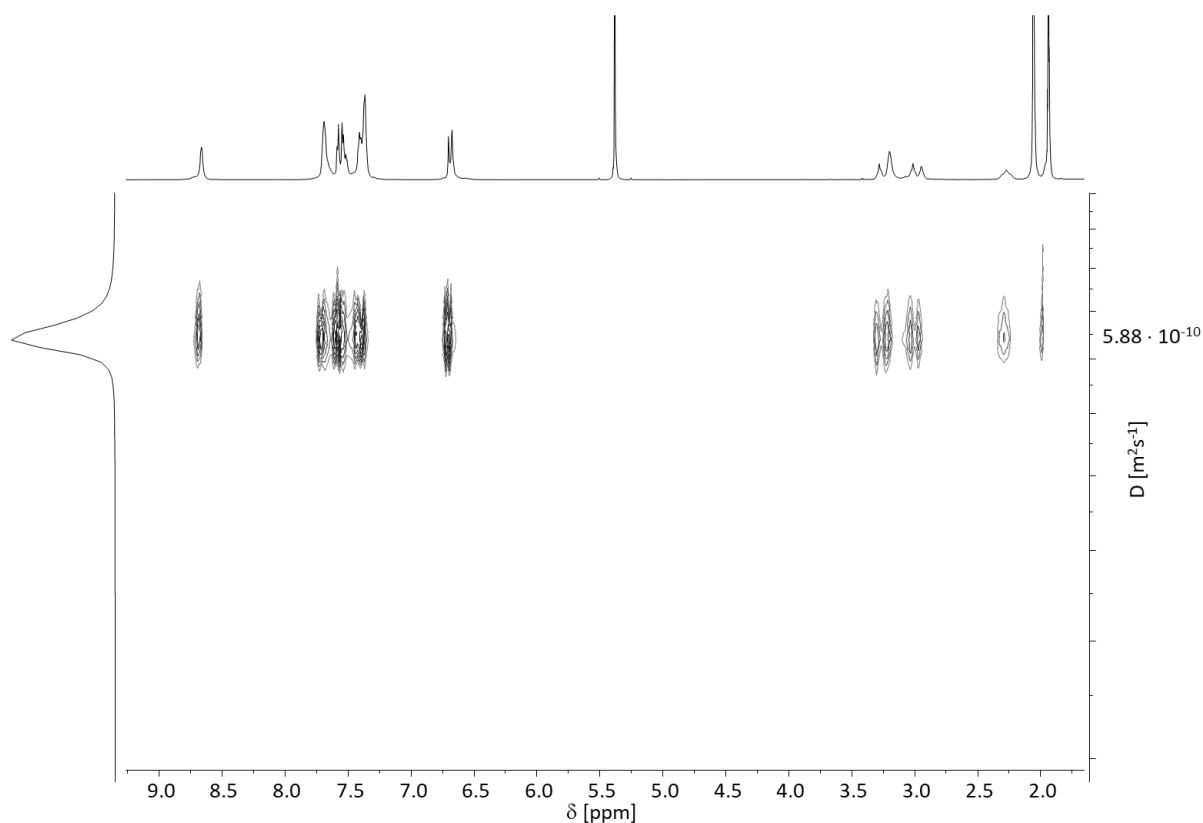


Figure S54: ^1H -DOSY NMR spectrum (700.4 MHz, $\text{CD}_3\text{CN}:\text{CD}_2\text{Cl}_2$ 1:1, 298 K) of $[\text{Pd}_2(\text{dppp})_2\{(\text{S}_p)\text{-4}\}_2](\text{OTf})_4$.

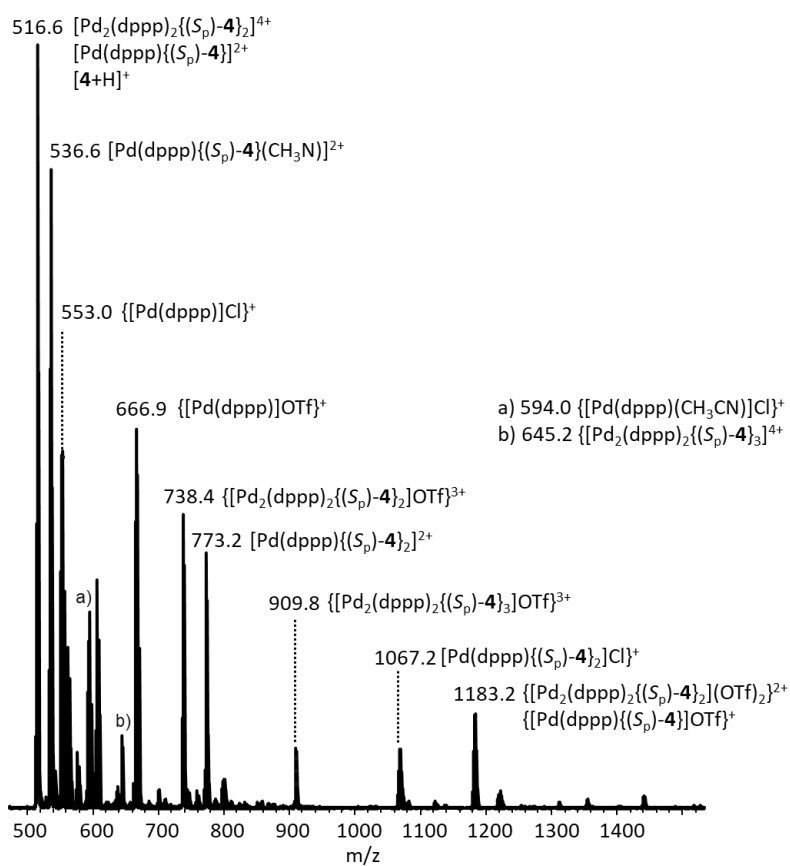


Figure S55: ESI positive mass spectrum of 1:1 mixture of $(\text{S}_p)\text{-4}$ and $[\text{Pd}(\text{dppp})](\text{OTf})_2$ in $\text{CD}_3\text{CN}:\text{CD}_2\text{Cl}_2$ 1:1 measured on a *micrOTOF-Q* time-of-flight mass spectrometer.

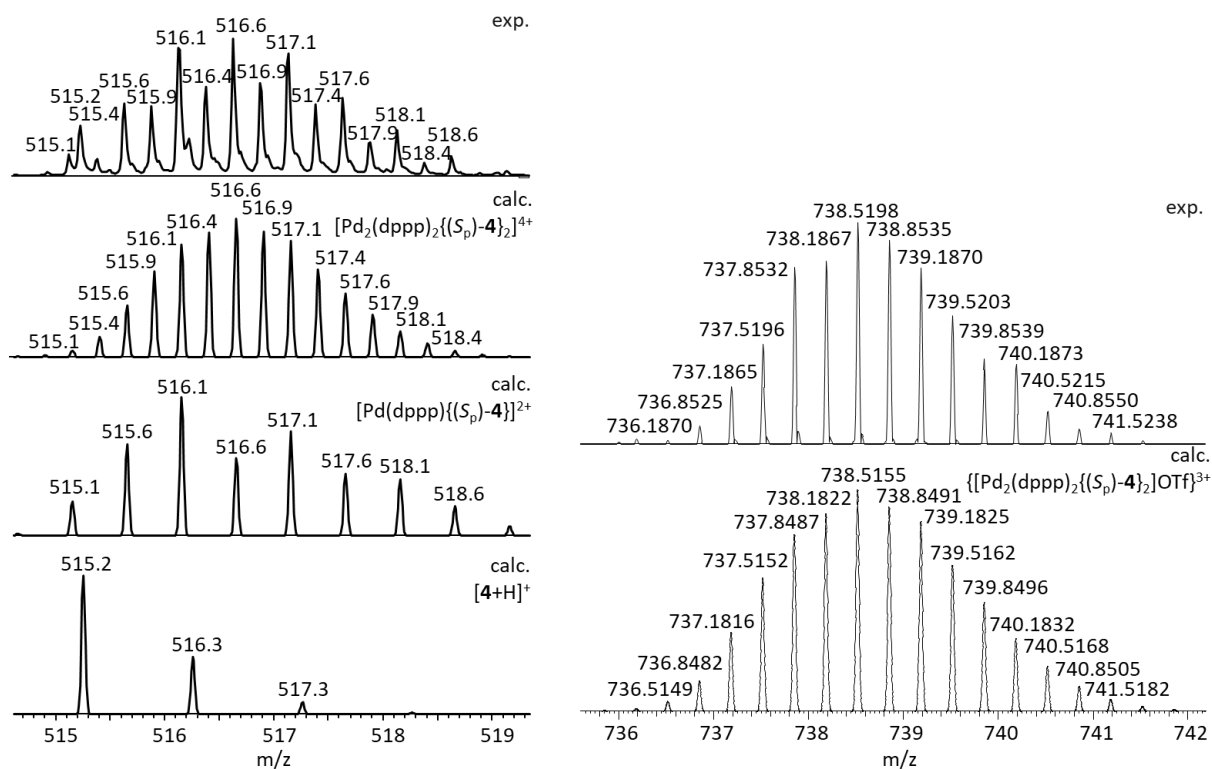


Figure S56: Experimental and calculated high resolution ESI positive mass spectra of $[\text{Pd}_2(\text{dppp})_2\{(\text{S}_p)\text{-4}\}_2]^{4+}$ (left) measured on a *micrOTOF-Q* time-of-flight mass spectrometer and $\{[\text{Pd}_2(\text{dppp})_2\{(\text{S}_p)\text{-4}\}_2]\text{OTf}\}^{3+}$ (right) in $\text{CD}_3\text{CN}:\text{CD}_2\text{Cl}_2$ 1:1 measured on an *Orbitrab XL* mass spectrometer.

$[\text{Pd}_2(\text{dppp})_2\{(\text{rac})\text{-4}\}_2](\text{OTf})_4$

^1H NMR (700.4 MHz, $\text{CD}_3\text{CN}:\text{CD}_2\text{Cl}_2$ 1:1, 298 K): δ [ppm] = 8.69-8.64 (m, 8H, H-23), 7.72-7.50 (m, 40H, H-18, H-19, $\text{dppp-Ph}_{\text{ortho}}$, $\text{dppp-Ph}_{\text{para}}$), 7.44-7.34 (m, 24H, H-22, $\text{dppp-Ph}_{\text{meta}}$), 6.72-6.65 (m, 12H, H-5, H-7, H-8, H-12, H-13, H-16), 3.32-2.90 (m, 24H, H-1, H-2, H-9, H-10, $\text{dppp-CH}_2\text{-PPh}_2$), 2.33-2.21 (m, 4H, dppp-CH_2).

^{13}C NMR (176.1 MHz, $\text{CD}_3\text{CN}:\text{CD}_2\text{Cl}_2$ 1:1, 298 K): δ [ppm] = 150.5 (C-23), 143.8*, 141.4*, 141.1*, 137.8*, 133.8*, 133.1*, 133.0*, 132.5*, 132.1*, 131.0*, 130.1*, 128.0*, 122.7*, 120.9*, 35.2*, 34.0*.

*Signals could not be unambiguously assigned.

^{31}P NMR (202.1 MHz, $\text{CD}_3\text{CN}:\text{CD}_2\text{Cl}_2$ 1:1, 298 K): δ [ppm] = 8.39 (s, dppp-P).

^1H -DOSY NMR (499.1 MHz, $\text{CD}_3\text{CN}:\text{CD}_2\text{Cl}_2$ 1:1, 298 K): $D = 4.51 \cdot 10^{-10} \text{ m}^2\text{s}^{-1}$, $R_H = 13.7 \text{ \AA}$.

MS (ESI+) m/z : 516.1530 $[\text{Pd}_2(\text{dppp})_2\{(\text{rac})\text{-4}\}_2]^{4+}$ and $[\text{Pd}(\text{dppp})\{(\text{rac})\text{-4}\}]^{2+}$, 536.6661 $[\text{Pd}(\text{dppp})\{(\text{rac})\text{-4}\}(\text{CH}_3\text{CN})]^{2+}$, 595.1025 $\{[\text{Pd}(\text{dppp})(\text{CH}_3\text{CN})]\text{Cl}\}^+$, 667.0122 $\{[\text{Pd}(\text{dppp})]\text{OTf}\}^+$, 738.5217 $\{[\text{Pd}_2(\text{dppp})_2\{(\text{rac})\text{-4}\}_2]\text{OTf}\}^{3+}$, 773.2753 $[\text{Pd}(\text{dppp})\{(\text{rac})\text{-4}\}]^{2+}$, 1182.2599 $\{[\text{Pd}_2(\text{dppp})_2\{(\text{rac})\text{-4}\}_2](\text{OTf})_2\}^{2+}$ and $\{[\text{Pd}(\text{dppp})\{(\text{rac})\text{-4}\}]\text{OTf}\}^+$.

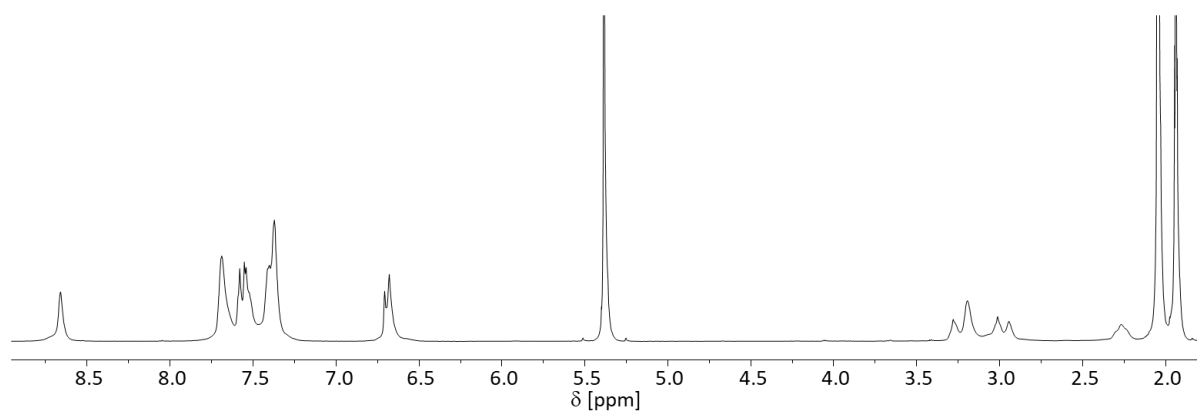


Figure S57: ^1H NMR spectrum (700.4 MHz, $\text{CD}_3\text{CN}:\text{CD}_2\text{Cl}_2$ 1:1, 298 K) of $[\text{Pd}_2(\text{dppp})_2\{(\text{rac})\text{-4}\}_2](\text{OTf})_4$.

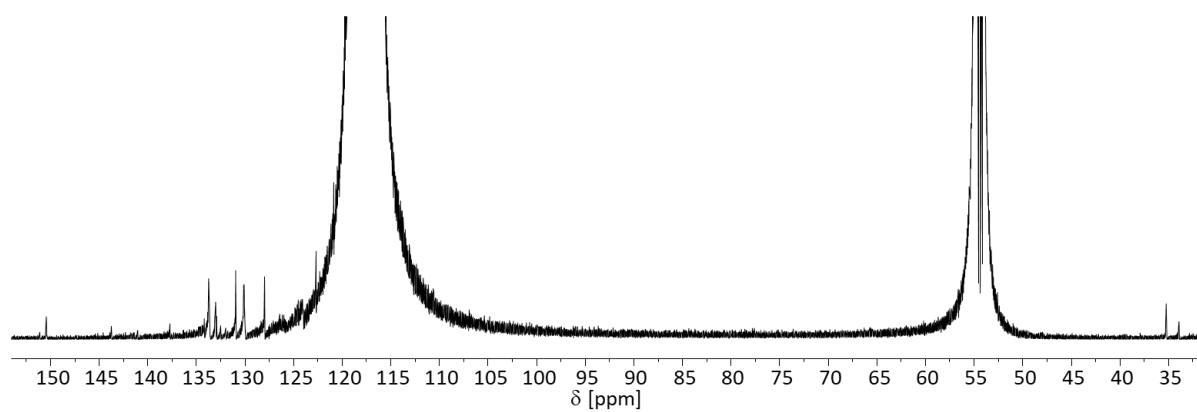


Figure S58: ^{13}C NMR spectrum (176.1 MHz, $\text{CD}_3\text{CN}:\text{CD}_2\text{Cl}_2$ 1:1, 298 K) of $[\text{Pd}_2(\text{dppp})_2\{(\text{rac})\text{-4}\}_2](\text{OTf})_4$.

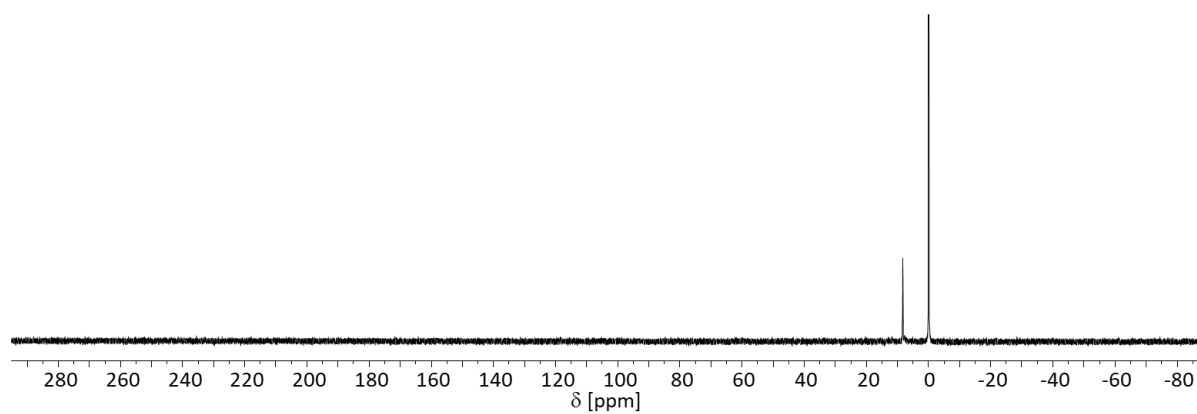


Figure S59: ^{31}P NMR spectrum (202.1 MHz, $\text{CD}_3\text{CN}:\text{CD}_2\text{Cl}_2$ 1:1, 298 K) of $[\text{Pd}_2(\text{dppp})_2\{(\text{rac})\text{-4}\}_2](\text{OTf})_4$.

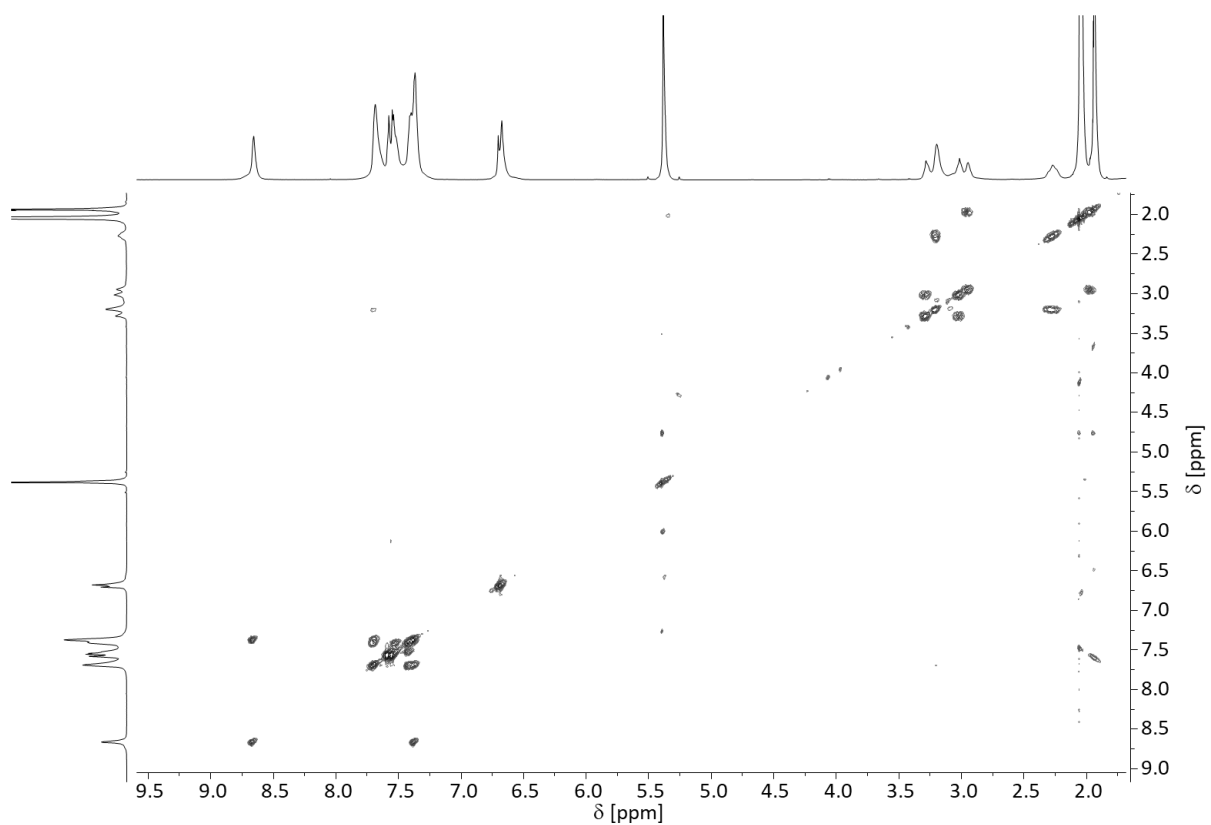


Figure S60: ^1H , ^1H -COSY NMR spectrum (700.4 MHz, $\text{CD}_3\text{CN}:\text{CD}_2\text{Cl}_2$ 1:1, 298 K) of $[\text{Pd}_2(\text{dppp})_2\{(\text{rac})\text{-4}\}_2](\text{OTf})_4$.

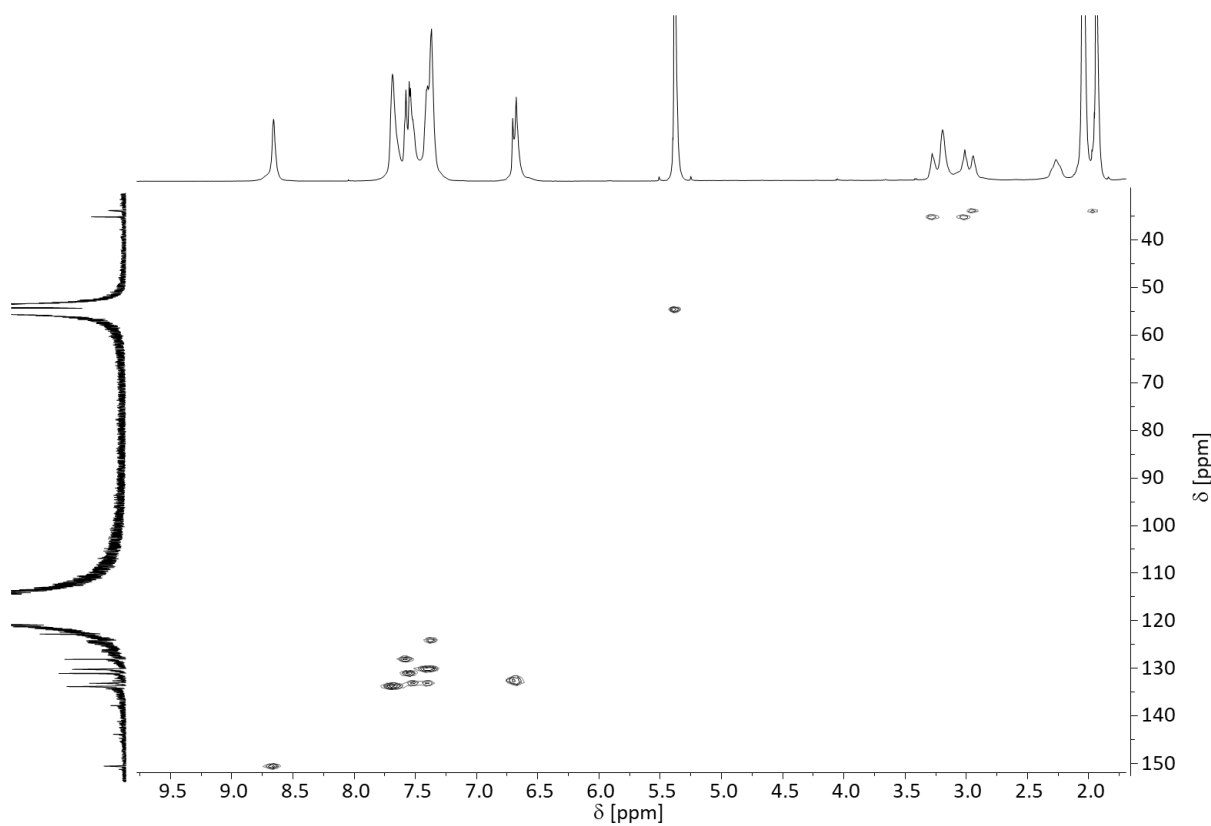


Figure S61: ^1H , ^{13}C -HSQC NMR spectrum (700.4 MHz, 176.1 MHz, $\text{CD}_3\text{CN}:\text{CD}_2\text{Cl}_2$ 1:1, 298 K) of $[\text{Pd}_2(\text{dppp})_2\{(\text{rac})\text{-4}\}_2](\text{OTf})_4$.

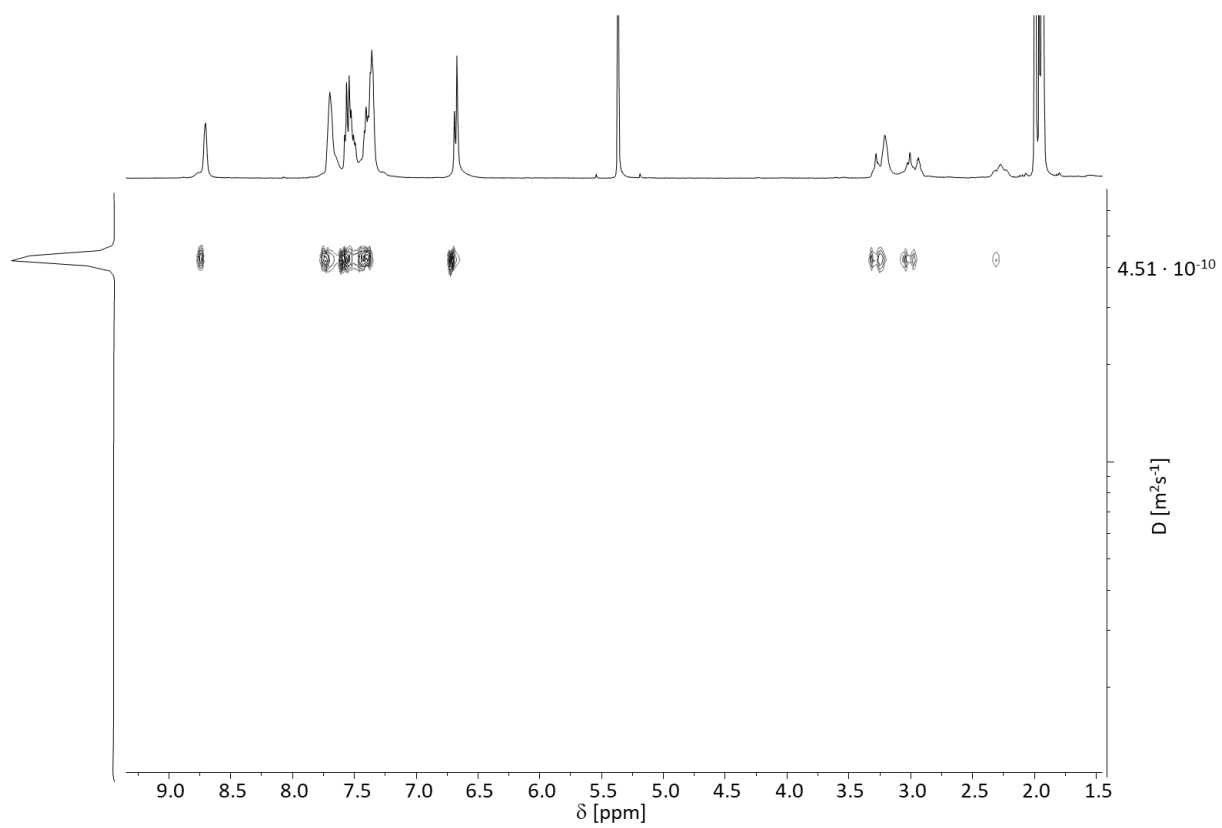


Figure S62: ^1H -DOSY NMR spectrum (499.1 MHz, $\text{CD}_3\text{CN}:\text{CD}_2\text{Cl}_2$ 1:1, 298 K) of $[\text{Pd}_2(\text{dppp})_2\{(\text{rac})\text{-4}\}](\text{OTf})_4$.

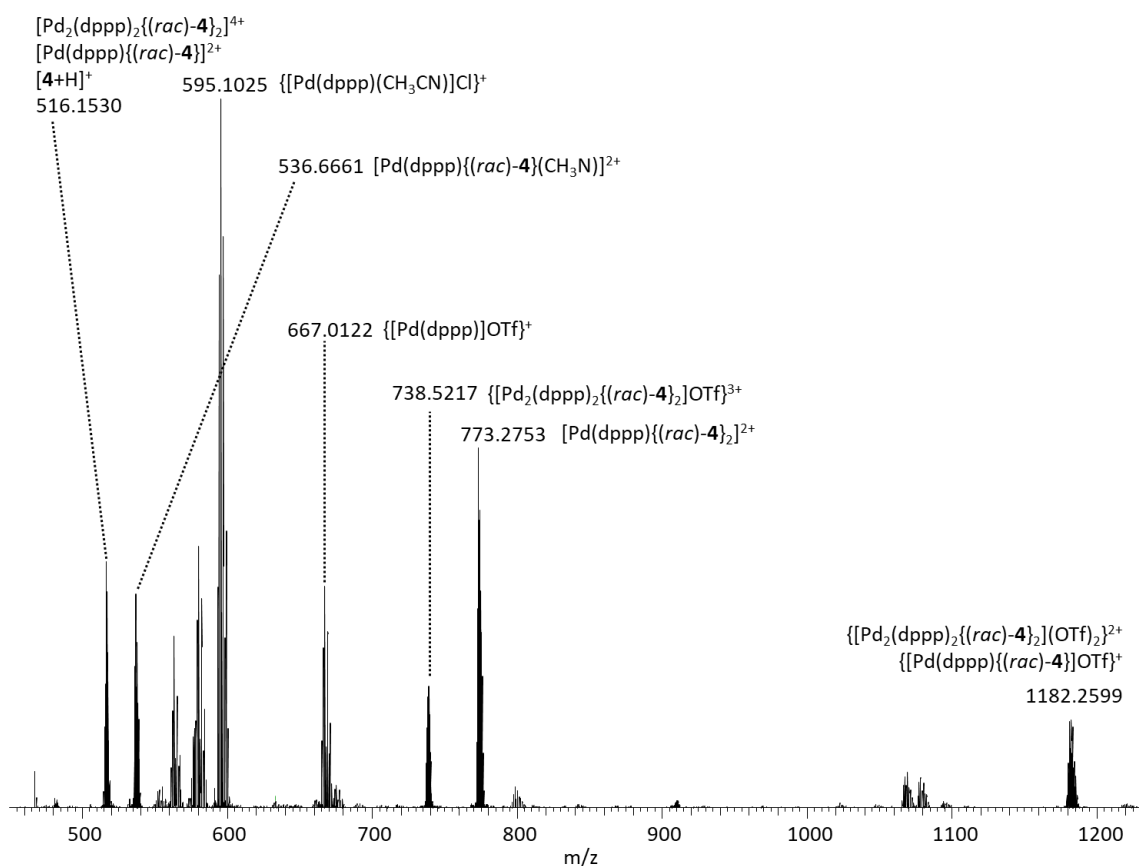


Figure S63: ESI positive mass spectrum of 1:1 mixture of *(rac)-4* and $[\text{Pd}(\text{dppp})](\text{OTf})_2$ in $\text{CD}_3\text{CN}:\text{CD}_2\text{Cl}_2$ 1:1 measured on a *micrOTOF-Q* time-of-flight mass spectrometer.

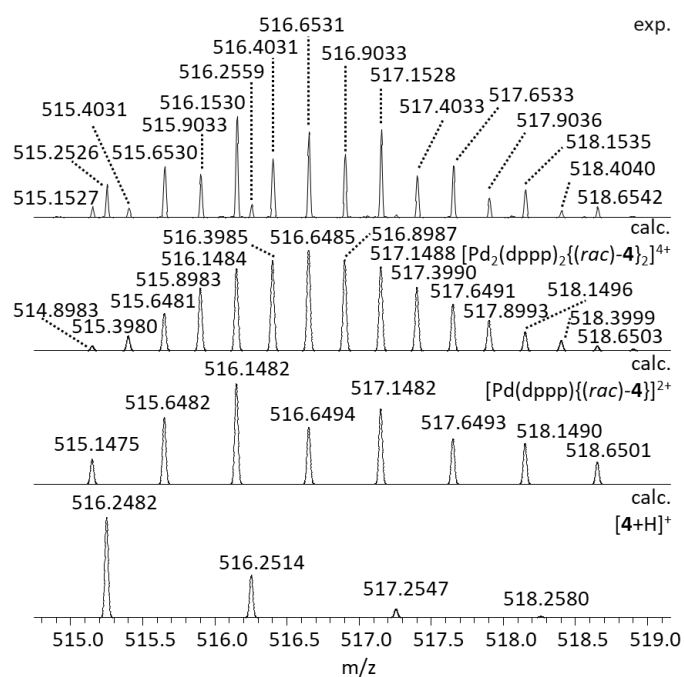


Figure S64: Experimental and calculated high resolution ESI positive mass spectra of $[\text{Pd}_2(\text{dppp})_2\{\text{(rac)-4}\}_2]^{4+}$ in $\text{CD}_3\text{CN}:\text{CD}_2\text{Cl}_2$ 1:1 measured on an *Orbitrap XL* mass spectrometer.

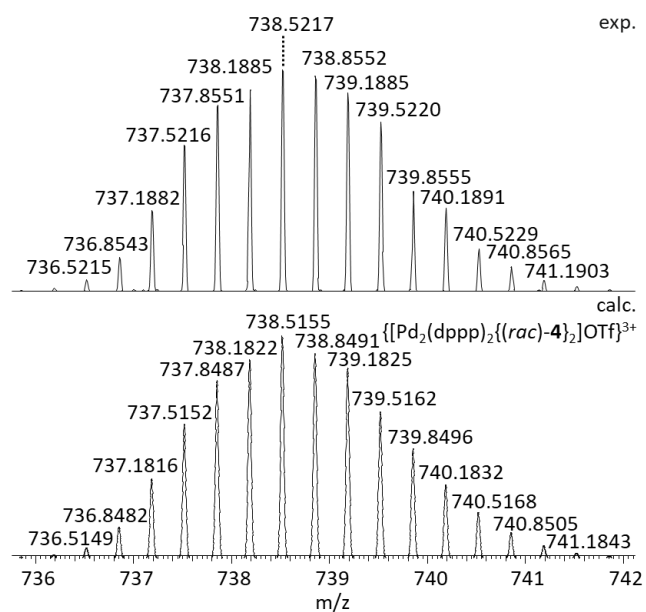
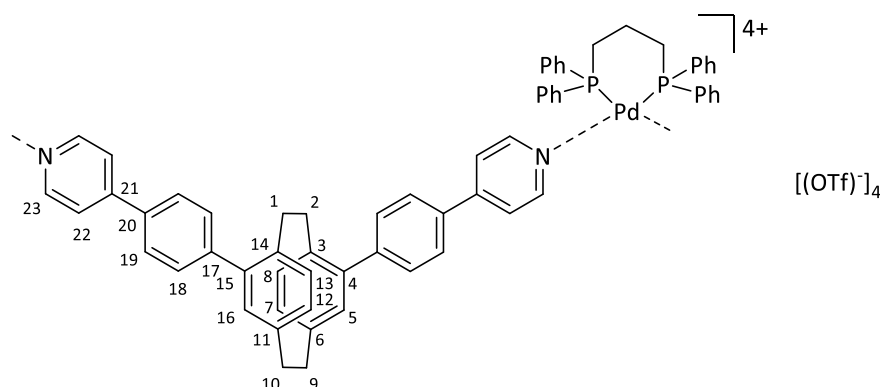


Figure S65: Experimental and calculated high resolution ESI positive mass spectra of $[[Pd_2(dppp)_2((rac)-4)_2]OTf]^{3+}$ in $CD_3CN:CD_2Cl_2$ 1:1 measured on an *Orbitrap XL* mass spectrometer.

[Pd₂(dppp)₂](OTf)₄ in acetonitrile

(*rac*)-, (*R_p*)- or (*S_p*)-**4** (2.05 mg, 3.98 μmol, 1.00 eq.) was dissolved in deuterated acetonitrile (0.5 mL) and a solution of [Pd(dppp)](OTf)₂ (3.27 mg, 4.00 μmol, 1.01 eq.) in deuterated acetonitrile (0.1 mL) was added. The mixture was filtrated.



[Pd₂(dppp)₂]{(*R_p*)-**4**}(OTf)₄

¹H NMR (499.1 MHz, CD₃CN, 298 K): δ [ppm] = 8.59-8.53 (m, 8H, H-23), 7.72-7.52 (m, 40H, H-18, H-19, dppp-Ph_{ortho}, dppp-Ph_{para}), 7.48-7.36 (m, 24H, H-22, dppp-Ph_{meta}), 6.78-6.70 (m, 8H, H-5, H-7, H-12, H-16), 6.69-6.64 (m, 4H, H-8, H-13), 3.32-2.94 (m, 24H, H-1, H-2, H-9, H-10, dppp-CH₂-PPh₂), 2.33-2.17 (m, 4H, dppp-CH₂).

¹³C NMR (125.5 MHz, CD₃CN, 298 K): δ [ppm] = 150.8 (C-23), 144.2*, 141.5*, 138.1*, 134.1*, 133.6*, 133.3*, 132.5*, 131.4*, 130.4*, 128.4*, 126.0*, 124.5*, 123.5*, 120.9*, 35.4*, 34.2*.

*Signals could not be unambiguously assigned.

³¹P NMR (202.1 MHz, CD₃CN, 298 K): δ [ppm] = 8.65 (s, dppp-P).

¹H-DOSY NMR (499.1 MHz, CD₃CN, 298 K): D = 5.15 · 10⁻¹⁰ m²s⁻¹, R_H = 13.2 Å.

MS (ESI+) *m/z*: 516.1512 [Pd₂(dppp)₂]{(*R_p*)-**4**}(OTf)₄⁴⁺ and [Pd(dppp)]{(*R_p*)-**4**}(OTf)₂²⁺, 536.6639 [Pd(dppp)]{(*R_p*)-**4**}(CH₃CN)²⁺, 667.0102 {[Pd(dppp)]OTf}⁺, 738.5190 {[Pd₂(dppp)₂]{(*R_p*)-**4**}(OTf)₃}³⁺, 773.2728 [Pd(dppp)]{(*R_p*)-**4**}(OTf)₂²⁺, 1181.2550 {[Pd₂(dppp)₂]{(*R_p*)-**4**}(OTf)₂}²⁺ and {[Pd(dppp)]{(*R_p*)-**4**}(OTf)}⁺.

UV-Vis (CH₃CN, c = 3.32 mM): λ [nm] = 275, 324.

CD (CH₃CN, c = 3.32 mM): λ [nm] (Δε [L/(mol cm)]) = [Pd₂(dppp)₂]{(*R_p*)-**4**}(OTf)₄: 214 (-25), 237 (+120), 257 (-3), 273 (+53), 291 (-1), 305 (+18), 338 (-236); [Pd₂(dppp)₂]{(*S_p*)-**4**}(OTf)₄: 214 (+33), 237 (-120), 258 (+4), 272 (-52), 291 (+2), 304 (-9), 337 (+247).

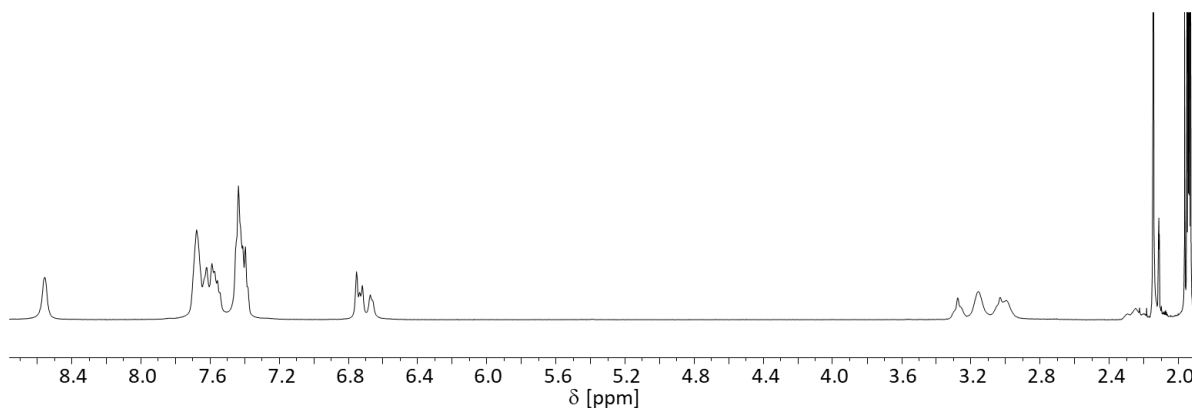


Figure S66: ¹H NMR spectrum (499.1 MHz, CD₃CN, 298 K) of [Pd₂(dppp)₂]{(*R_p*)-**4**}(OTf)₄.

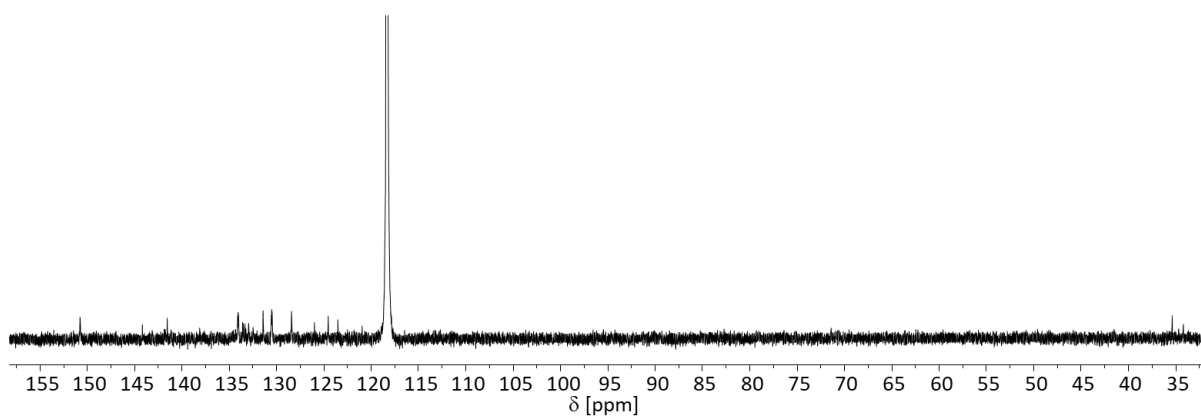


Figure S67: ^{13}C NMR spectrum (125.5 MHz, CD_3CN , 298 K) of $[\text{Pd}_2(\text{dppp})_2\{(\text{R}_p)\text{-4}\}_2](\text{OTf})_4$.

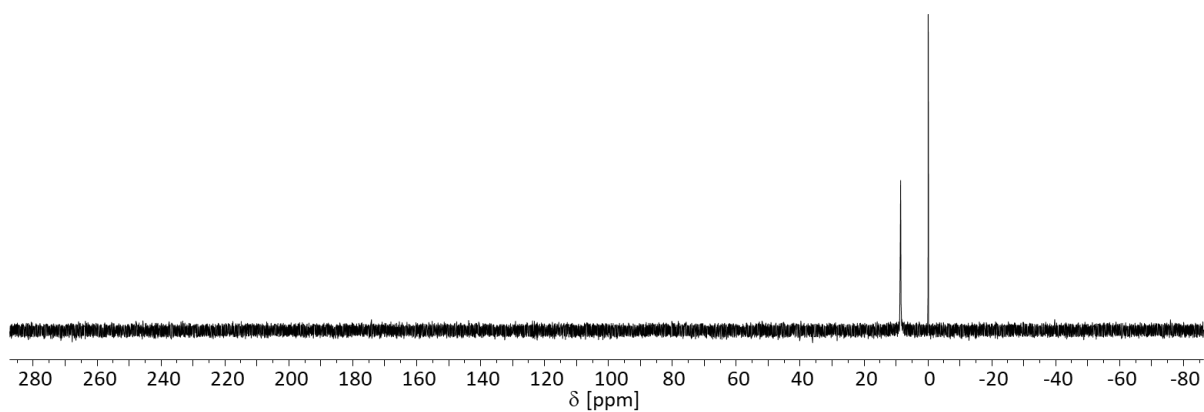


Figure S68: ^{31}P NMR spectrum (202.1 MHz, CD_3CN , 298 K) of $[\text{Pd}_2(\text{dppp})_2\{(\text{R}_p)\text{-4}\}_2](\text{OTf})_4$.

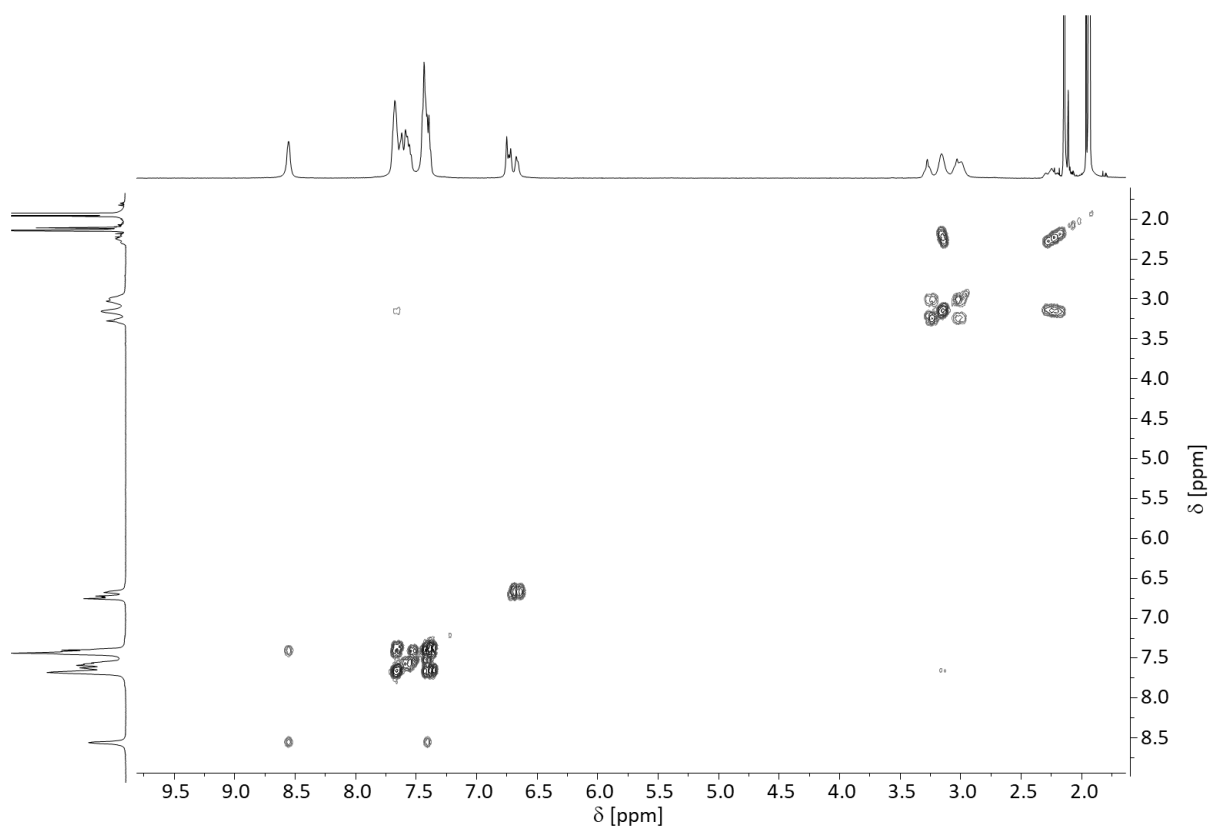


Figure S69: ^1H , ^1H -COSY NMR spectrum (499.1 MHz, CD_3CN , 298 K) of $[\text{Pd}_2(\text{dppp})_2\{(\text{R}_p)\text{-4}\}_2](\text{OTf})_4$.

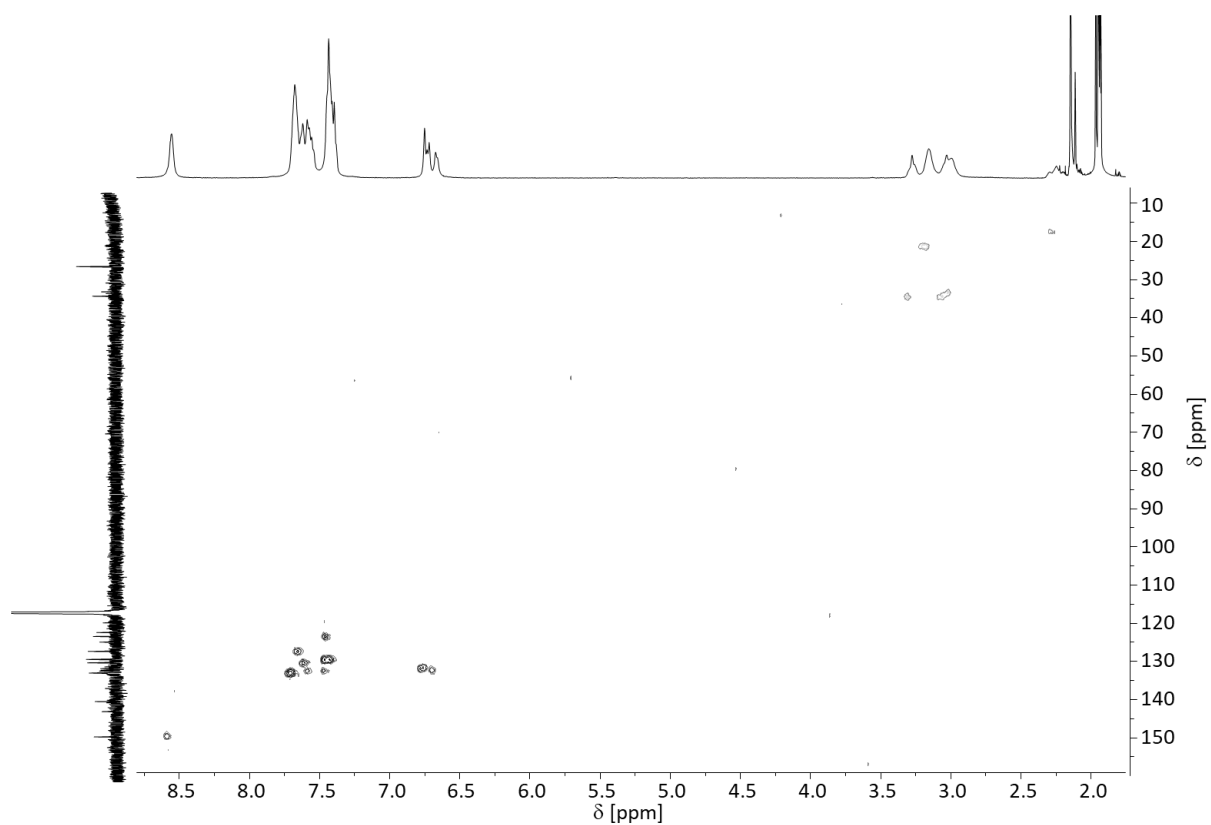


Figure S70: ^1H , ^{13}C -HSQC NMR spectrum (499.1 MHz, 125.5 MHz, CD_3CN , 298 K) of $[\text{Pd}_2(\text{dppp})_2\{(\text{R}_p)\text{-4}\}_2](\text{OTf})_4$.

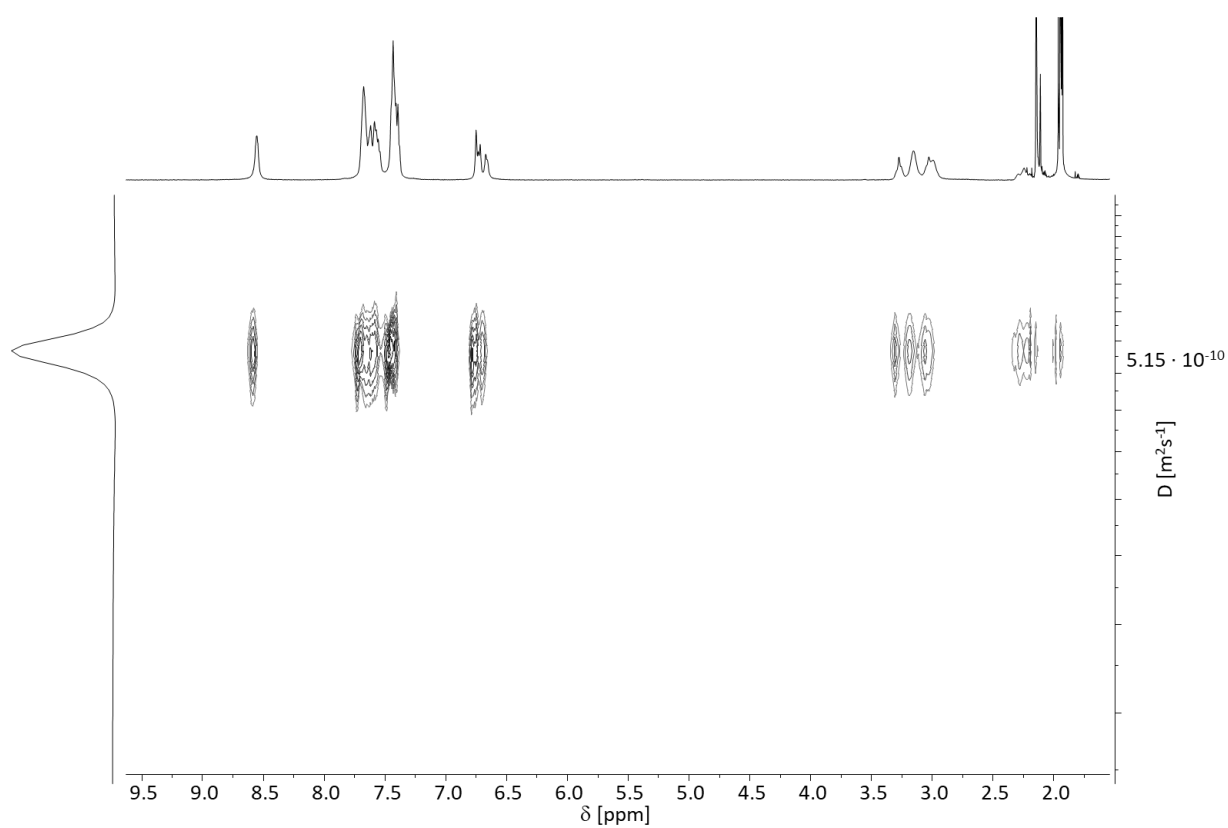


Figure S71: ^1H -DOSY NMR spectrum (499.1 MHz, CD_3CN , 298 K) of $[\text{Pd}_2(\text{dppp})_2\{(\text{R}_p)\text{-4}\}_2](\text{OTf})_4$.

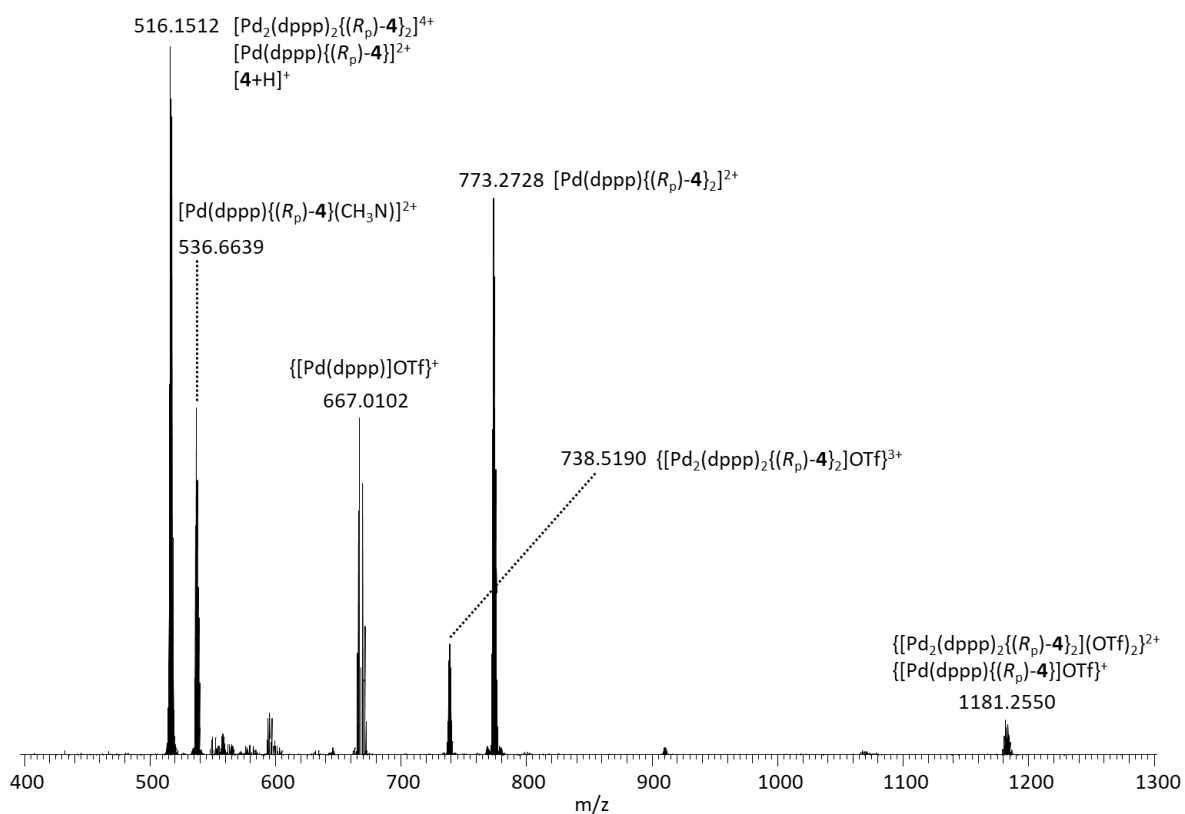


Figure S72: ESI positive mass spectrum of 1:1 mixture of $(\text{R}_p)\text{-4}$ and $[\text{Pd}(\text{dppp})](\text{OTf})_2$ in CD_3CN measured on an *Orbitrap XL* mass spectrometer.

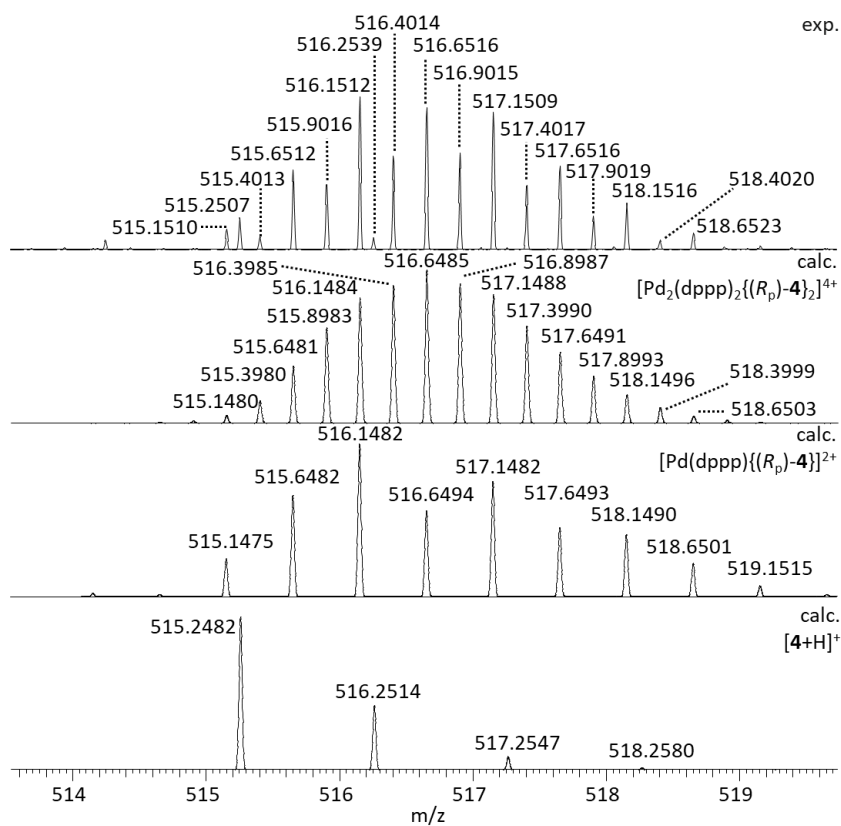


Figure S73: Experimental and calculated high resolution ESI positive mass spectra of $[\text{Pd}_2(\text{dppp})_2\{(\text{R}_p)\text{-4}\}_2]^{4+}$ in CD_3CN measured on an *Orbitrap XL* mass spectrometer.

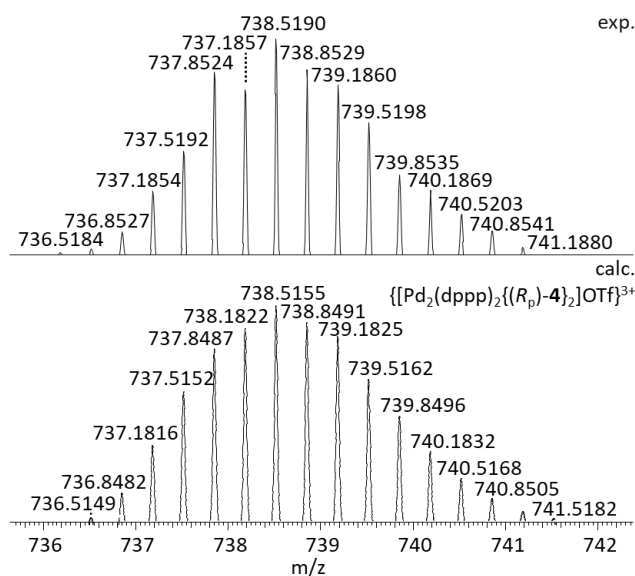


Figure S74: Experimental and calculated high resolution ESI positive mass spectra of $\{[\text{Pd}_2(\text{dppp})_2\{(\text{R}_p)\text{-4}\}_2]\text{OTf}\}^{3+}$ in CD_3CN measured on an *Orbitrap XL* mass spectrometer.

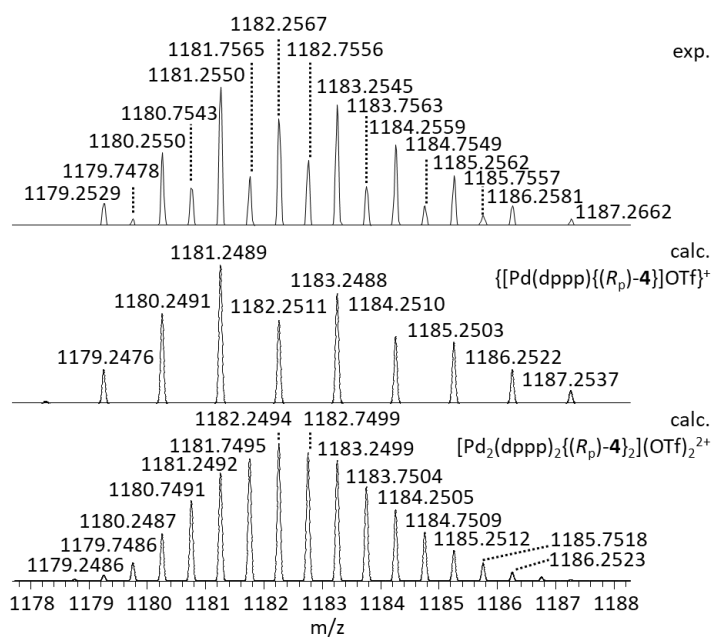


Figure S75: Experimental and calculated high resolution ESI positive mass spectra of $\{[\text{Pd}_2(\text{dppp})_2\{(\text{R}_p)\text{-4}\}_2]\text{OTf}\}^{2+}$ in CD_3CN measured on an *Orbitrap XL* mass spectrometer.

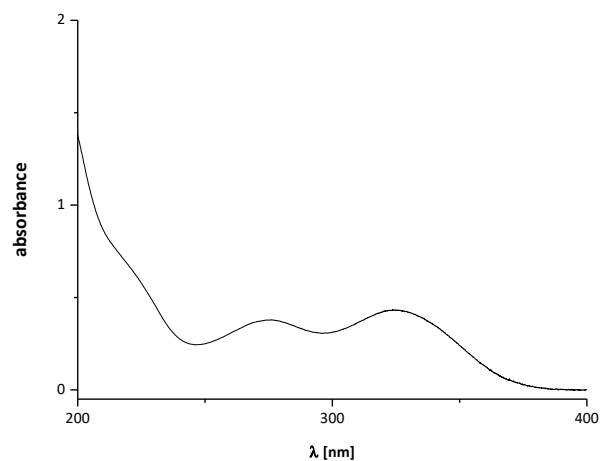


Figure S76: Non-normalized UV-Vis spectrum of $[\text{Pd}_2(\text{dppp})_2\mathbf{4}_2](\text{OTf})_4$ ($c = 3.32 \text{ mM}$ in CH_3CN).

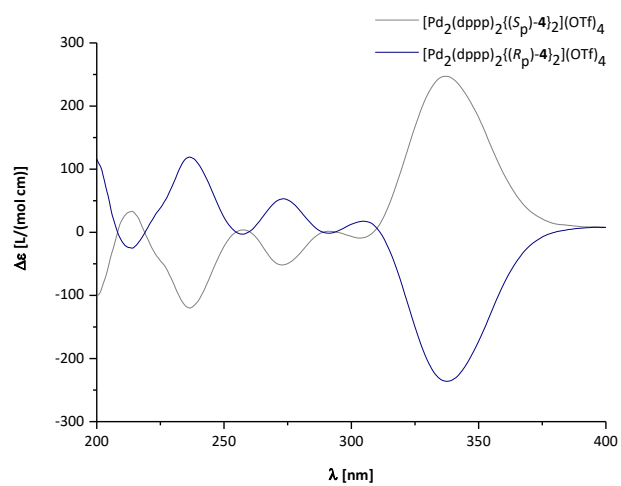


Figure S77: CD spectra of $[\text{Pd}_2(\text{dppp})_2\mathbf{4}_2](\text{OTf})_4$ ($c = 3.32 \text{ mM}$, CH_3CN).

[Pd₂(dppp)₂{(rac)-4}₂](OTf)₄

¹H NMR (499.1 MHz, CD₃CN, 298 K): δ [ppm] = 8.59-8.53 (m, 8H, H-23), 7.72-7.52 (m, 40H, H-18, H-19, dppp-Ph_{ortho}, dppp-Ph_{para}), 7.48-7.36 (m, 24H, H-22, dppp-Ph_{meta}), 6.78-6.70 (m, 8H, H-5, H-7, H-12, H-16), 6.69-6.64 (m, 4H, H-8, H-13), 3.32-2.94 (m, 24H, H-1, H-2, H-9, H-10, dppp-CH₂-PPh₂), 2.33-2.17 (m, 4H, dppp-CH₂).

¹³C NMR (125.5 MHz, CD₃CN, 298 K): δ [ppm] = 150.7 (C-23), 144.1*, 141.5*, 138.1*, 134.0*, 133.5*, 133.3*, 132.9*, 131.4*, 130.5*, 128.4*, 126.0*, 124.6*, 123.5*, 120.9*, 35.4*, 34.2*.

*Signals could not be unambiguously assigned.

³¹P NMR (202.1 MHz, CD₃CN, 298 K): δ [ppm] = 8.65 (s, dppp-P).

¹H-DOSY NMR (499.1 MHz, CD₃CN, 298 K): D = 4.89 · 10⁻¹⁰ m²s⁻¹, R_H = 13.9 Å.

MS (ESI+) *m/z*: 516.1529 [Pd₂(dppp)₂{(rac)-4}₂]⁴⁺ and [Pd(dppp){(rac)-4}]²⁺, 536.1661 [Pd(dppp){(rac)-4}(CH₃CN)]²⁺, 595.1030 [[Pd(dppp)(CH₃CN)]Cl]⁺, 667.0126 [[Pd(dppp)]OTf]⁺, 738.51220 [[Pd₂(dppp)₂{(rac)-4}₂]OTf]³⁺, 773.2757 [Pd(dppp){(rac)-4}]²⁺, 1181.2600 [[Pd₂(dppp)₂{(rac)-4}₂](OTf)₂]²⁺ and [[Pd(dppp){(rac)-4}]OTf]⁺.

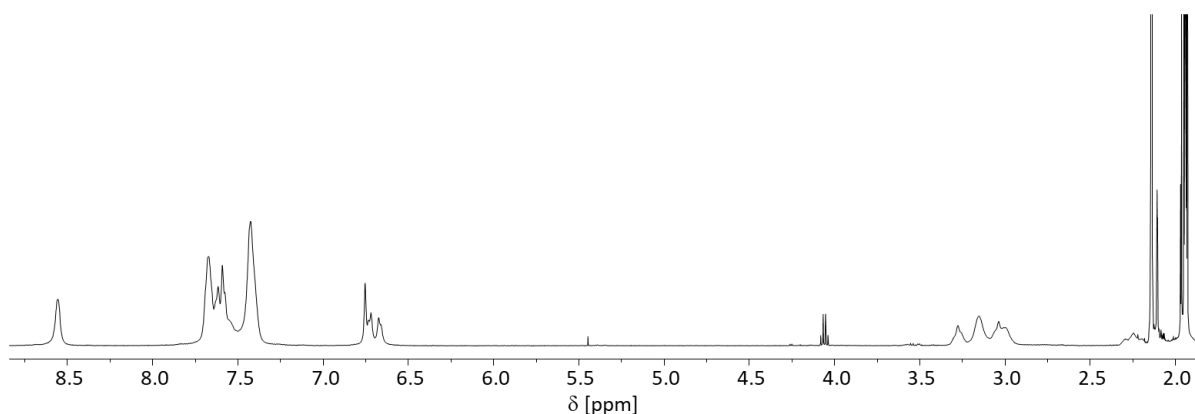


Figure S78: ¹H NMR spectrum (499.1 MHz, CD₃CN, 298 K) of [Pd₂(dppp)₂{(rac)-4}₂](OTf)₄.

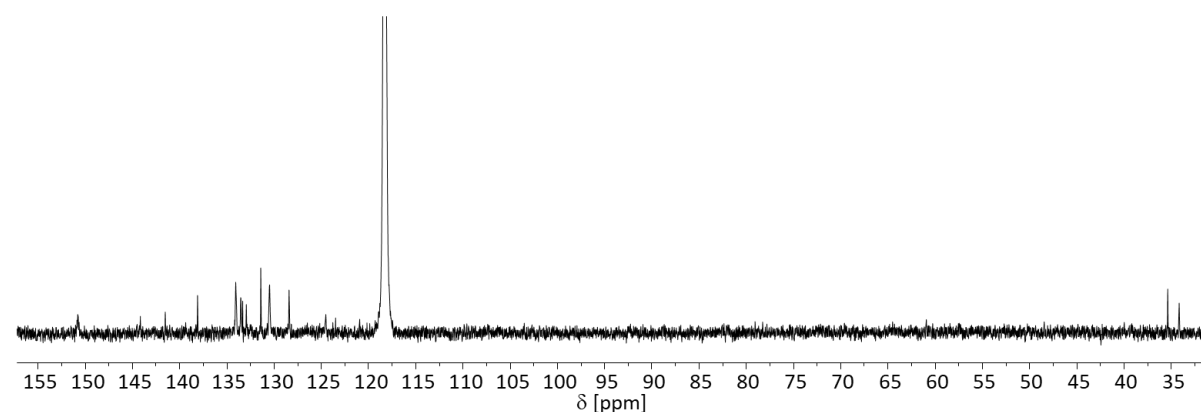


Figure S79: ¹³C NMR spectrum (125.5 MHz, CD₃CN, 298 K) of [Pd₂(dppp)₂{(rac)-4}₂](OTf)₄.

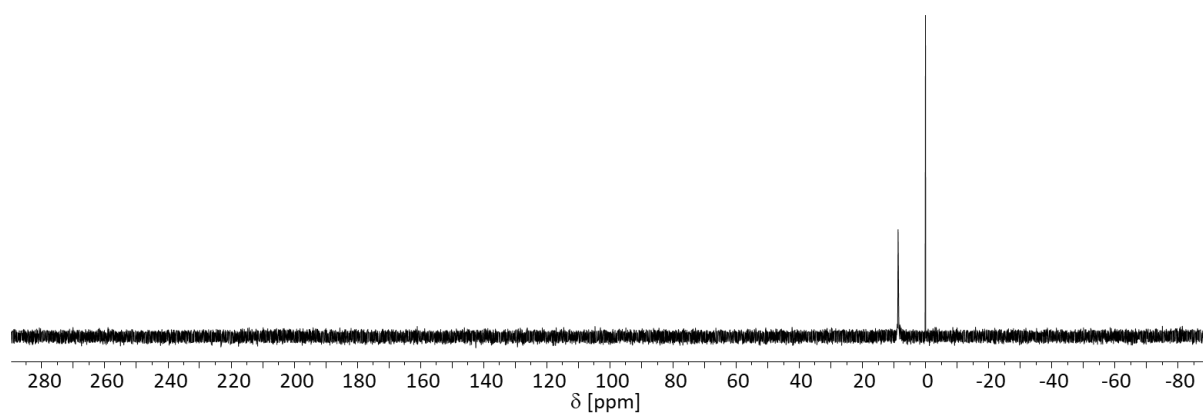


Figure S80: ^{31}P NMR spectrum (202.1 MHz, CD_3CN , 298 K) of $[\text{Pd}_2(\text{dppp})_2\{(\text{rac})\text{-4}\}_2](\text{OTf})_4$.

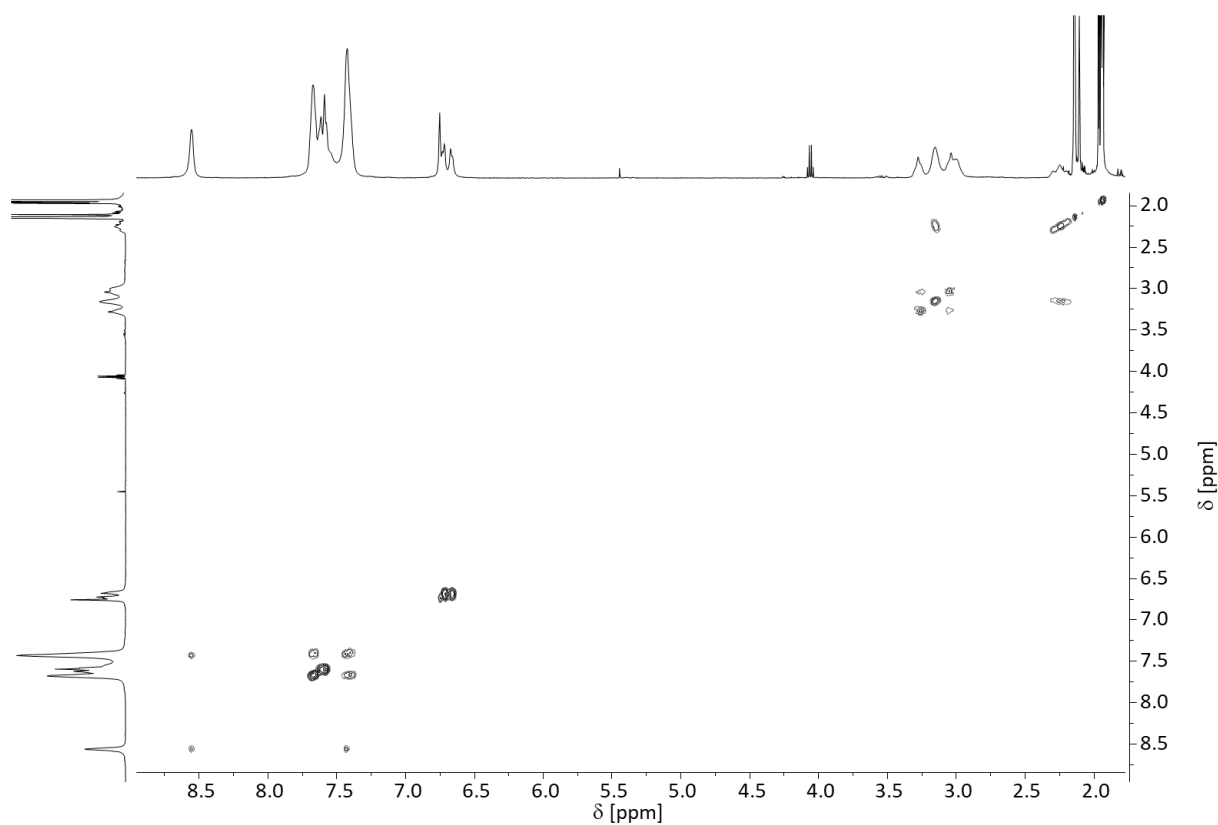


Figure S81: ^1H , ^1H -COSY NMR spectrum (499.1 MHz, CD_3CN , 298 K) of $[\text{Pd}_2(\text{dppp})_2\{(\text{rac})\text{-4}\}_2](\text{OTf})_4$.

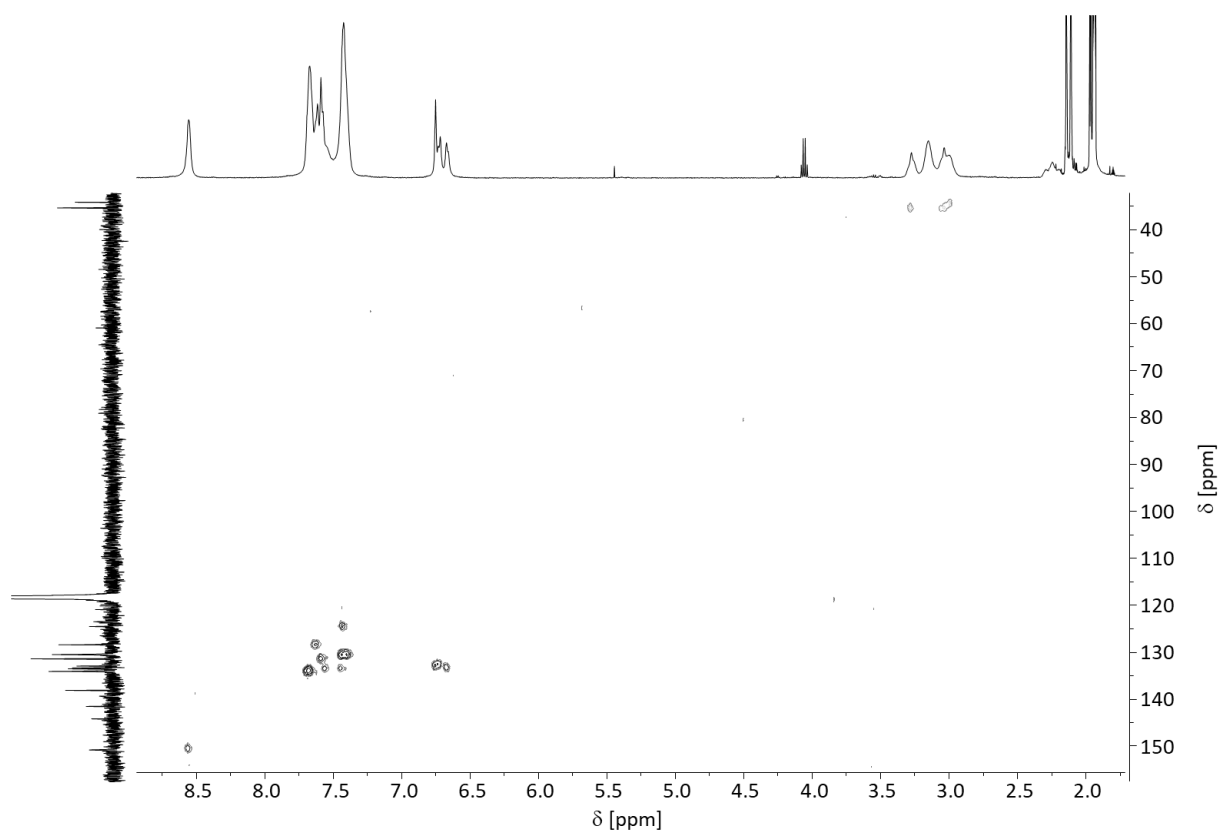


Figure S82: ^1H , ^{13}C -HSQC NMR spectrum (499.1 MHz, 125.5 MHz, CD_3CN , 298 K) of $[\text{Pd}_2(\text{dppp})_2\{\text{rac}\}\text{-4}\}_2](\text{OTf})_4$.

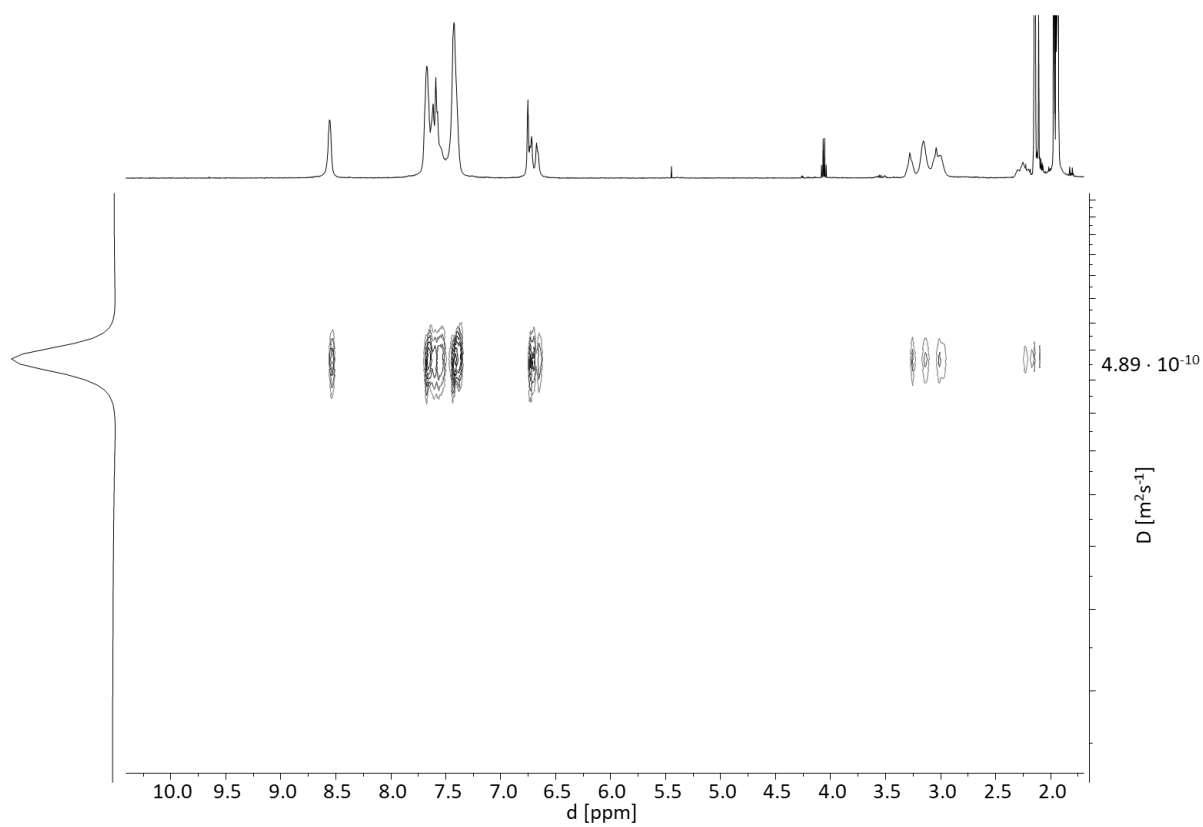


Figure S83: ^1H -DOSY NMR spectrum (499.1 MHz, CD_3CN , 298 K) of $[\text{Pd}_2(\text{dppp})_2\{\text{rac}\}\text{-4}\}_2](\text{OTf})_4$.

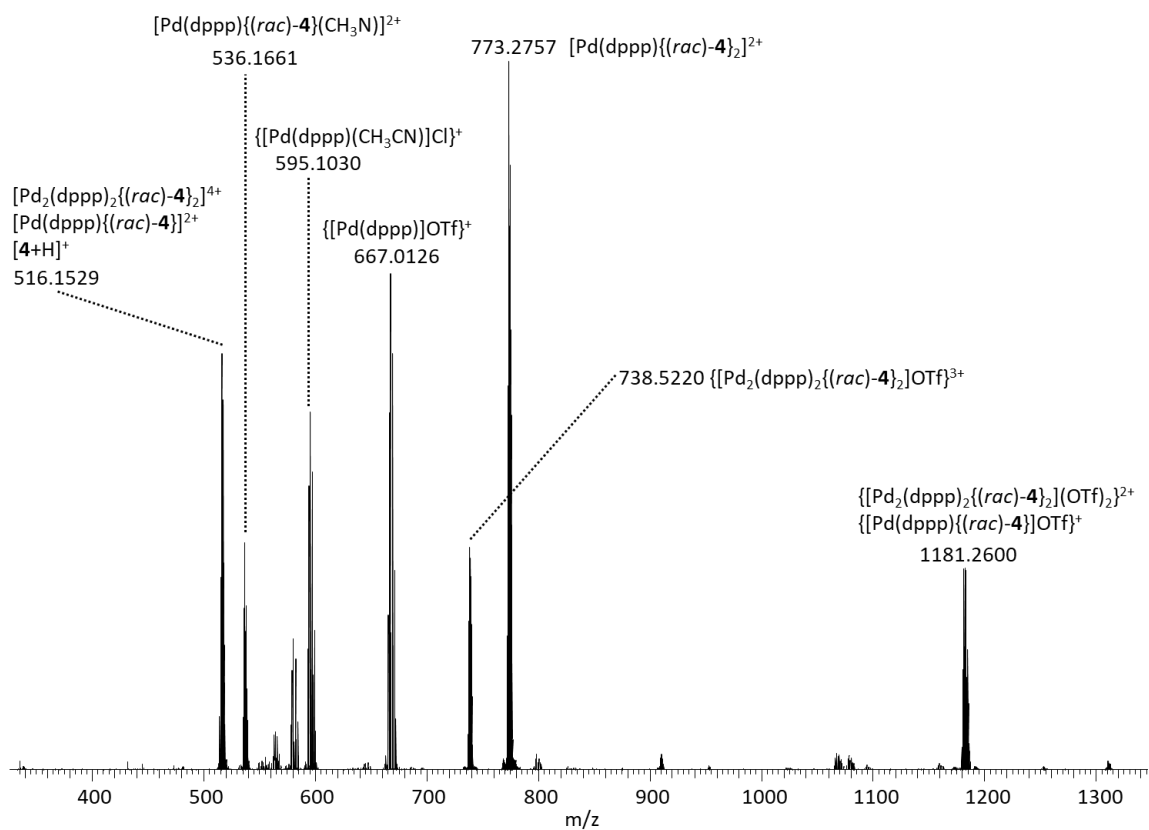


Figure S84: ESI positive mass spectrum of 1:1 mixture of *(rac)*-**4** and $[\text{Pd}(\text{dppp})](\text{OTf})_2$ in CD_3CN measured on an *Orbitrap XL* mass spectrometer.

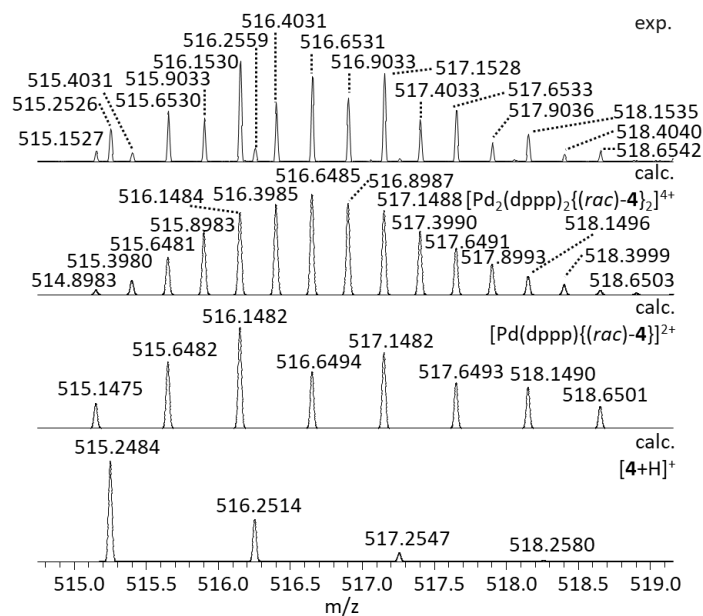


Figure S85: Experimental and calculated high resolution ESI positive mass spectra of $[\text{Pd}_2(\text{dppp})_2\{(\text{rac})\text{-4}\}_2]^{4+}$ in CD_3CN measured on an *Orbitrap XL* mass spectrometer.

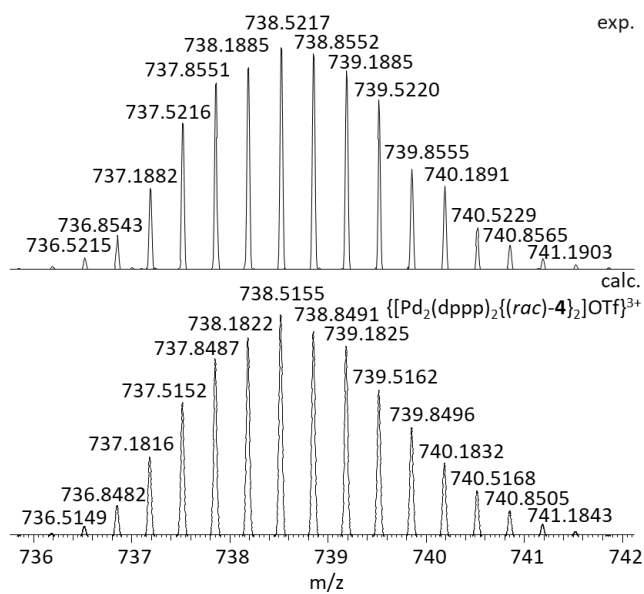
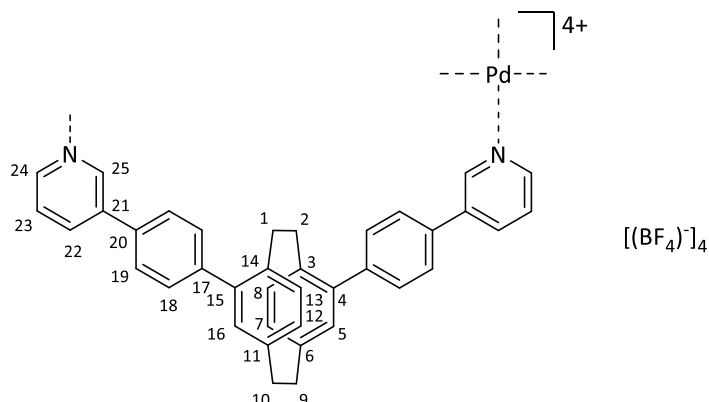


Figure S86: Experimental and calculated high resolution ESI positive mass spectra of $\{[Pd_2(dppp)_2((rac)-4)_2]OTf\}^{3+}$ in CD_3CN measured on an *Orbitrap XL* mass spectrometer.

[Pd₂5₄](BF₄)₄ in acetonitrile

(rac)-, (R_p)- or (S_p)-**5** (4.00 mg, 7.77 μmol, 1.00 eq.) was dissolved in deuterated acetonitrile (1 mL) and a solution of [Pd(CH₃CN)₄](BF₄)₂ (1.76 mg, 3.96 μmol, 0.51 eq.) in deuterated acetonitrile (0.5 mL) was added. The mixture was stirred at 70 °C for 15 h and then filtrated.



[Pd₂{(R_p)-**5**}]₄(BF₄)₄

¹H NMR (499.1 MHz, CD₃CN, 298 K): δ [ppm] = 9.47 (d, 8 H, H-25, ⁴J_{25,22} = 2.0 Hz), 9.13 (dd, 8H, H-24, ³J_{24,23} = 5.7 Hz, ⁴J_{24,22} = 1.3 Hz), 8.32 (ddd, 8H, H-22, ³J_{22,23} = 8.00 Hz, ⁴J_{22,25} = 2.0 Hz, ⁴J_{22,24} = 1.3 Hz), 7.75 (dd, 8H, H-23, ³J_{23,22} = 8.0 Hz, ³J_{23,24} = 5.7 Hz), 7.68-7.65 (m, 16H, H-19), 7.65-7.62 (m, 16H, H-18), 6.75 (d, 8H, H-5, H-16, ⁴J_{5,7} = ⁴J_{16,12} = 1.5 Hz), 6.64-6.59 (m, 16H, H-8, H-13, H-7, H-12), 3.42-3.34 (m, 8H, H-1, H-2), 3.25-3.17 (m, 8H, H-9, H-10), 3.06-3.97 (m, 8H, H-9, H-10), 2.51-2.42 (m, 8H, H-1, H-2).

¹³C NMR (125.5 MHz, CD₃CN, 298 K): δ [ppm] = 150.9 (C-24), 149.7 (C-25), 143.2 (C-17), 141.8 (C-4, C-15), 141.7 (C-6, C-11), 140.9 (C-21), 140.3 (C-22), 137.5 (C-3, C-14), 134.6 (C-20), 133.5* (C-7, C-8, C-12, C-13), 133.1 (C-5, C-16), 132.6* (C-7, C-8, C-12, C-13), 131.5 (C-19), 128.6 (C-23), 128.5 (C-18), 35.3 (C-9, C-10), 34.8 (C-1, C-2).

* Signals could not be unambiguously assigned.

¹⁹F NMR (469.6 MHz, CD₃CN, 298 K): δ [ppm] = -151.74 (s, BF₄), -151.79 (s, BF₄).

¹H-DOSY NMR (499.1 MHz, CD₃CN, 298 K): D = 5.49 · 10⁻¹⁰ m²s⁻¹, R_H = 10.2 Å.

MS (ESI+) *m/z*: 567.7 [Pd₂{(R_p)-**5**}]₄⁴⁺, 786.0 {[Pd₂{(R_p)-**5**}]₄(BF₄)₃}³⁺, 1222.5 {[Pd₂{(R_p)-**5**}]₄(BF₄)₂}²⁺.

UV-Vis (CH₃CN, c = 3.24 mm): λ [nm] = 275, 324.

CD (CH₃CN, c = 3.24 mm): λ [nm] (Δε [L/(mol cm)]) = [Pd₂{(R_p)-**5**}]₄(BF₄)₄: 211 (-66), 236 (+137), 249 (+102), 259 (+107), 272 (+53), 282 (+63), 323 (-470); [Pd₂{(S_p)-**5**}]₄(BF₄)₄: 212 (+52), 236 (-101), 248 (-70), 255 (-72), 271 (-11), 285 (-34), 322 (+358).

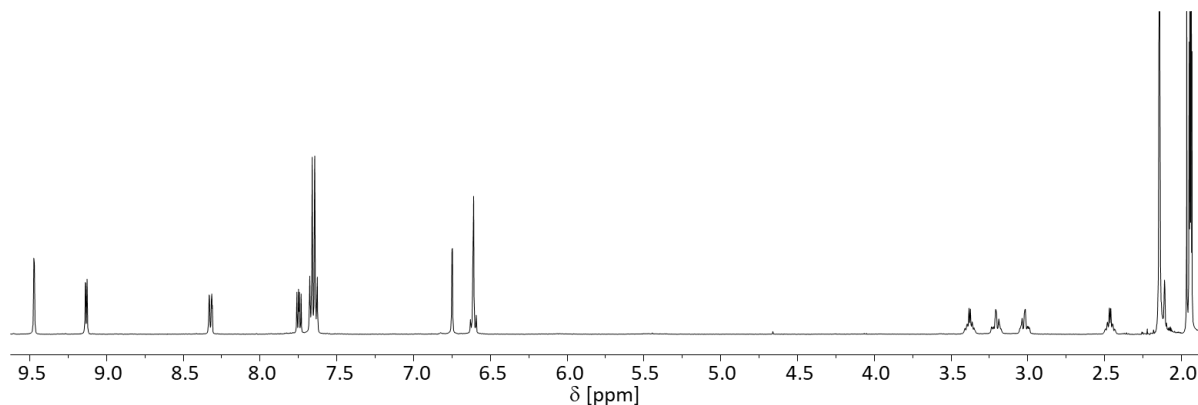


Figure S87: ¹H NMR spectrum (499.1 MHz, CD₃CN, 298 K) of [Pd₂{(R_p)-**5**}]₄(BF₄)₄.

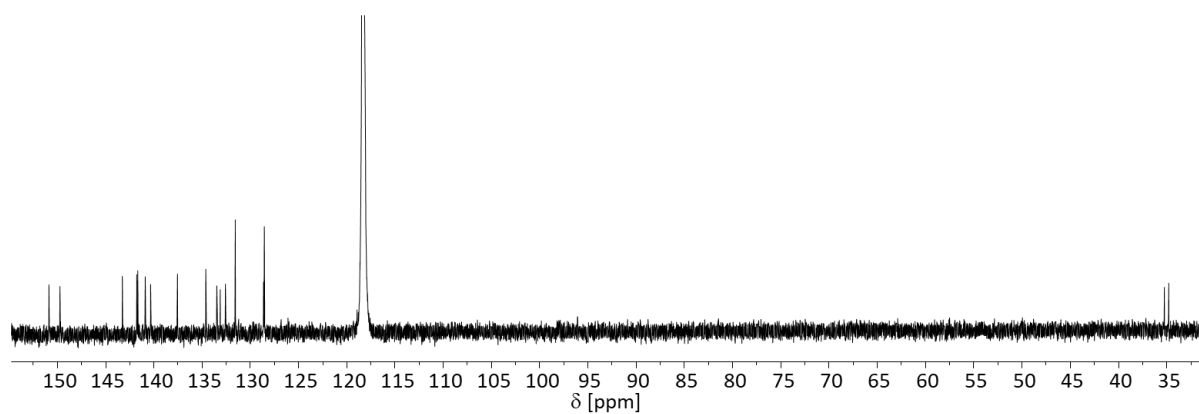


Figure S88: ^{13}C NMR spectrum (125.5 MHz, CD_3CN , 298 K) of $[\text{Pd}_2\{(\text{R}_p)\text{-5}\}_4](\text{BF}_4)_4$.

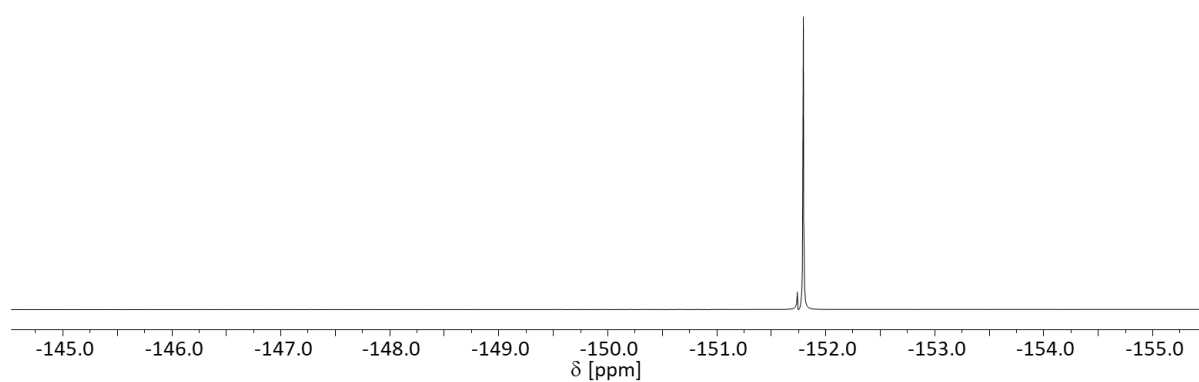


Figure S89: ^{19}F NMR spectrum (469.6 MHz, CD_3CN , 298 K) of $[\text{Pd}_2\{(\text{R}_p)\text{-5}\}_4](\text{BF}_4)_4$.

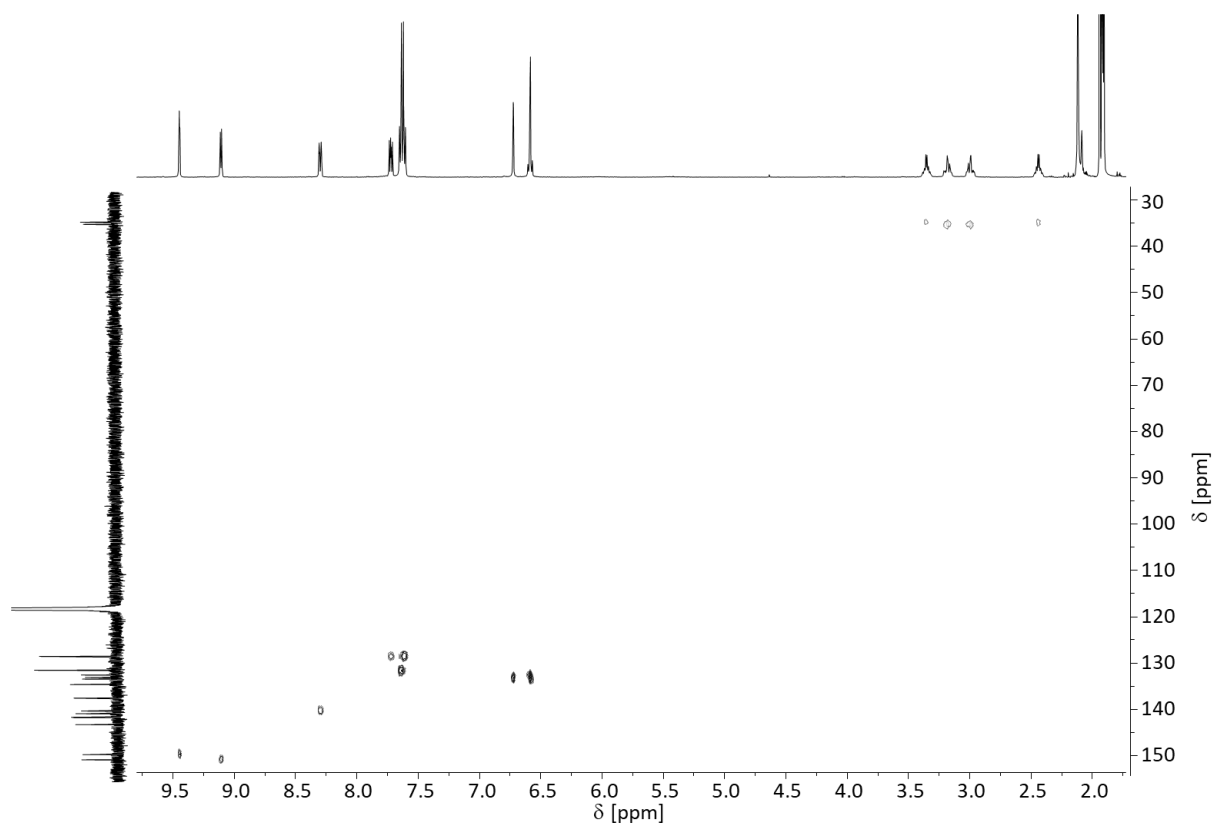


Figure S90: ^1H , ^{13}C -HSQC NMR spectrum (499.1 MHz, 125.5 MHz, CD_3CN , 298 K) of $[[\text{Pd}_2\{(\text{R}_p)\text{-5}\}_4](\text{BF}_4)_4$.

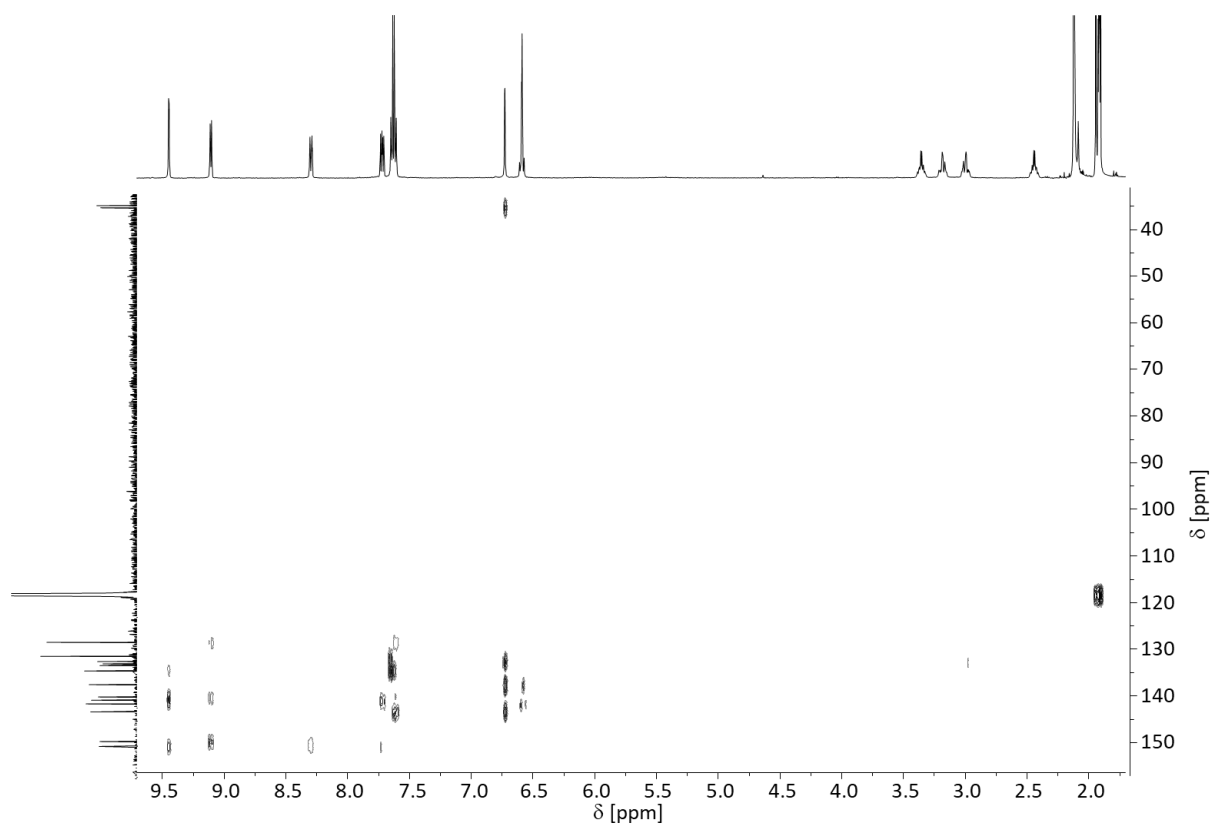


Figure S91: ^1H , ^{13}C -HMBC NMR spectrum (499.1 MHz, 125.5 MHz, CD_3CN , 298 K) of $[\text{Pd}_2\{(\text{R}_p)\text{-5}\}_4](\text{BF}_4)_4$.

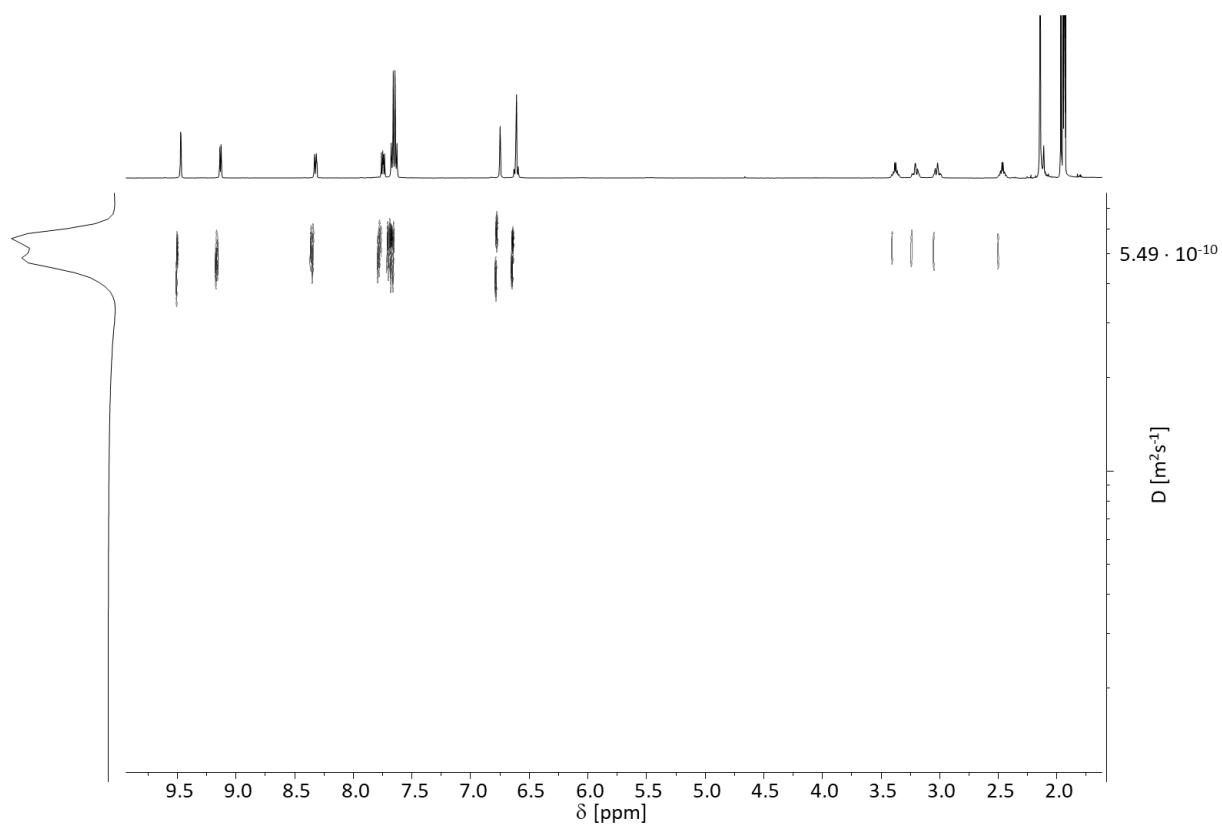


Figure S92: ^1H -DOSY NMR spectrum (499.1 MHz, CD_3CN , 298 K) of $[\text{Pd}_2\{(\text{R}_p)\text{-5}\}_4](\text{BF}_4)_4$.

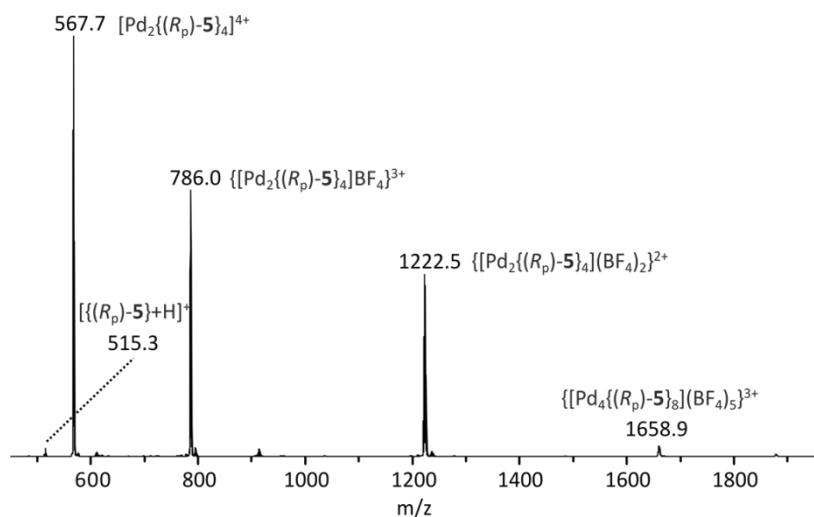


Figure S93: ESI positive mass spectrum of 2:1 mixture of (*R_p*)-5 and [Pd(CH₃CN)₄](BF₄)₂ in CD₃CN measured on a *micrOTOF-Q* time-of-flight spectrometer.

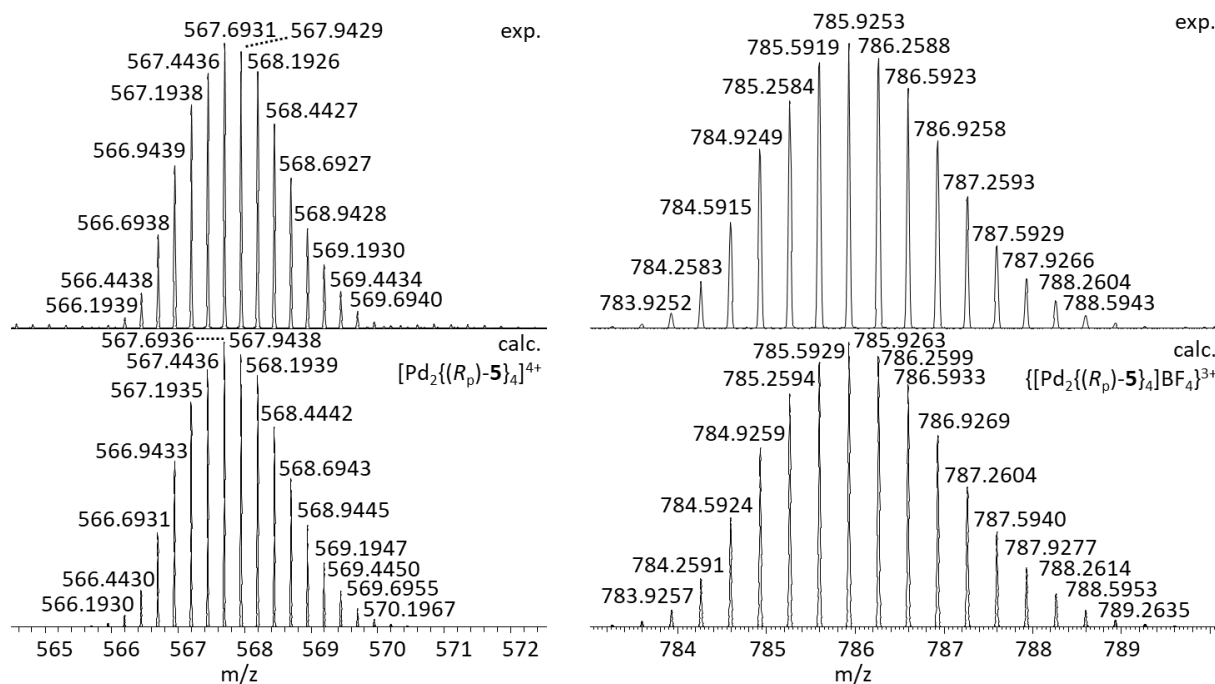


Figure S94: Experimental and calculated high resolution ESI positive mass spectra of [Pd₂{(*R_p*)-5}₄]⁴⁺ (left) and {[Pd₂{(*rac*)-5}₄]BF₄]³⁺ (right) in CD₃CN measured on an *Orbitrap XL* mass spectrometer.

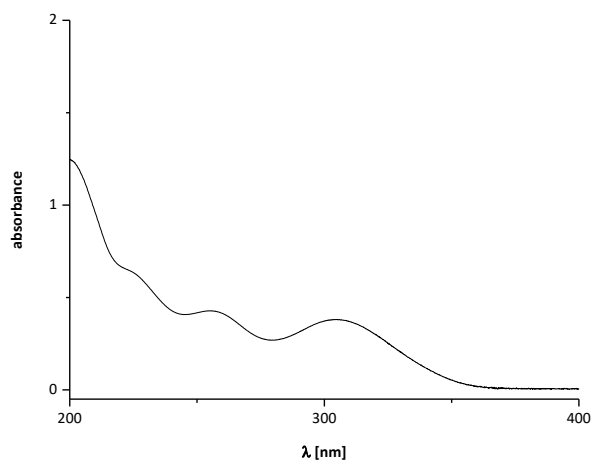


Figure S95: Non-normalized UV-Vis spectrum of $[\text{Pd}_2\mathbf{5}_4](\text{BF}_4)_4$ ($c = 3.24 \text{ mM}$ in CH_3CN).

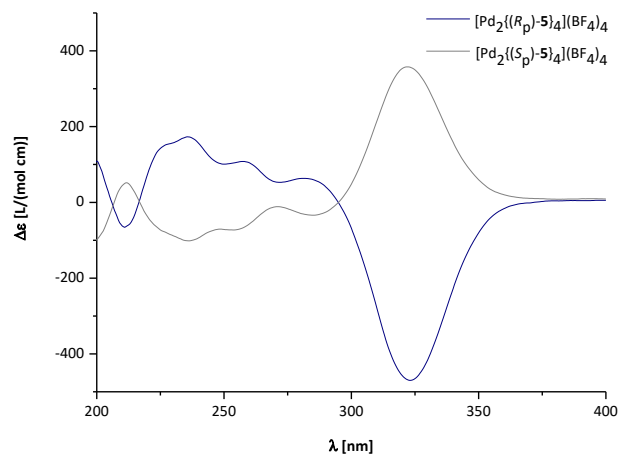


Figure S96: CD spectra of $[\text{Pd}_2\mathbf{5}_4](\text{BF}_4)_4$ ($c = 3.24 \text{ mM}$, CH_3CN).

[Pd₂{(rac)-5₄}] (BF₄)₄

¹⁹F NMR (469.6 MHz, CD₃CN, 298 K): δ [ppm] = -151.60 (s, BF₄), -151.65 (s, BF₄).

¹H-DOSY NMR (700.4 MHz, CD₃CN, 298 K): D = 6.52 · 10⁻¹⁰ m²s⁻¹, R_H = 10.4 Å.

MS (ESI+) m/z: 567.8 [Pd₂{(rac)-5₄}]⁴⁺, 786.0 {[Pd₂{(rac)-5₄}] (BF₄)₃}³⁺, 1222.5 {[Pd₂{(rac)-5₄}] (BF₄)₂}²⁺.

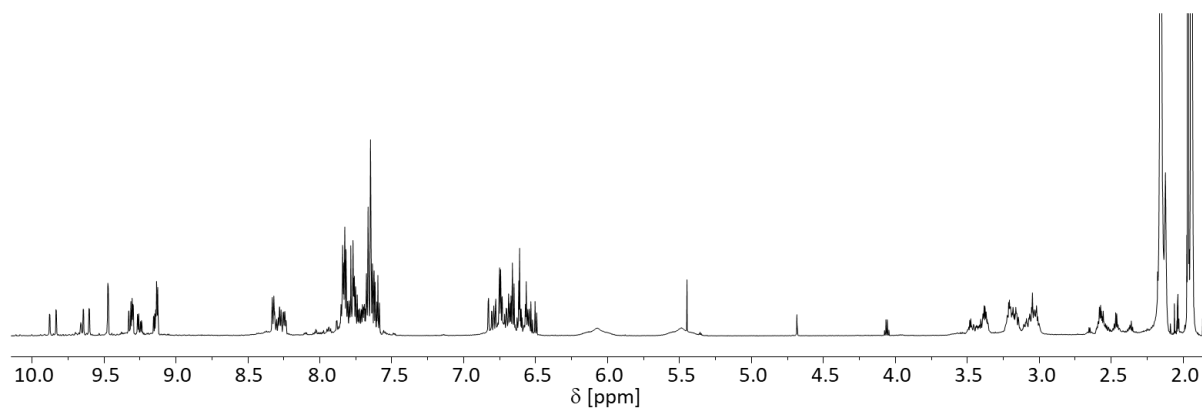


Figure S97: ¹H NMR spectrum (700.4 MHz, CD₃CN, 298 K) of [Pd₂{(rac)-5₄}] (BF₄)₄.

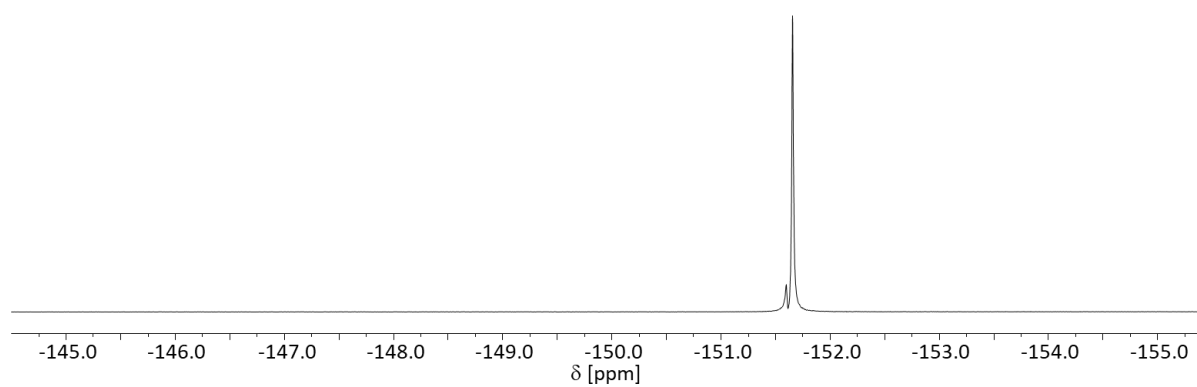


Figure S98: ¹⁹F NMR spectrum (469.6 MHz, CD₃CN, 298 K) of [Pd₂{(rac)-5₄}] (BF₄)₄.

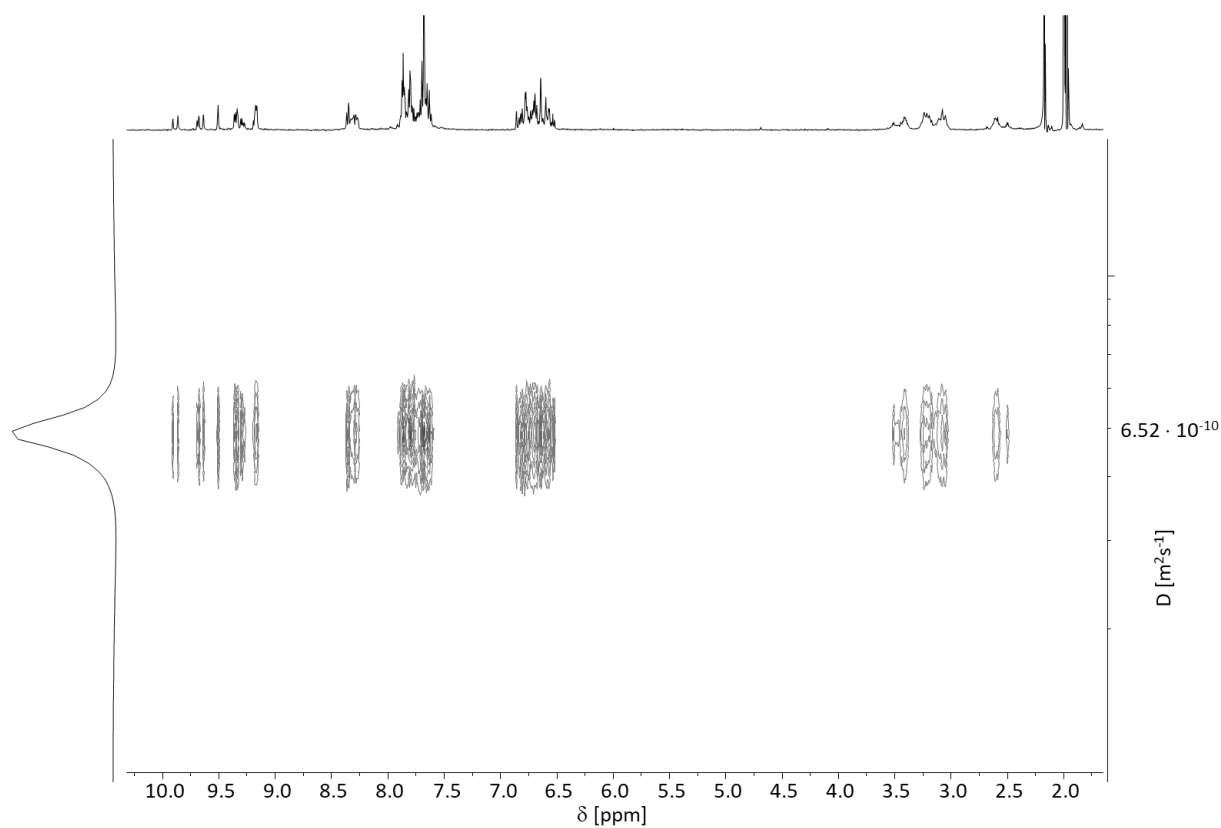


Figure S99: ^1H -DOSY NMR spectrum (499.1 MHz, CD_3CN , 298 K) of $[\text{Pd}_2\{(\text{rac})\text{-5}\}_4](\text{BF}_4)_4$.

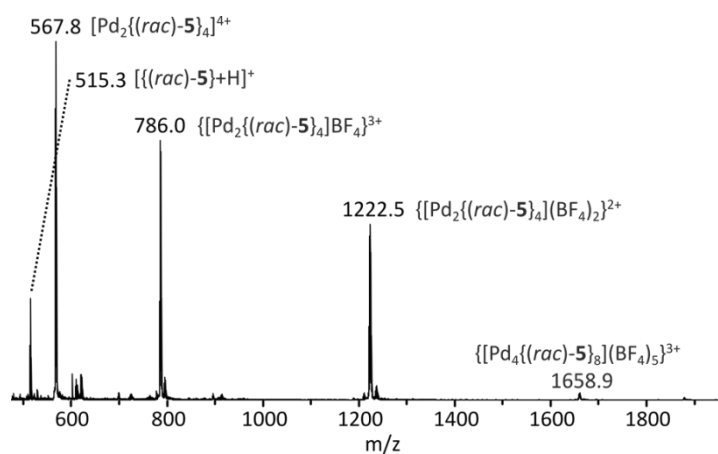


Figure S100: ESI positive mass spectrum of 2:1 mixture of $(\text{rac})\text{-5}$ and $[\text{Pd}(\text{CH}_3\text{CN})_4](\text{BF}_4)_2$ in CD_3CN measured on a *micro*TOF-Q time-of-flight spectrometer.

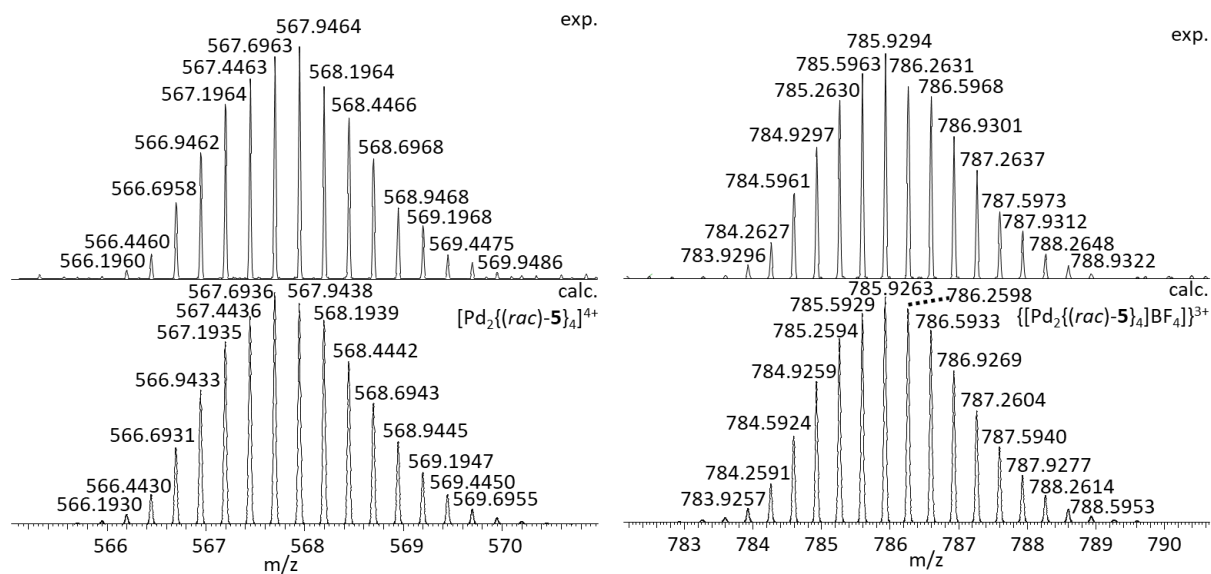
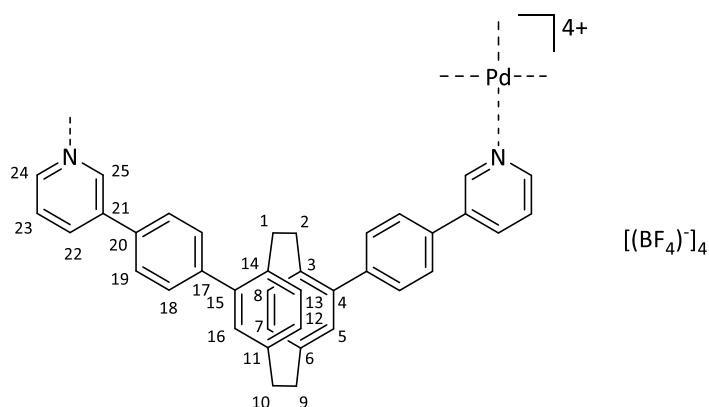


Figure S101: Experimental and calculated high resolution ESI positive mass spectra of $[\text{Pd}_2\{(\text{rac})\text{-5}\}_4]^{4+}$ (left) and $\{[\text{Pd}_2\{(\text{rac})\text{-5}\}_4]\text{BF}_4\}^{3+}$ (right) in CD_3CN measured on an *Orbitrap XL* mass spectrometer.

[Pd₂5₄](BF₄)₄ in dimethyl sulfoxide

(*rac*)-, (*R_p*)- or (*S_p*)-**5** (4.00 mg, 7.77 μmol, 1.00 eq.) was dissolved in deuterated dimethyl sulfoxide (1 mL) and a solution of [Pd(CH₃CN)₄](BF₄)₂ (1.76 mg, 3.96 μmol, 0.51 eq.) in deuterated dimethyl sulfoxide (0.5 mL) was added. The mixture was stirred at 70 °C for 15 h and then filtrated.



[Pd₂{(*R_p*)-**5**}]₄(BF₄)₄

¹H NMR (700.4 MHz, DMSO-*d*₆, 298 K): δ [ppm] = 9.67 (d, 8H, H-25, ⁴J_{25,22} = 2.4 Hz), 9.35 (dd, 8H, H-24, ³J_{24,23} = 5.7 Hz, ⁴J_{24,22} = 1.4 Hz), 8.45-8.42 (m, 8H, H-22), 7.90 (dd, 8H, H-23, ³J_{23,22} = 7.8 Hz, ³J_{23,24} = 5.7 Hz), 7.71-7.68 (m, 16H, H-19), 7.65-7.62 (m, 16H, H-18), 6.7 (d, 8H, H-5, H-16, ⁴J_{5,7} = ⁴J_{16,12} = 2.2 Hz), 6.67-6.64 (m, 8H, H-7, H-12), 6.51 (d, 8H, H-8, H-13, ³J_{8,7} = ³J_{13,12} = 7.8 Hz), 3.36-3.30* (m, 8H, H-1, H-2, H-9, H-10), 3.18-3.12* (m, 8H, H-1, H-2, H-9, H-10), 2.98-2.92* (m, 8H, H-1, H-2, H-9, H-10), 2.31-2.25* (m, 8H, H-1, H-2, H-9, H-10).

* Signals could not be unambiguously assigned.

¹³C NMR (176.1 MHz, DMSO-*d*₆, 298 K): δ [ppm] = 150.2 (C-24), 148.8 (C-25), 141.5 (C-17), 140.2 (C-4, C-15), 139.2 (C-22), 138.4 (C-21), 135.4 (C-3, C-14), 133.4 (C-20), 132.3 (C-8, C-13), 132.1 (C-5, C-16), 131.3 (C-7, C-12), 130.2 (C-18), 127.5 (C-19), 127.4 (C-23), 118.1 (C-6, C-11), 34.1 (C-1, C-2, C-9, C-10).

¹⁹F NMR (469.6 MHz, DMSO-*d*₆, 298 K): δ [ppm] = -148.8 (s, BF₄), -167.6 (s, BF₄).

¹H-DOSY NMR (700.4 MHz, DMSO-*d*₆, 298 K): D = 1.04 · 10⁻¹⁰ m²s⁻¹, R_H = 10.6 Å.

MS (ESI+) *m/z*: 567.6956 [Pd₂{(*R_p*)-**5**}]₄⁴⁺, 785.9290 {[Pd₂{(*R_p*)-**5**}]₄(BF₄)₃}³⁺, 1221.3960 {[Pd₂{(*R_p*)-**5**}]₄(BF₄)₂}²⁺.

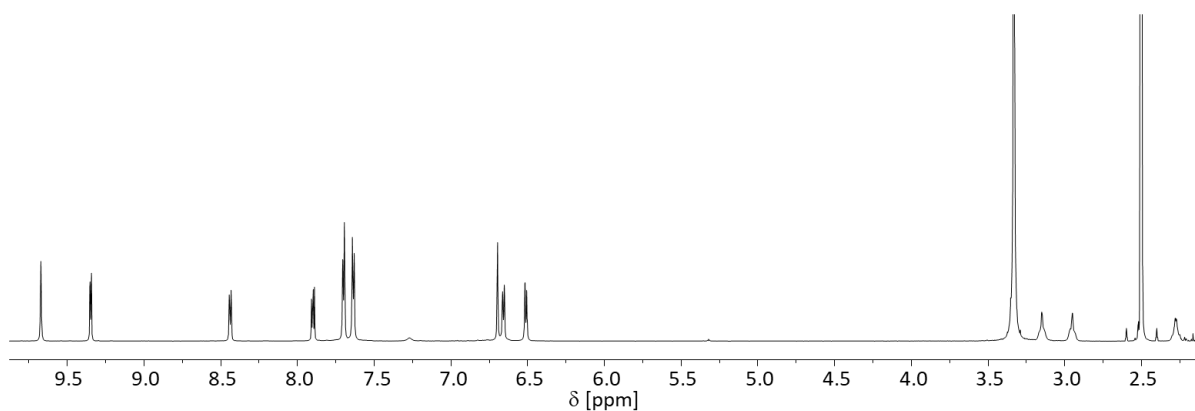


Figure S102: ¹H NMR spectrum (700.4 MHz, DMSO-*d*₆, 298 K) of [Pd₂{(*R_p*)-**5**}]₄(BF₄)₄.

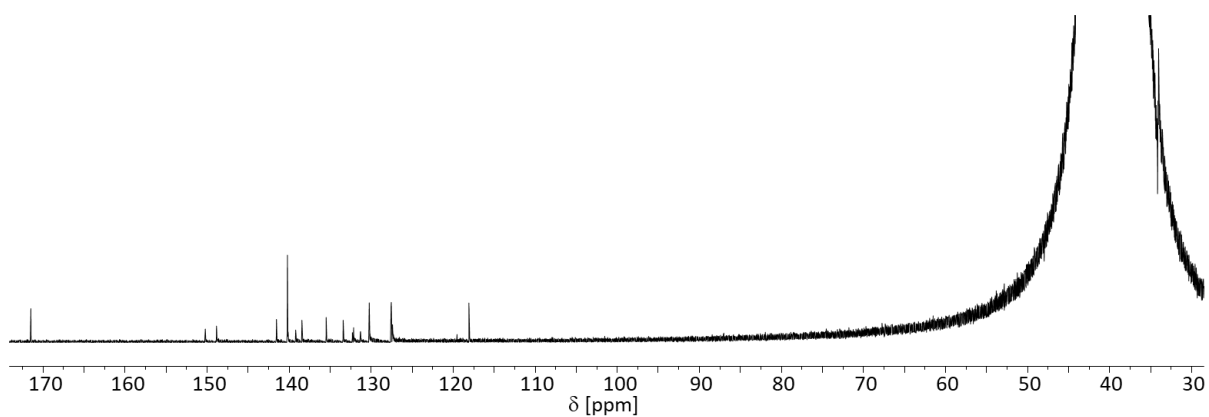


Figure S103: ^{13}C NMR spectrum (176.1 MHz, $\text{DMSO-}d_6$, 298 K) of $[\text{Pd}_2\{(\text{R}_p)\text{-5}\}_4](\text{BF}_4)_4$.

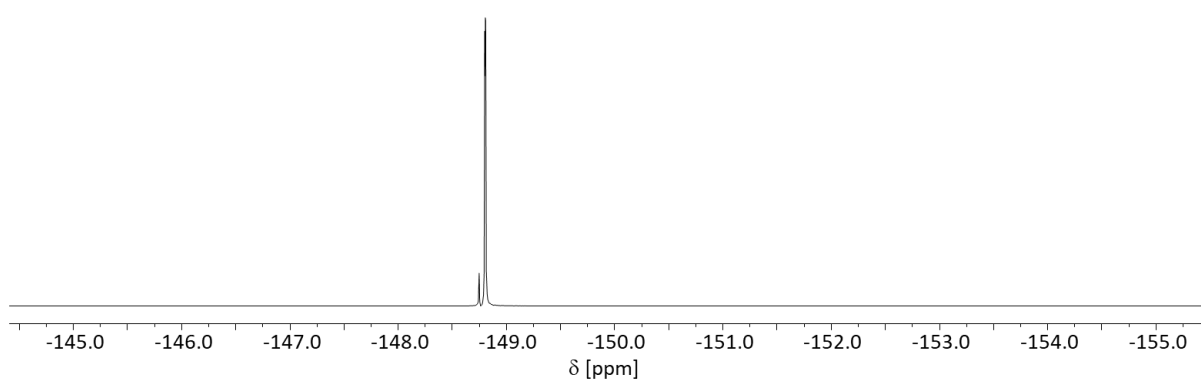


Figure S104: ^{19}F NMR spectrum (469.6 MHz, $\text{DMSO-}d_6$, 298 K) of $[\text{Pd}_2\{(\text{R}_p)\text{-5}\}_4](\text{BF}_4)_4$.

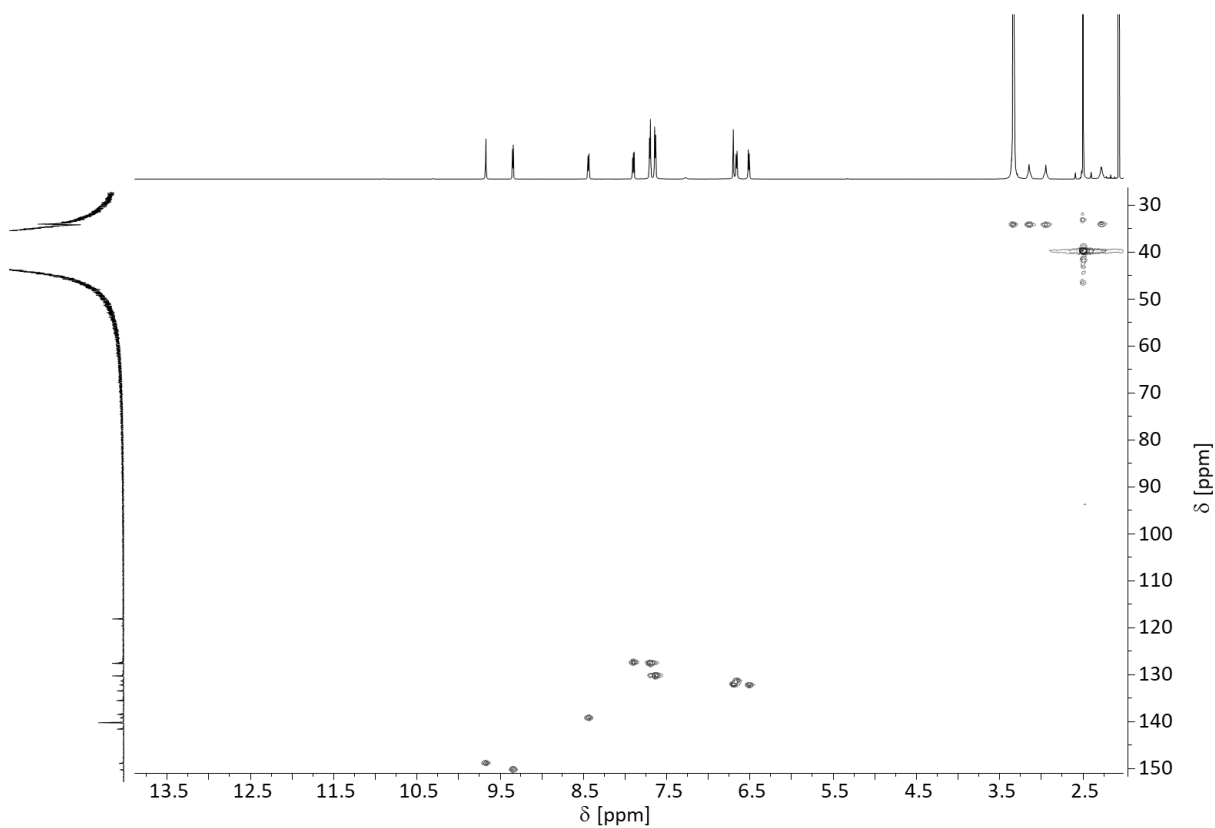


Figure S105: ^1H , ^{13}C -HSQC NMR spectrum (700.4 MHz, 176.1 MHz, $\text{DMSO-}d_6$, 298 K) of $[[\text{Pd}_2\{(\text{R}_p)\text{-5}\}_4](\text{BF}_4)_4$.

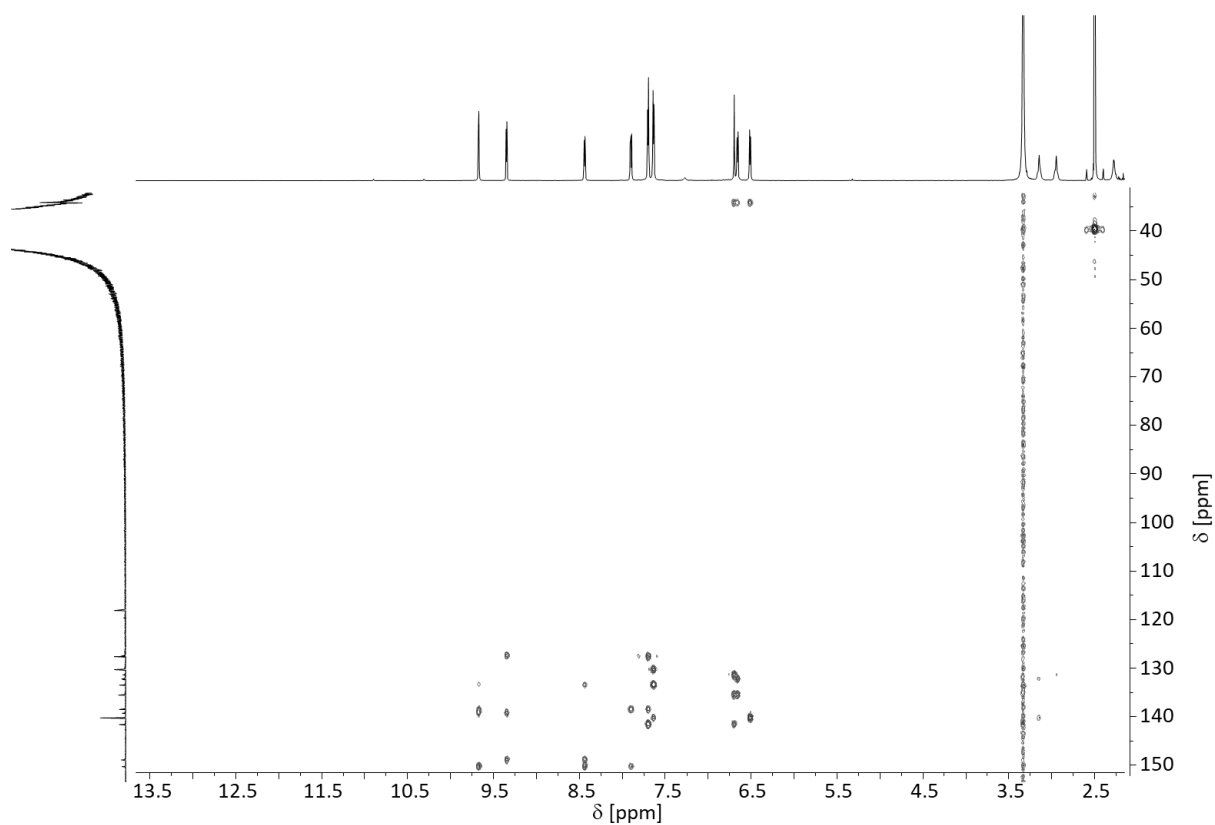


Figure S106: ^1H , ^{13}C -HMBC NMR spectrum (700.4 MHz, 176.1 MHz, $\text{DMSO-}d_6$, 298 K) of $[[\text{Pd}_2\{(\text{R}_p)\text{-5}\}_4](\text{BF}_4)_4$.

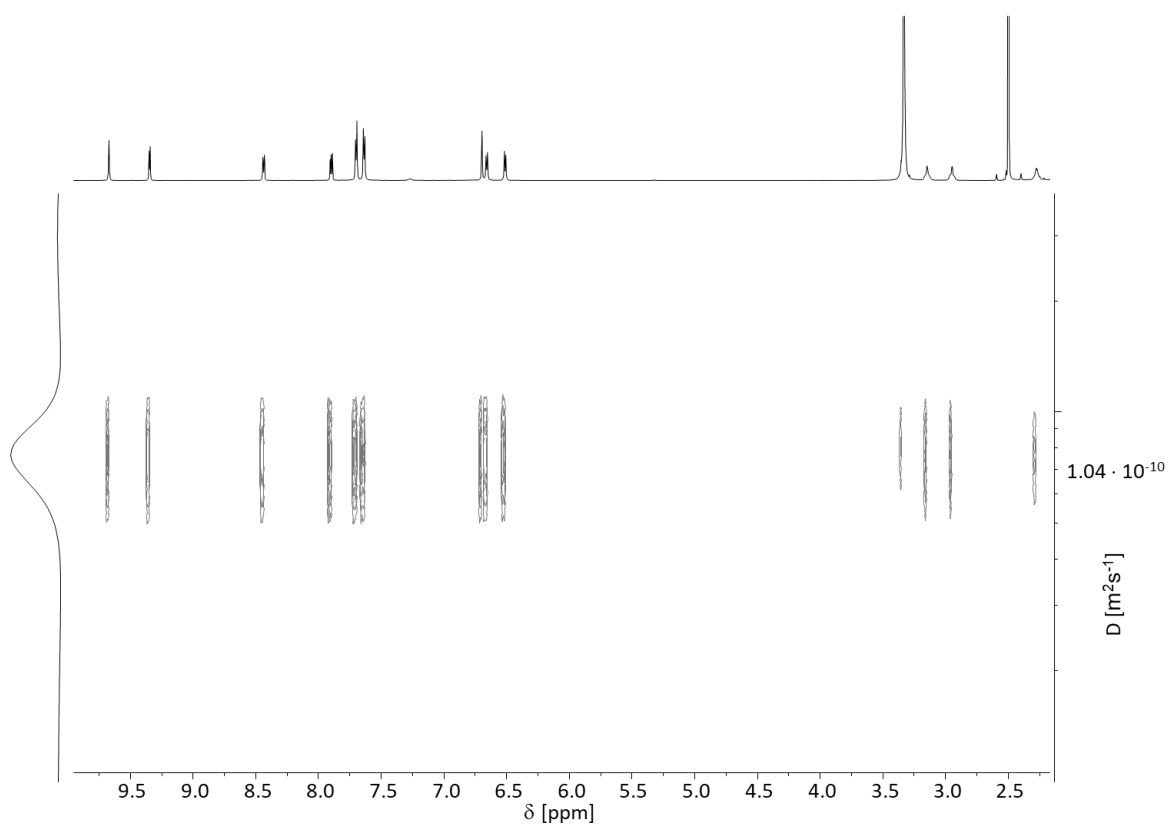


Figure S107: ^1H -DOSY NMR spectrum (499.1 MHz, $\text{DMSO-}d_6$, 298 K) of $[\text{Pd}_2\{(\text{R}_p)\text{-5}\}_4](\text{BF}_4)_4$.

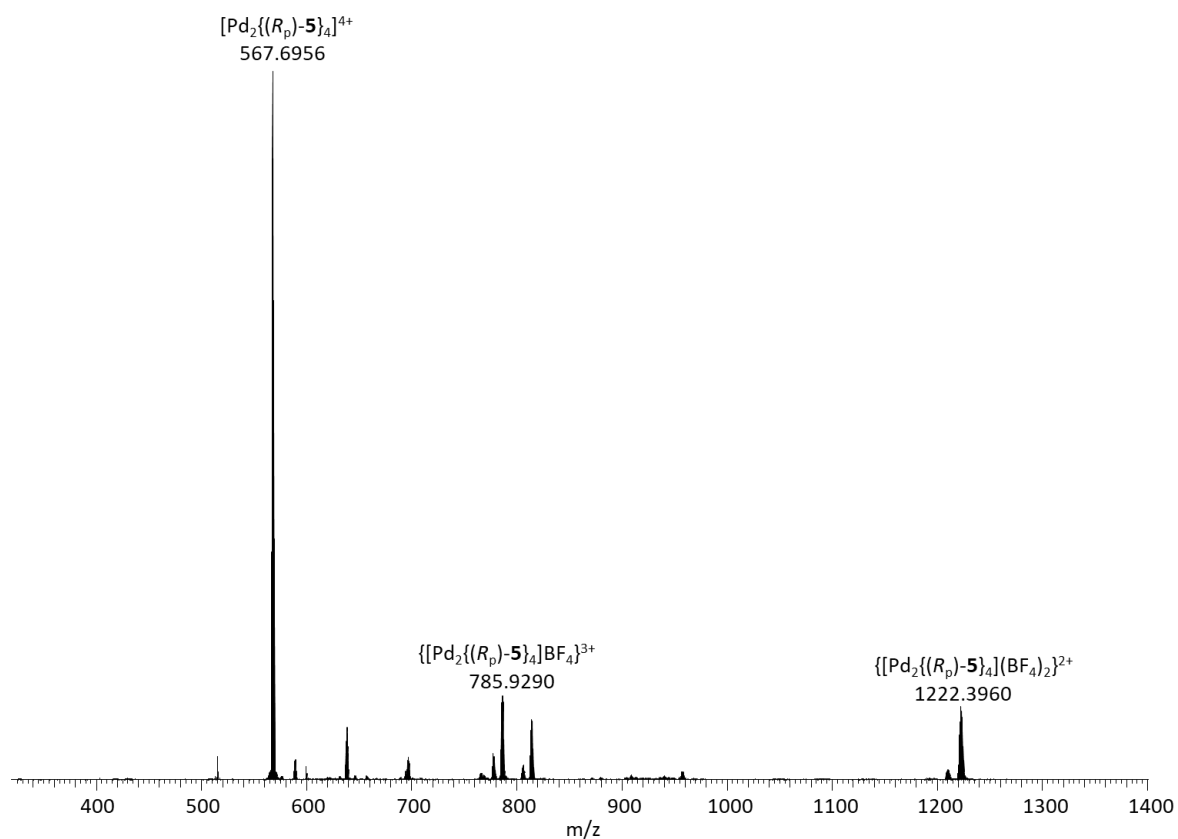


Figure S108: ESI positive mass spectrum of 2:1 mixture of $(\text{R}_p)\text{-5}$ and $[\text{Pd}(\text{CH}_3\text{CN})_4](\text{BF}_4)_2$ in $\text{DMSO-}d_6$ measured on an *Orbitrap XL* mass spectrometer.

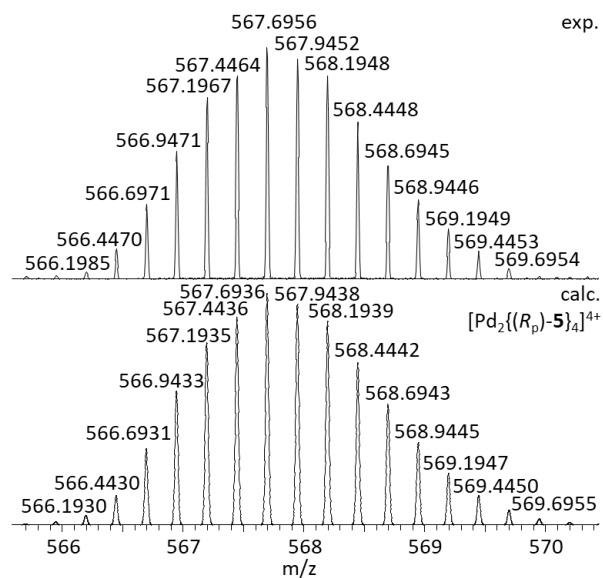


Figure S109: Experimental and calculated high resolution ESI positive mass spectra of $[\text{Pd}_2\{(\text{R}_p)\text{-5}\}_4\text{BF}_4]^{3+}$ in $\text{DMSO-}d_6$ measured on an *Orbitrap XL* mass spectrometer.

[Pd₂{(rac)-5₄}] (BF₄)₄

¹⁹F NMR (469.6 MHz, DMSO-*d*₆, 298 K): δ [ppm] = -148.74(s, BF₄), -148.79(-148.81) (m, BF₄).

¹H-DOSY NMR (700.4 MHz, DMSO-*d*₆, 298 K): D = 1.06 · 10⁻¹⁰ m²s⁻¹, R_H = 10.4 Å.

MS (ESI+) *m/z*: 567.6967 [Pd₂{(rac)-5₄}]⁴⁺, 785.9302 {[Pd₂{(rac)-5₄}] (BF₄)³⁺, 1222.8984 {[Pd₂{(rac)-5₄}] (BF₄)₂}²⁺.

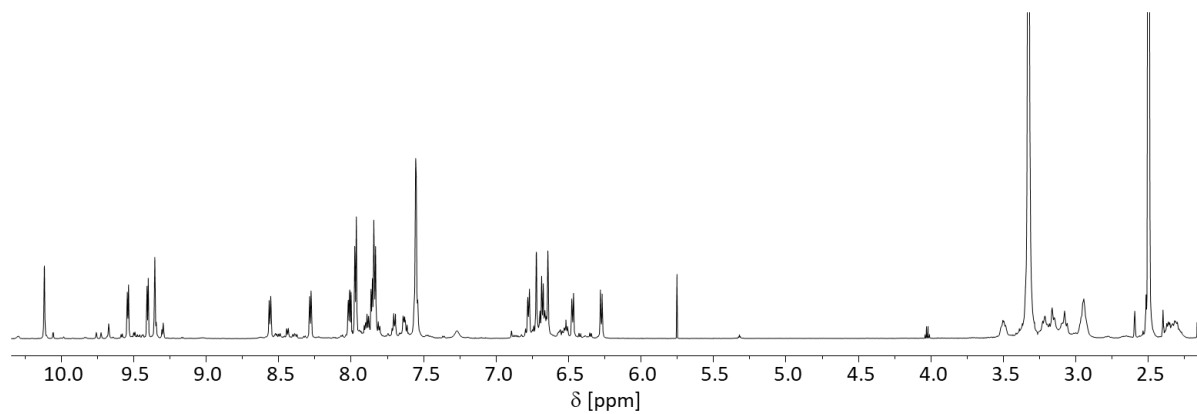


Figure S110: ¹H NMR spectrum (700.4 MHz, DMSO-*d*₆, 298 K) of [Pd₂{(rac)-5₄}] (BF₄)₄.

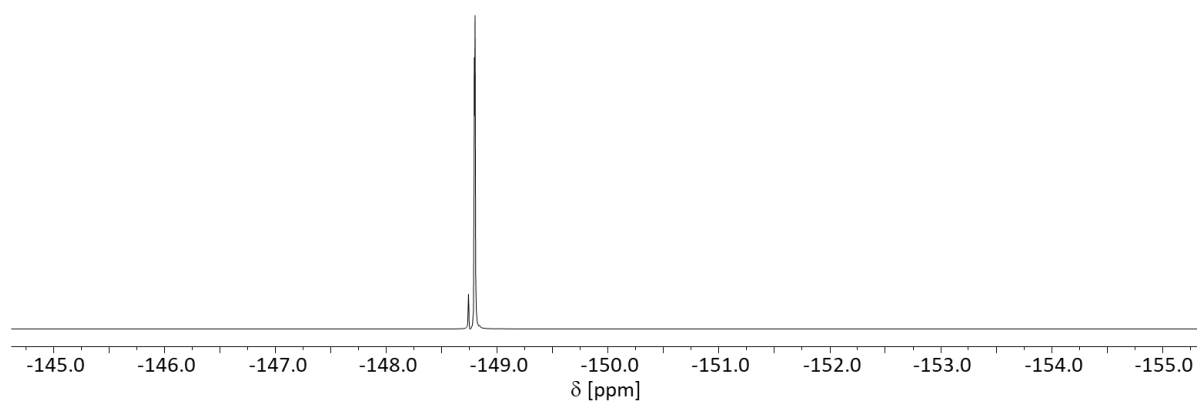


Figure S111: ¹⁹F NMR spectrum (469.6 MHz, DMSO-*d*₆, 298 K) of [Pd₂{(rac)-5₄}] (BF₄)₄.

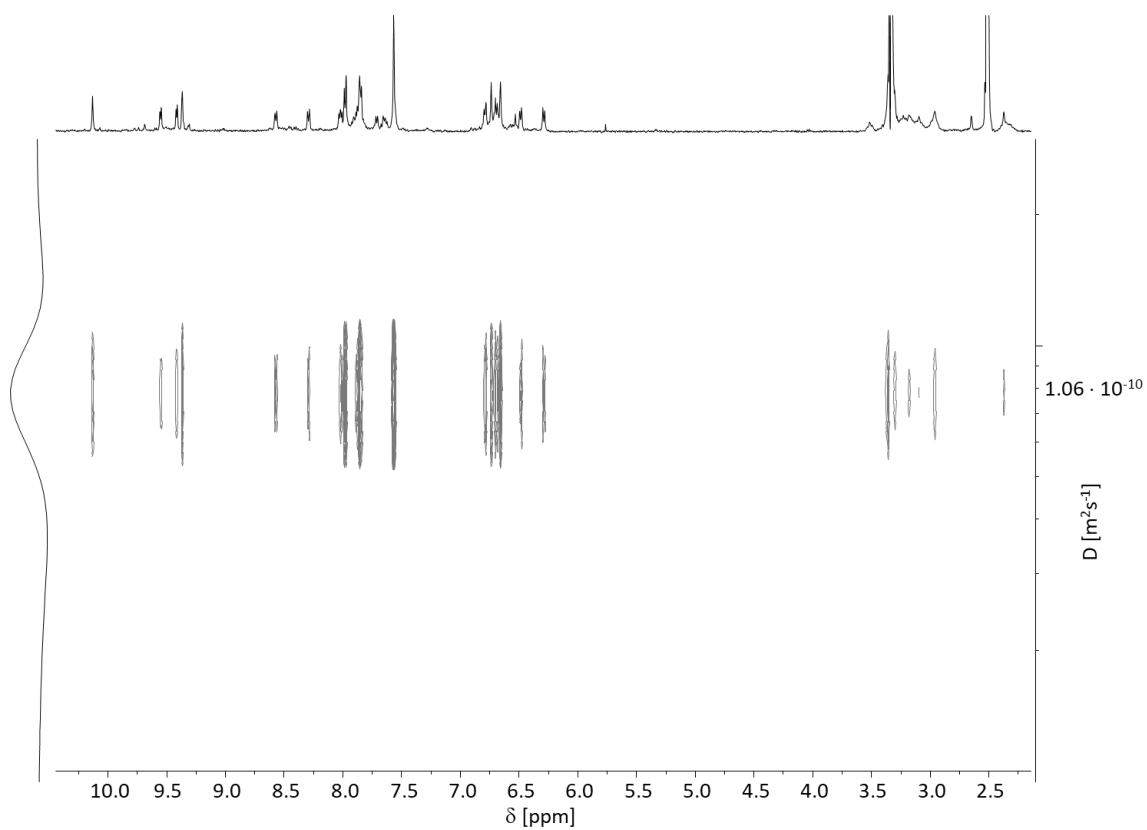


Figure S112: ^1H -DOSY NMR spectrum (499.1 MHz, $\text{DMSO-}d_6$, 298 K) of $[\text{Pd}_2\{(\text{rac})\text{-5}\}_4](\text{BF}_4)_4$.

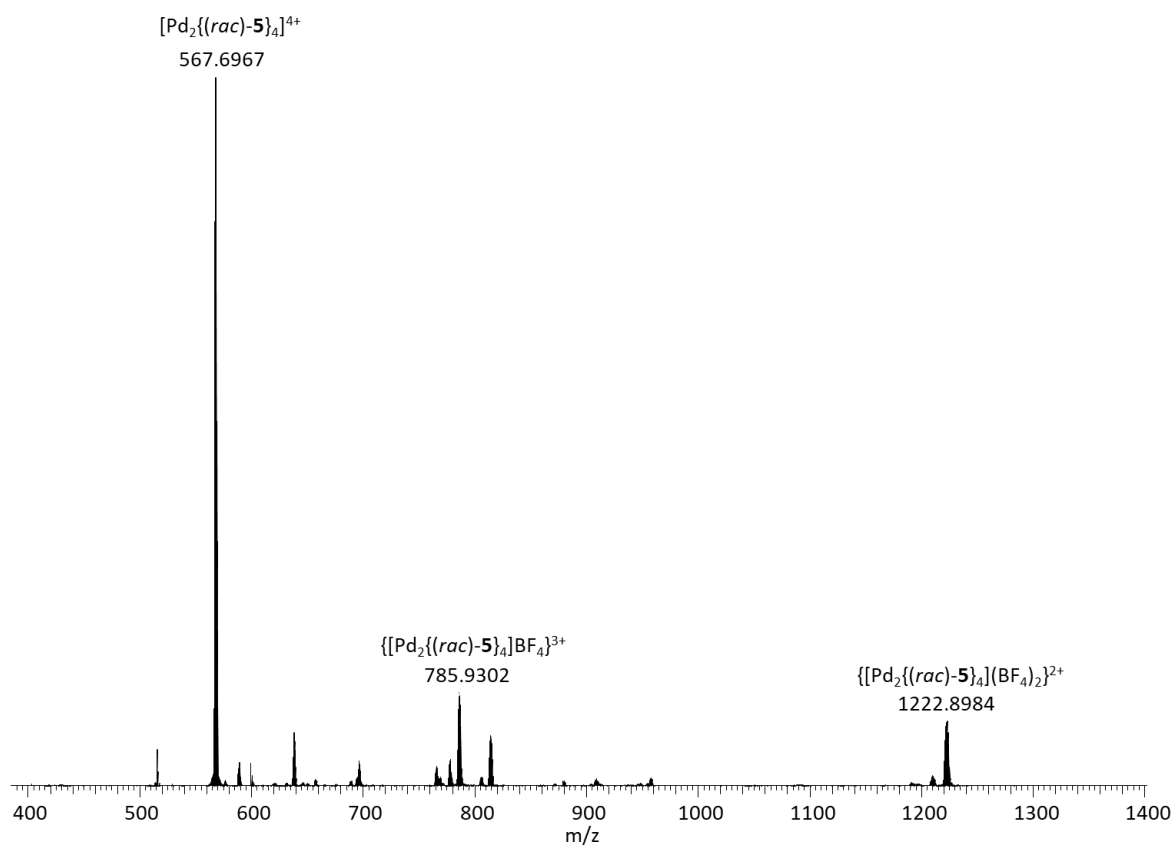


Figure S113: ESI positive mass spectrum of 2:1 mixture of $(\text{rac})\text{-5}$ and $[\text{Pd}(\text{CH}_3\text{CN})_4](\text{BF}_4)_2$ in $\text{DMSO-}d_6$ measured on an *Orbitrap XL* mass spectrometer.

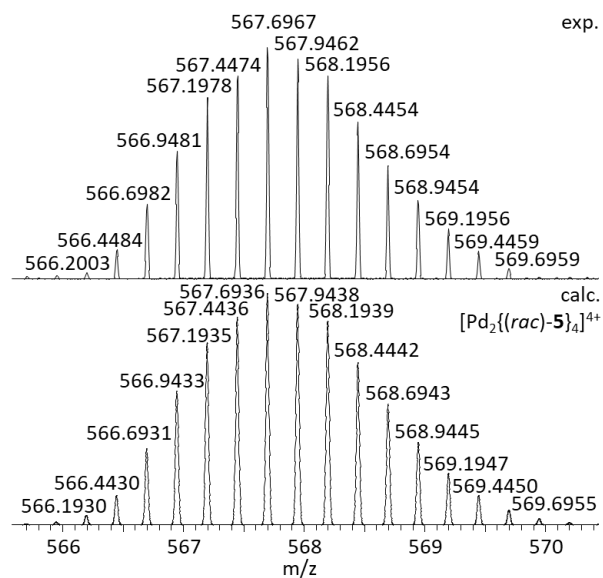


Figure S114: Experimental and calculated high resolution ESI positive mass spectra of $[\text{Pd}_2\{(\text{rac})\text{-5}\}_4]^{3+}$ in $\text{DMSO-}d_6$ measured on an *Orbitrap XL* mass spectrometer.

NMR experiments concerning the kinetics of structural rearrangements upon mixing of preassembled enantiomerically pure complexes $[\text{Pd}_2\{(R_p)\text{-5}\}_4](\text{BF}_4)_4$ and $[\text{Pd}_2\{(S_p)\text{-5}\}_4](\text{BF}_4)_4$

(R_p) - and (S_p) -5 (4.00 mg, 7.77 μmol , 1.00 eq.) were each dissolved in deuterated acetonitrile or deuterated dimethyl sulfoxide (1 mL) and a solution of $[\text{Pd}(\text{CH}_3\text{CN})_4](\text{BF}_4)_2$ (1.76 mg, 3.96 μmol , 0.51 eq.) in deuterated acetonitrile or dimethyl sulfoxide (0.5 mL) were added to each ligand solution. Both mixtures were stirred at 70 °C for 15 h. The enantiomerically pure complex solutions were mixed and analysed by NMR spectroscopy.

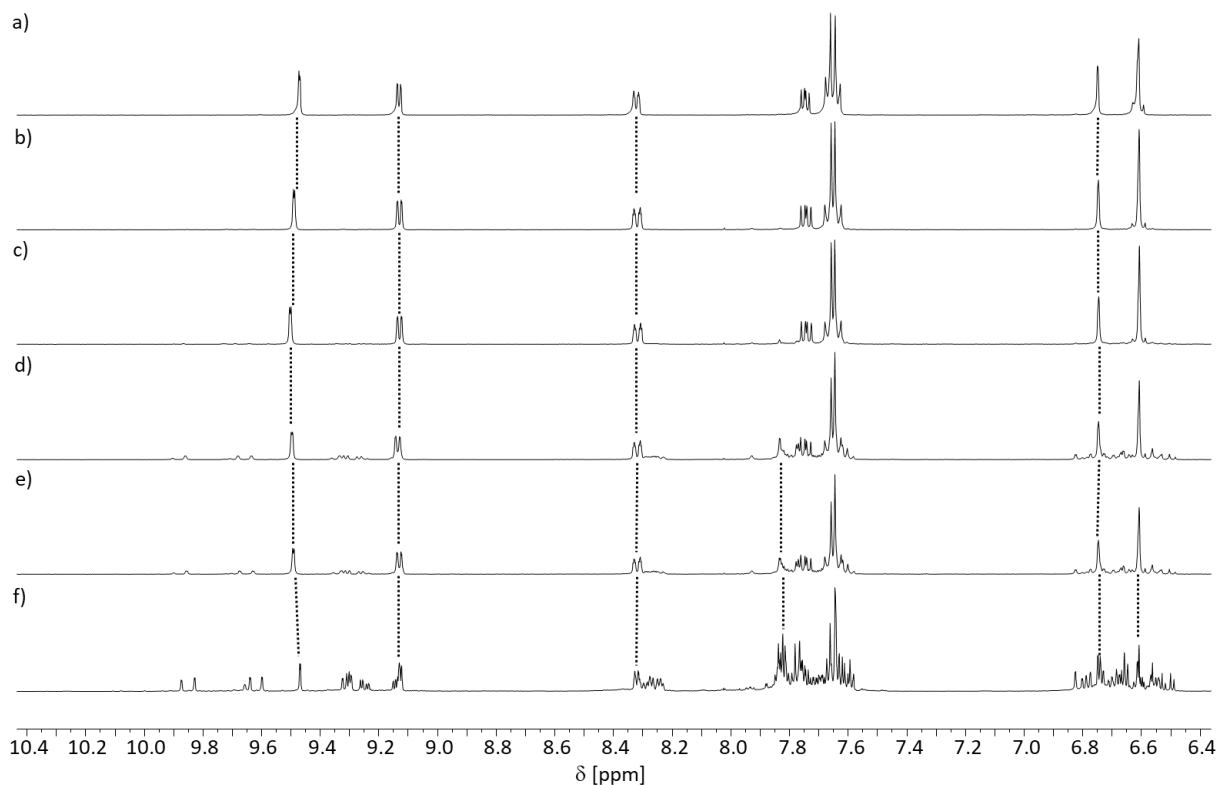


Figure S115: ^1H NMR spectra (400.1 MHz, $\text{ACN-}d_3$, 298 K) of a) $[\text{Pd}_2\{(R_p)\text{-5}\}_4](\text{BF}_4)_4$, b) mixture of $[\text{Pd}_2\{(R_p)\text{-5}\}_4](\text{BF}_4)_4$ and $[\text{Pd}_2\{(S_p)\text{-5}\}_4](\text{BF}_4)_4$ immediately after mixing, c) mixture of $[\text{Pd}_2\{(R_p)\text{-5}\}_4](\text{BF}_4)_4$ and $[\text{Pd}_2\{(S_p)\text{-5}\}_4](\text{BF}_4)_4$ after 12 h at room temperature, d) mixture of $[\text{Pd}_2\{(R_p)\text{-5}\}_4](\text{BF}_4)_4$ and $[\text{Pd}_2\{(S_p)\text{-5}\}_4](\text{BF}_4)_4$ after another 15 h at 70 °C, e) mixture of $[\text{Pd}_2\{(R_p)\text{-5}\}_4](\text{BF}_4)_4$ and $[\text{Pd}_2\{(S_p)\text{-5}\}_4](\text{BF}_4)_4$ again after another 15 h and f) $[\text{Pd}_2\{(rac)\text{-5}\}_4](\text{BF}_4)_4$.

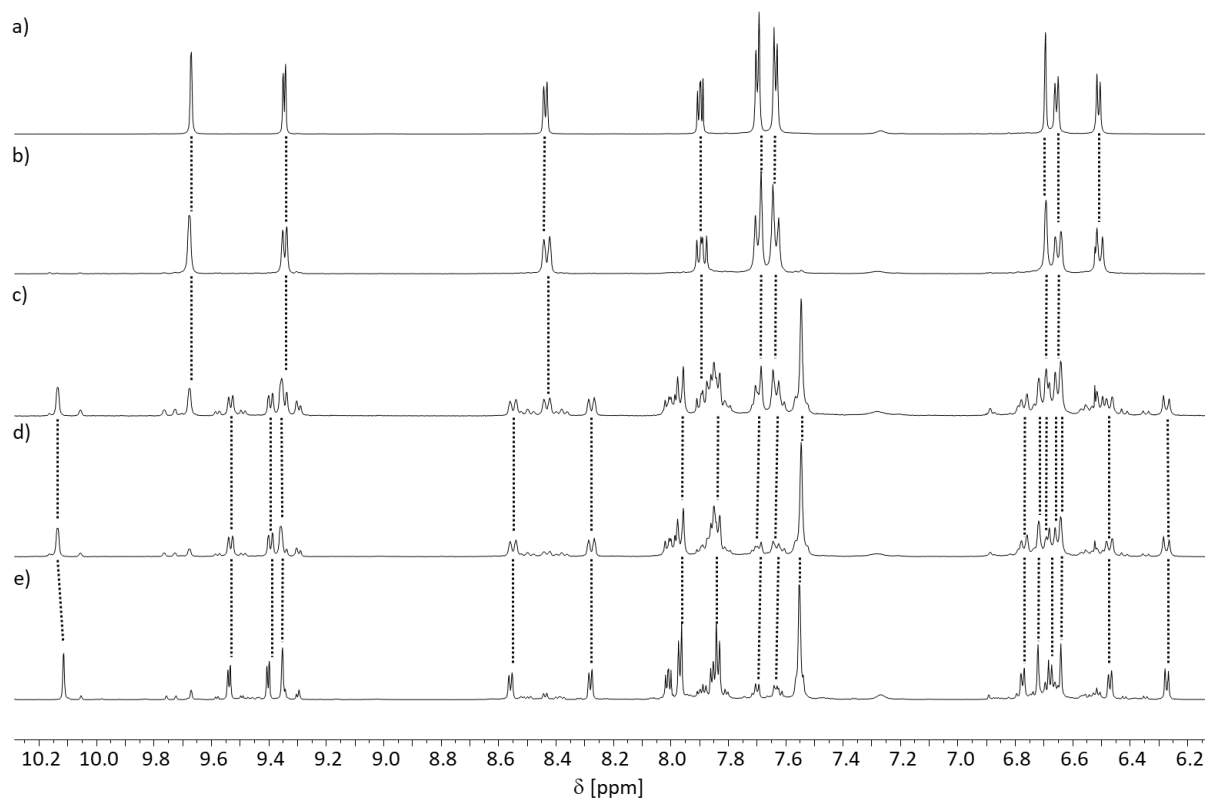


Figure S116: ^1H NMR spectra (400.1 MHz, $\text{DMSO-}d_6$, 298 K) of a) $[\text{Pd}_2\{(\text{R}_p)\text{-5}\}_4](\text{BF}_4)_4$, b) mixture of $[\text{Pd}_2\{(\text{R}_p)\text{-5}\}_4](\text{BF}_4)_4$ and $[\text{Pd}_2\{(\text{S}_p)\text{-5}\}_4](\text{BF}_4)_4$ immediately after mixing, c) mixture of $[\text{Pd}_2\{(\text{R}_p)\text{-5}\}_4](\text{BF}_4)_4$ and $[\text{Pd}_2\{(\text{S}_p)\text{-5}\}_4](\text{BF}_4)_4$ after 12 h at room temperature, d) mixture of $[\text{Pd}_2\{(\text{R}_p)\text{-5}\}_4](\text{BF}_4)_4$ and $[\text{Pd}_2\{(\text{S}_p)\text{-5}\}_4](\text{BF}_4)_4$ after another 15 h at 70 °C, e) $[\text{Pd}_2\{(\text{rac})\text{-5}\}_4](\text{BF}_4)_4$.

X-ray crystallography

X-Ray experimental details for (R_p) -**4**, the racemic mixture of $[\text{Pd}_2(\text{dppp})_2\{(R_p)\text{-4}\}_2](\text{OTf})_4$ & $[\text{Pd}_2(\text{dppp})_2\{(S_p)\text{-4}\}_2](\text{OTf})_4$ and $[\text{Pd}_2\{(R_p)\text{-5}\}_4](\text{BF}_4)_4$ are below. The single-crystal X-ray data for (R_p) -**4** were measured on a *Rigaku SuperNova* diffractometer equipped with an *Eos CCD* detector using mirror-monochromated Mo-K α ($\lambda = 0.71073 \text{ \AA}$) radiation. Data for the racemic mixture of $[\text{Pd}_2(\text{dppp})_2\{(R_p)\text{-4}\}_2](\text{OTf})_4$ & $[\text{Pd}_2(\text{dppp})_2\{(S_p)\text{-4}\}_2](\text{OTf})_4$ and $[\text{Pd}_2\{(R_p)\text{-5}\}_4](\text{BF}_4)_4$ were measured using a dual-source *Rigaku SuperNova* diffractometer equipped with an *Atlas* detector using mirror-monochromated Cu-K α ($\lambda = 1.54184 \text{ \AA}$) radiation. The data collection and reduction were performed using the program *CrysAlisPro*⁶ and Gaussian face index absorption correction method was applied.⁶ The structure was solved with direct methods (*SHELXS*)⁷ and refined by full-matrix least squares on F^2 using the *OLEX2*⁸ software which utilizes the *SHELXL-2015* module.⁷ In $[\text{Pd}_2\{(R_p)\text{-5}\}_4](\text{BF}_4)_4$ one tetrafluoroborate anion could not be found using electron fourier difference map. This is due to weakly diffracting power of the crystals and disordered solvent molecules. Therefore, one tetrafluoroborate anion is modelled and thermal movement of fluorine atoms on both tetrafluoroborate anions were physically restrained to give roughly tetrahedral geometry.

Crystal data for (R_p) -**4**: CCDC-1893943, $\text{C}_{40}\text{H}_{34}\text{I}_3\text{N}_3$, $M = 937.40$, light orange plate, $0.174 \times 0.075 \times 0.068 \text{ mm}^3$, tetragonal, space group $P 4_12_12$, $a = 13.41045(10) \text{ \AA}$, $b = 13.41045(10) \text{ \AA}$, $c = 40.0935(5) \text{ \AA}$, $\alpha = 90^\circ$, $\beta = 90^\circ$, $\gamma = 90^\circ$, $V = 7210.41(14) \text{ \AA}^3$, $Z = 8$, $D_c = 1.727 \text{ g/cm}^3$, $F000 = 3632$, $\mu = 2.633 \text{ mm}^{-1}$, $T = 120.00(16) \text{ K}$, $\theta_{\text{max}} = 29.06^\circ$, 99031 total reflections, 8071 with $I_o > 2\sigma(I_o)$, $R_{\text{int}} = 0.0525$, 9148 data, 416 parameters, 0 restraints, $\text{Goof} = 1.106$, $R = 0.0448$ and $wR = 0.1136 [I_o > 2\sigma(I_o)]$, $R = 0.0551$ and $wR = 0.1188$ (all reflections), $1.120 < d\Delta\rho < -0.876 \text{ e/\AA}^3$, $\text{Flack} = -0.004(8)$.

Crystal data for $[\text{Pd}_2\{(R_p)\text{-5}\}_4](\text{BF}_4)_4$: CCDC-1893944, $\text{C}_{152}\text{H}_{120}\text{B}_4\text{F}_{16}\text{N}_8\text{Pd}_2$, $M = 2618.59$, colourless needle, $0.176 \times 0.079 \times 0.048 \text{ mm}^3$, tetragonal, space group $P4_12_12$, $a = 32.9899(5) \text{ \AA}$, $b = 32.9899(5) \text{ \AA}$, $c = 14.3593(4) \text{ \AA}$, $\alpha = 90^\circ$, $\beta = 90^\circ$, $\gamma = 90^\circ$, $V = 15627.7(6) \text{ \AA}^3$, $Z = 4$, $D_c = 1.113 \text{ g/cm}^3$, $F000 = 5376$, $\mu = 2.397 \text{ mm}^{-1}$, $T = 120.01(10) \text{ K}$, $\theta_{\text{max}} = 66.748^\circ$, 48137 total reflections, 10932 with $I_o > 2\sigma(I_o)$, $R_{\text{int}} = 0.0493$, 13861 data, 806 parameters, 31 restraints, $\text{Goof} = 1.031$, $R = 0.0861$ and $wR = 0.2445 [I_o > 2\sigma(I_o)]$, $R = 0.0997$ and $wR = 0.2598$ (all reflections), $1.233 < d\Delta\rho < -1.572 \text{ e/\AA}^3$, $\text{Flack} = 0.049(6)$.

Crystal data for [the racemic mixture of $[\text{Pd}_2(\text{dppp})_2\{(R_p)\text{-4}\}_2](\text{OTf})_4$ & $[\text{Pd}_2(\text{dppp})_2\{(S_p)\text{-4}\}_2](\text{OTf})_4$]: CCDC-1893945, $\text{C}_{280}\text{H}_{248}\text{F}_{24}\text{N}_8\text{O}_{27}\text{P}_8\text{Pd}_4\text{S}_8$, $M = 5542.69$, colourless plate, $0.256 \times 0.226 \times 0.079 \text{ mm}^3$, monoclinic, space group $C2/c$, $a = 46.6905(8) \text{ \AA}$, $b = 26.3232(3) \text{ \AA}$, $c = 31.9982(5) \text{ \AA}$, $\alpha = 90^\circ$, $\beta = 97.750(2)^\circ$, $\gamma = 90^\circ$, $V = 38968.0(10) \text{ \AA}^3$, $Z = 4$, $D_c = 0.945 \text{ g/cm}^3$, $F000 = 11392$, $\mu = 2.653 \text{ mm}^{-1}$, $T = 120.01(10) \text{ K}$, $\theta_{\text{max}} = 66.749^\circ$, 109627 total reflections, 25716 with $I_o > 2\sigma(I_o)$, $R_{\text{int}} = 0.0411$, 34510 data, 1732 parameters, 97 restraints, $\text{Goof} = 1.033$, $R = 0.0815$ and $wR = 0.2423 [I_o > 2\sigma(I_o)]$, $R = 0.0992$ and $wR = 0.2681$ (all reflections), $4.275 < d\Delta\rho < -1.553 \text{ e/\AA}^3$.

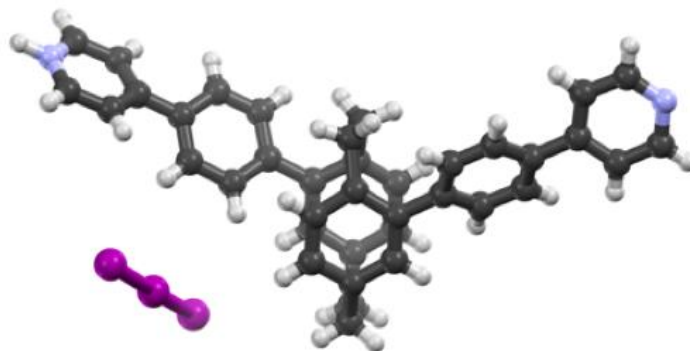


Figure S117. X-Ray crystal structure of (*R_p*)-**4** in ball & stick model (acetonitrile solvent is omitted for viewing clarity; colour code: grey – carbon, white – hydrogen, blue – nitrogen, purple – iodine)

References

- 1 G. Meyer-Eppler, R. Sure, A. Schneider, G. Schnakenburg, S. Grimme, A. Lützen, *J. Org. Chem.*, 2014, **79**, 6679.
- 2 S. S. Zaleskiy, V. P. Ananikov, *Organometallics*, 2012, **31**, 2302.
- 3 T. G. Appleton, M. A. Bennett, I. B. Tomkins, *J. Chem. Soc. Dalton Trans.*, 1976, 439.
- 4 P. J. Stang, D. H. Cao, S. Saito, A. M. Arif, *J. Am. Chem. Soc.*, 1995, **117**, 6273.
- 5 a) K. E. Van Holde, *Physical Biochemistry*, Prentice-Hall, Englewood Cliffs (1971); b) A. Macchioni, G. Ciancaleoni, C. Zuccaccia, D. Zuccaccia, *Chem. Soc. Rev.*, 2008, **37**, 479.
- 6 Rigaku Oxford Diffraction, 2017, *CrysAlisPro* Software system, version 38.46, Rigaku Corporation, Oxford, UK.
- 7 a) G. M. Sheldrick, *Acta Crystallogr. Sect. C*, 2015, **71**, 3; b) G. M. Sheldrick, *Acta Crystallogr. Sect. A*, 2015, **71**, 3.
- 8 O. V Dolomanov, L. J. Bourhis, R. J. Gildea, J. A. K. Howard and H. Puschmann, *J. Appl. Crystallogr.*, 2009, **42**, 339.